MINISTERE DES AFFAIRES ECONOMIQUES
SERVICE GEOLOGIQUE DE BELGIQUE · BELGISCHE GEOLOGISCHE DIENST
MINISTERIE VAN ECONOMISCHE ZAKEN

IN SITU PARAMETERS FROM THE EARTH TIDAL AND BAROMETRIC RESPONSES IN THE BOREHOLE AT THE ROYAL OBSERVATORY OF BELGIUM. THE EFFECT ON GRAVITY OF THE WATER-LEVELS VARIATIONS

by

Micheline DELCOURT-HONOREZ

1990

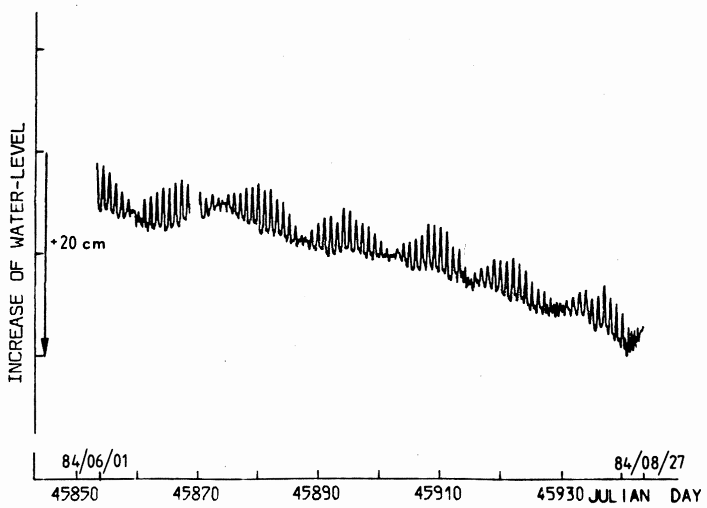

PROFESSIONAL PAPER 1990/3 — Nr 244

IN SITU PARAMETERS FROM THE EARTH TIDAL AND BAROMETRIC RESPONSES IN THE BOREHOLE AT THE ROYAL OBSERVATORY OF BELGIUM. THE EFFECT ON GRAVITY OF THE WATER-LEVELS VARIATIONS

by

Micheline DELCOURT-HONOREZ

Dr. Micheline DELCOURT-HONOREZ
ROYAL OBSERVATORY OF BELGIUM
CENTRE DE GEOPHYSIQUE INTERNE
Avenue Circulaire, 3
B 1180 BRUXELLES

PROFESSIONAL PAPER 1990/3 — Nr 244

Abstract.

A borehole has been drilled in January 1984 under the responsibility of the Belgian Geological Survey at the Royal Observatory of Belgium in Brussels. The profile drawn up by the Geological Survey shows eight different layers. In this multiple aquifer-aquitard system, three layers are aquifer layers : a water table aquifer in the Brussels sand, an intermediate aquifer in the tuf of Lincent and a deep aquifer in the bedrock.

Various kinds of water-levels variations are registered : long term and short term variations and, in the intermediate and deep wells, periodic oscillations that are due to Earth tidal phenomena. Moreover, the water table and the pressure heads respond to the atmospheric pressure variations.

We estimate the water-levels variations perturbing effects on the superconducting gravimeter registrations (the borehole at the Observatory is next to this gravimeter), i.e. the land surface displacement, the gravitational, barometric and Earth tidal effects. The land surface displacement is studied by the combined problem that includes the hydraulic problem and the consolidation problem. To estimate the gravitational effect induced by the variable watermasses, we enlarge the classical Bouguer's formula in theories taking into account the nature of the layers, the expansions or compressions of each layer and the total land surface displacement; moreover, for the effect of the water table variations, we propose a theory in which we consider the various hydrostatic occurences of phases in porous media. In a confined aquifer, we show that the effect of the attraction variation is depending on the fluid compressibility. We also generalize the Bouguer's theory, valid for a thin layer, to the case of a finite thickness layer, by a numerical integration.

We conclude that the water-levels variations in the intermediate and deep aquifers (at long term, at short term and those due to the barometric and tidal responses) are inducing very small indeed negligible perturbing effects on the superconducting gravimeter registrations. Moreover the effect of the long term water table drift is at the limit of the actual precision of the gravimeter registrations.

On the other hand, for each of the three well-aquifer systems, we study the barometric and tidal responses to estimate the in situ parameters of both the aquifers and the aquifer system (porosity, specific storage, vertical compressibility and permeability). The estimated values are in good agreement with those deduced by using hydrogeological, soil and rock mechanics considerations.

The research we present mainly concerning the ROB station can be also applied to any other station with any complexity.

The values of the in situ parameters estimated from the Earth tides observations in the wells can be of great interest for the stocking of the nuclear and toxic waste products.

Figures and Tables are separated at the end of this paper.

Notations. Chapter 2

a_v	: coefficient of compressibility	$M^{-1}LT^2$
b	: thickness of an aquifer layer	L
b'	: thickness of an aquitard layer	L
b_L	: distance to a drainage face in an aquitard layer	L
c	: depth of the center of a layer	L
c_m	: uniaxial compaction coefficient	$M^{-1}LT^2$
c_c	: coefficient of consolidation	L^2T^{-1}
e	: void ratio	/
g	: acceleration due to gravity	LT^{-2}
h	: piezometric head	L
$i^{z}{}_R$	: influence factor	/
k_D	: Darcy's coefficient (aquifer)	LT^{-1}
k'_D	: Darcy's coefficient (aquitard)	LT^{-1}
p	: fluid pressure	$ML^{-1}T^{-2}$
p_e	: pore water pressure in excess of hydrostatic	$ML^{-1}T^{-2}$
r	: radial coordinate direction	L
s	: drawdown	L
t	: time	T
t_R	: reservoir compaction	L
z	: radial coordinate direction	L
$z_{i,F}$	: initial, final water table	L
A^*	: expansion constant	/
C^*	: compaction constant	/
C_c	: compression index	/
E	: Young's modulus	$ML^{-1}T^{-2}$
E_s	: compressibility modulus of the aquifer skeleton	$ML^{-1}T^{-2}$
E'_c	: bulk modulus of compression	$ML^{-1}T^{-2}$
F_t	: time factor	/
$I^{q}{}_i$	: Hankel integral	/
$J_{a,b}$	: Bessel's functions of the first kind of the orders a,b	
K_b	: bulk modulus	$ML^{-1}T^{-2}$
K_{ij}	: components of permeability tensor	LT^{-1}
Q_i	: leakage term	LT^{-1}
R	: radius of an aquifer	L
S	: storage coefficient of an aquifer	/
S'	: storage coefficient of an aquitard	/
S_s	: specific storage of an aquifer	L^{-1}
S'_s	: specific storage of an aquitard	L^{-1}
T	: transmissivity	L^2T^{-1}
$T_{ix,y}$	: transmissivity tensor components in the directions x and y	L^2T^{-1}
V_v	: voids volume	L^3
V_s	: solid volume	L^3
W	: parameter	/

α	: skeleton aquifer vertical compressibility (= $1/E_s$)	$M^{-1}LT^{2}$
α'	: skeleton aquitard vertical compressibility	$M^{-1}LT^{2}$
α_b	: bulk compressibility	$M^{-1}LT^{2}$
α_g	: compressibility of the solid grains	$M^{-1}LT^{2}$
β	: fluid compressibility	$M^{-1}LT^{2}$
β^*	: constant	/
γ	: unit weight (= ρ g)	$ML^{-2}T^{-2}$
γ_k	: unit weight of the material without void	$ML^{-2}T^{-2}$
γ_n	: unit weight of the layer n	$ML^{-2}T^{-2}$
γ_w	: unit weight of water	$ML^{-2}T^{-2}$
δ_{ij}	: Kronecker symbol	/
ϵ	: cubic dilatation	/
ϵ_{ij}	: strain tensor	/
ζ	: constant (=1 - α_g K_b)	/
λ	: Lamé parameter	$ML^{-1}T^{-2}$
μ	: Lamé parameter, rigidity modulus	$ML^{-1}T^{-2}$
ν_p	: Poisson's coefficient	/
ξ	: displacement (ξ_x, ξ_y, ξ_z)	L
ξ^*	: displacement (unit volume and unit pressure change)	L
$\lvert\xi_z\rvert$	: expansion or compaction of an aquifer layer	L
$\lvert\xi'_z\rvert$	: expansion or compaction of an aquitard layer	L
ρ	: volumic mass	ML^{-3}
ρ_w	: fluid volumic mass	ML^{-3}
σ	: total stress	$ML^{-1}T^{-2}$
σ_{ij}	: stress tensor	$ML^{-1}T^{-2}$
σ_{ij}	: effective stress tensor	$ML^{-1}T^{-2}$
σ_z	: effective stress	$ML^{-1}T^{-2}$
Δ	: increment	/
Σ	: sommation	/
Φ_o	: volume porosity	/
$\hat{\Phi}$	: internal friction angle	/
∇	: gradient	L^{-1}
∇^2	: Laplace's operator	L^{-2}

Notations. Chapter 3

b_j	:	thickness of the j^{th} layer	L
b_s	:	thickness of the layer s of the bedrock	L
c	:	depth of a layer	L
c_s	:	depth of the layer s of the bedrock	L
e	:	void ratio	/
g	:	acceleration due to gravity	LT^{-2}
h_{wt}	:	water table variation	L
h_c	:	capillary water height	L
h_f	:	funicular zone height	L
h_p	:	pendular zone height	L
$\{i^j{}_R\}_{i,F}$	:	influence factor of the stratum j, at the initial, final state	/
l	:	subscript of a substratum of the stratum j	/
m	:	number of substrata of the stratum j	/
n	:	number of layers	/
z_i, z_F	:	initial, final water table	L
$(z_s)_{i,F}$	:	vertical coordinate of the land surface at the initial, final state	L
ΔA_j	:	attraction variation of the j^{th} layer	LT^{-2}
$(A_{j,l})_{i,F}$	:	attraction of a substratum l of the j^{th} layer at the initial, final state	LT^{-2}
G	:	gravitation constant	$M^{-1}L^3T^{-2}$
R	:	aquifer radius	L
S	:	storage coefficient of an aquifer	/
S_s	:	specific storage of an aquifer	L^{-1}
β	:	fluid compressibility	$M^{-1}LT^2$
γ_w	:	fluid unit weight	$ML^{-2}T^{-2}$
γ_k	:	unit weight of the material without void	$ML^{-2}T^{-2}$
γ_p	:	unit weight of the pendular zone	$ML^{-2}T^{-2}$
Δ	:	increment	
ϵ_c	:	thickness of a thin circular slab	L
$\lvert \xi_{zj} \rvert$	:	expansion or compaction along z of the j^{th} layer	L
$\lvert \xi_z \rvert$	:	total expansion or compaction along z	L
ρ_w	:	fluid volumic mass	ML^{-3}
$(\rho)_{i,F}$	:	fluid volumic mass at the initial, final state	ML^{-3}
Φ_o	:	volume porosity	/
ξ_j	:	unit expansion of the j^{th} layer	/

Notations. Chapter 5

b	confined aquifer thickness	L
b_{wt}	unconfined aquifer thickness	L
f	pipe friction	/
g	acceleration due to gravity	LT^{-2}
h	piezometric head	L
h_o	pressure head fluctuation	L
k_D	permeability	LT^{-1}
n_p	parameter	/
p	fluid pressure	$ML^{-1}T^{-2}$
p_a	atmospheric pressure	$ML^{-1}T^{-2}$
r_e	effective radius	L
r_i	influence region radius	L
r_w	well radius	L
t	time	T
x_o	water-level well oscillation amplitude	L
A, A'	amplification factors	/
BE	barometric efficiency	/
H	water column height above the aquifer	L
H_e	effective water column height	L
K_b	bulk modulus	$ML^{-1}T^{-2}$
S	storage coefficient (of the aquifer)	/
S_s	specific storage (of the aquifer)	L^{-1}
T	transmissivity	L^2T^{-1}
T_r	retardation time	T
TE	Tidal Efficiency	/
α	aquifer skeleton vertical compressibility	$M^{-1}LT^2$
α_w	parameter	/
β	fluid compressibility	$M^{-1}LT^2$
β_w	parameter	/
ϵ_t	tidal dilatation	/
ϵ_{pa}	cubic dilatation due to p_a	/
ν_p	Poisson's coefficient	/
ρ	fluid volumic mass	ML^{-3}
τ_p	wave period	T
$\emptyset$	water-level phase lag	/
ω	wave frequency	T^{-1}
ω_w	parameter	T^{-1}
$\emptyset_o$	volume porosity	/

CHAPTER 1. WATER-LEVELS REGISTRATIONS

1. Observations

In January 1984, the Belgian Geological Survey has drilled a borehole with three observation wells at the Royal Observatory of Belgium (afterwards referred as "ROB"), in Brussels (Laga & Delcourt, 1990).
The profile drawn up by the Belgian Geological Survey shows that eight different layers belong to a multiple aquifer-aquitard system, down to a 140 meter depth (figure 1.1). Three of these layers has been considered as aquifers: a water table aquifer in the Brussels sand, which the phreatic level appears at the depth of about 35.60 m, an intermediate aquifer in the tuf of Lincent and a deep aquifer in the fissured bedrock, in which the pressure heads are respectively rising at the depths of about 61.50 m and 67.00 m. The technical description of the borehole and the complete geological study can be found in Laga & Delcourt (1990). The water-levels variations are registered by capacitive transducers "Nivocaps" (Van Ruymbeke & Delcourt, 1986). All the observations are converted into the standard format used by the "ICET", International Centre for the Earth Tides (Ducarme, 1975, 1978).

In the water-levels registrations, three kinds of variations are detected : long term variations (i.e. over one year or more), short term variations which correspond to pressure heads declines during pumping (of about two hours duration) and periodic fluctuations in the intermediate and deepest wells. We shall see that those oscillations are due to tidal phenomena. The water table doesn't show any periodic fluctuations of that kind. We use the now available water-levels hourly readings set, i.e. 4 years and six months observations, from June 1984 to December 1988. (Delcourt-Honorez, afterwards referred as "DH", 1990a).

2. Water-levels barometric responses (at long term)

Water-levels in wells especially tapping confined aquifer are affected by changes in the atmospheric pressure (e.g. Jacob, 1950, Melchior et al., 1956, Sterling, 1964, De Wiest, 1966, Walton, 1970, Sterling & Smets, 1971). At the ROB, each of the three well-aquifer systems is sensitive to the atmospheric pressure variations.

We obtain the bi-hourly readings set of the atmospheric pressure in Brussels from the Royal Meteorological Institute of Belgium, Brussels. A polynomial fitting is applied to get one data every hour.

At long term, we remove the barometric effects by using the Multiple Input Single Output method (De Meyer, 1982) and by determining the transfer functions. The impulse responses are given in the table 1.1. respectively for the water table, for the intermediate and deep wells. The pressure p_t are expressed in millibar and the numerical coefficients are expressed in millimeter of water.millibar-1. For each water-level, the static response corresponding to the zero frequency is represented by the "static admittance or efficiency", also called the "Observed Efficiency" $|BE|_{obs}$. This efficiency is obtained by adding the coefficients of the expressions (1.1a), (1.1b) and (1.1c) respectively for each water-level. $|BE|_{obs}$ is given in the last column of the table 1.1.

3. Water-levels data

We obtain the long term water-levels variations by direct measurements with the meter and by extrapolation using the registrations of the nivocap transducer. From the data files we can establish the list of the largest variations in the three wells; we present that list in the table 1.2.

The figure 1.2. displays the long term variations of the water-levels registered in the three wells during the first year of observations (84/06/01 — 85/07/09). On this figure, the water-levels are represented at the same scale : that shows that the water table (1) is varying (a maximum rise of 0.07 m) less than the pressure heads in the intermediate (2) and deep wells (3) (respectively pressure heads increases of 1.40 m and of 0.95 m). On the figures 1.3 to 1.5, we see the 34 months data sets (84/06/01 — 87/03/09), respectively for the water-table, the intermediate and deep wells. On the figures 1.6 to 1.8, the complete data sets (84/06/01 — 88/12/02) for the water table, the intermediate and deep wells are presented. The curves (a) are the water-levels that are not corrected from the atmospheric pressure effect, the curves (b) are the water-levels from which the barometric effect has been removed.

From those figures and from the table 1.2 (DH, 1989b) we can conclude that the water-levels are not very stable. In the water table after the first year, the registrations show larger variations, e.g. a 10 cm decline (from 86/06/01 to 86/10/31), a 16 cm rise (from 87/09/29 to 88/04/25) and a 18 cm rise (from 88/04/25 to 88/11/04).
In the intermediate and deep aquifer, after the one year recovery phase of about one meter, the pressure heads show decreases and increases of the order of 10 cm resulting in a total decrease of 60 cm in the tuf and of 38 cm in the bedrock (Comments on water-levels variations can be found in DH, 1986a, b, 1988, 1989a, b, 1990a).

The short term variations corresponding to pressure heads losses during pumpings are registered with amplitudes of 0.01 m to 0.07 m in the intermediate well and of 0.01 m to 0.11 m in the deep well.

In the aim to calculate the effect of the water-levels variations on gravity (mainly on the superconducting gravimeter registrations at the ROB), we have to estimate the land subsidence (cf chapter 2) and the gravitational effect (cf chapter 3). We call these two effects the "hydrogeological perturbing effect".

CHAPTER 2. LAND SUBSIDENCE

1. Introduction

The land subsidence due to ground-water, oil and gaz withdrawal is a well known phenomenon. Observed subsidences in the San Joaquin Valley (for instance Lofgren, 1975, Bull & Poland, 1975, Poland et al., 1975, etc.), above the gaz reservoir at Groningen (Geertsma, 1973) and in the Venetian lagoon (Gambolati & Freeze, 1973) are largely reported.

The water-levels fluctuations are modifying the effective stress in the strata; those effective stress changes are resulting in the beds deformation.

Various types of compression are involved, mainly elastic or instantaneous compression of elastic media (such as a sand aquifer) and non elastic or plastic deformation (of beds of clay in or adjacent to the aquifer); the clay bed settlement is depending on the time and it is described by the consolidation theory.

In aquifers and aquitards (porous or fissured media), we have to deal with the poro-elasticity equations (Biot, 1941, 1955, 1956) of which the resolution leads to the land displacement.

To calculate the total effect of several water-levels of an aquifer system and in the aim to estimate hydrogeological perturbing effect at other stations than at the ROB, we preliminarily analyse each kind of the following phenomena :

- the land displacement induced by water-table variations.
- the land displacement due to the pressure head changes in a confined aquifer.
- the consolidation of an aquitard.

We study the land subsidence in a multi-aquifer-aquitard system by the combined problem.

The mean vertical gradient of the gravity (Melchior, 1971)

$$\Delta g \approx - 3.086 \ \mu\text{Gal. cm}^{-1}, \tag{2.1}$$

allows, from the total land displacement, to calculate the total effect of the water-levels variations on the superconducting gravimeter registrations.

Most of reports on the land surface change describe the land surface response to declines of the water-levels. In this larger study, we have also to consider the opposite phenomenon, i.e. the response to the rises of the water-levels too.

2. Definitions of the storage coefficient (S) and of the specific storage (S_c)

The storage coefficient S and the specific storage S_s of an aquifer are hydrogeological parameters that allow to connect Earth tides to hydrogeology.
It must be noticed that in hydrogeology, various definitions are used for S and for S_s. We have chosen for S_s the expression :

$$S_s = \rho g \ (\alpha + \emptyset_o \ \beta), \qquad (2.2)$$

in which ρ , α, β and $\emptyset_o$ are respectively the fluid volumic mass, the skeleton aquifer vertical compressibility, the fluid compressibility and the volume porosity of the layer. In (2.2) , it is assumed that the solid grains are incompressible so that volume changes of the formation are taken as equal to changes of the pore volume. If the compressibility of the solids α_g ($M^{-1}LT^2$) is not neglected, the specific storage $S_s{}^c$ is defined as :

$$S_s{}^c = \rho g \ \left\{(\alpha_b - \alpha_g) \left[1 - \frac{2(\alpha_b - \alpha_g)(1-2 \ \nu_p)}{3 \ \alpha_b \ (1- \nu_p)} \right] + \emptyset_o \ (\beta - \alpha_g)\right\}, \qquad (2.3)$$

derived from the generalized stress law (cf.(2.6)) of Biot-Willis-Nur-Byerlee (1971) and from the general three dimensional equations for the interaction of stress and fluid pressures in a homogeneous porous medium by Van der Kamp & Gale (1983); α_b is the bulk compressibility ($M^{-1}LT^2$) and ν_p is the Poisson's coefficient.
It is evident that if the compressibility of the solid grains α_g is neglected in (2.3), this latter equation becomes simplified in (2.2).

For the storage coefficient S of a confined aquifer with thickness b, we choose

$$S = S_s b \qquad (2.4)$$

The S_s dimensions are L^{-1} , S has no dimension. Several arguments justify our choices of S_s and S definitions (DH 88).

3. Effective stress law

In a porous medium of two phases, fluid-solid, as aquifers or aquitards, the Terzaghi's law (1925) states that the total stress σ , total of the effective stress σ_z borne by the skeleton and of the fluid pressure p, is constant :

$$\sigma = \sigma_z + p \tag{2.5}$$

For instance, for a constant total stress, a decline in the fluid pressure increases the effective stress of the aquifer skeleton and that results in a reservoir compaction.

The Terzaghi's law is generalized for a fissured rock in the expression of Biot-Willis-Nur-Byerlee (1971), firstly suggested by Geertsma (1957) and Skempton (1961) who adjusted Biot's equations to convenient experimental procedures for the determination of the deformation constants and adapted Biot's theory to various types of reservoir rock :

$$\sigma_{ij} = \sigma_{ij} - \zeta p \, \delta_{ij} \tag{2.6}$$

σ_{ij} are the effective stress tensor components,

σ_{ij} the components of the total stress tensor and the fluid pressure.

ζ is a constant defined by

$$\zeta = 1 - K_b \, \alpha_g \tag{2.7}$$

{K_b is the bulk modulus ($ML^{-1}T^{-2}$) and α_g the grain compressibility ($M^{-1}LT^2$)}.
If α_g is neglected, the law (2.6) becomes simplified in the Terzaghi's law (2.5). Gar & Nur (1973) present a discussion of the validity of the law (2.6) demonstrated for small deformations. Their considerations are based on the "TINC" (Theory of Interacting Continua) that uses developments in series of K_b, α_g, ...; that theory is introduced by Morland (1972) who deduces expressions describing the well response to a tidal force; we shall meet Morland's expressions in the study on the Earth tides in the wells, in the chapter 5.
The generalized form (2.6) allows to define the specific storage $S_s{}^c$ (cf (2.3)) for a medium with compressible grains.

Any water table change has an effect on lower-zone applied stress (Bull & Poland, 1975, Martin & Louis, 1973). Mainly, as it can be seen on the σ_z - depth diagram of the figure 2.1, a decline from the initial water table z_i to the final water table z_F, increases the effective stress of ρ g (z_i - z_F), which is transmitted to the lower layers.

4. Vertical displacement induced by the water table variations

The vertical displacement induced by the water table variations can be considered as time-independent and thus instantaneous : soil compaction and expansion can be estimated with the same model.

The Terzaghi's expression (1925) allows to calculate the compaction ξ_z of a layer with thickness b, induced by the $\Delta\sigma_z$ variation in the effective stress σ_z :

$$\frac{\xi_z}{b} = \frac{1}{A^*,C^*} \ln \frac{\sigma_z + i_R^z \Delta\sigma_z}{\sigma_z} ; \qquad (2.8)$$

in (2.8) :

- i_R^z is the influence factor for a normal uniform load over a circular area with radius R (De Beer, 1949)

$$i_R^z = \left\{ 1 - \frac{1}{\left[\left[\frac{R}{r}\right]^2 + 1 \right]^{3/2}} \right\} \qquad (2.9)$$

- C* and A* are respectively the compaction constant and the expansion constant defined by (e.g. for C*)

$$C^* = \frac{d(\ln p)}{d\,\epsilon_v} \qquad (2.10)$$

(ϵ_v is the deformation)

(2.8) is also written as :

$$\frac{\xi_z}{b} = \frac{C_c}{1 + e} \log \frac{\sigma_z + i_R^z \;\Delta\sigma_z}{\sigma_z} , \qquad (2.11)$$

in which e is the void ratio, i.e. the ratio of the voids volume V_v to the solid volume V_s or :

$$e = \frac{V_v}{V_s}, \tag{2.12}$$

and C_c , compression index, is defined as

$$C_c = - \frac{de}{d(\log \sigma_z)} \tag{2.13}$$

For an infinite extent load, i_R^z is equal to 1 : (2.8) becomes :

$$\frac{\xi_z}{b} = \frac{1}{A^*, C^*} \ln \frac{\sigma_z + \Delta\sigma_z}{\sigma_z} \tag{2.14}$$

(2.14) is the classical Terzaghi's expression also used to calculate the compaction of a confined aquifer and the settlement (at the equilibrium) of an aquitard (see § 5 and 6).

5. Displacement induced by the fluid pressure variations in a confined aquifer.

5.1. The poro-elasticity

The decline of fluid pressure in connection with the withdrawal of fluid from an underground reservoir gives rise to change in volume of both reservoir fluids and reservoir rocks.

Terzaghi's treatment is restricted to the one-dimensional problem of the response of a soil under a constant load. A study was carried out by Biot who first extended the theory of deformations of porous materials (Biot, 1941) to the three-dimensional case and established the equations valid for any arbitrary load variable with time in an isotropic medium. Biot generalized this theory to an anisotropic medium (Biot, 1955, 1956), writing the well-known" poro-elasticity equations". Those equations link the fluid flow field to the stress field.

In an isotropic porous material, the four equations of the poro-elasticity lead to (Gambolati, 1972):

$$\frac{\partial p}{\partial t} = \frac{k_D}{\rho g(\alpha + \emptyset_o \beta)} \nabla^2 p, \tag{2.15}$$

in which ∇^2 is the Laplace's operator, p is the pressure head and k_D, the Darcy's coefficient.
The diffusion equation (2.15) describes the piezometric decline resulting from depletion in the aquifer and also allows to study the subsidence problem. Gambolati & Freeze (1973) simplified the Biot's three-dimensional anisotropic equations by establishing the "pseudo-tridimensional" equation :

$$\frac{\partial h}{\partial t} = \frac{1}{\rho g(\alpha+\emptyset_o\beta)} \nabla . (K_{ij} \nabla h), \qquad (2.16)$$

in which h is the piezometric head or fluid potential in the aquifer.

5.2. Strain nucleus concept

The equation describing the interaction between the pore-pressure and the strain field can be solved making use of the concept of the "strain nucleus". Each volume element (fig 2.2) at a point Z (o,c) contributes to the potential at P in proportion to the fluid pressure prevailing at Z. The same applies to the potential gradients, i.e. the displacements $\bar{\xi}$. Therefore (Geertsma, 1973).

$$\bar{\xi} = \int_V p(Z) \; \xi^* \; (P,Z) \; d \; V \; (Z), \qquad (2.17)$$

where ξ^* represents the displacement at P resulting from a unit pressure at Z in volume element dV, forming there a "nucleus of strain". The function ξ^* can be considered as the Green function for the displacements. (A strain nucleus also named stress nucleus and tension center is then a cavity in which the pressure is varying).

5.3. The homogeneous elastic model (McCann and Wills, 1951)

<u>Hypotheses</u> : the subsoil is made to approximate a homogeneous, isotropic, semi-infinite elastic medium, delimited by a flat, free upper surface.

Starting from the equations of the theory of elasticity, Mc Cann & Wilts (1951) obtain the distribution of the displacements provoked in the medium by a unitary variation of radial tension acting at the boundary of a (spherical) cavity of unitary volume (tension center)

The vertical component of the displacement ξ^*_z in P (see fig 2.2) is

$$\xi^*_z = - \frac{3}{8} \frac{1+\nu_p}{\pi E} \left(\frac{c-z}{R_1^3} + \frac{z+3c-4\nu_p(z+c)}{R_2^3} + \frac{6z\,(z+c)^2}{R_2^5} \right) \qquad (2.18)$$

$$R_1 = \sqrt{r^2 + (c-z)^2} \quad (2.19)$$

$$R_2 = \sqrt{r^2 + (c+z)^2} \quad (2.20)$$

or

$$\overset{*}{\xi}_z = -\frac{3}{8}\,\frac{1+\nu_p}{\pi E}\, f\,(c,\ z,\ r,\ \nu_p), \quad (2.21)$$

with ν_p , the Poisson's coefficient, E the Young's modulus ; we also write (2.21) as a function of the volume compressibility α_b (the inverse of the bulk modulus K_b):

$$\overset{*}{\xi}_z = -\frac{1+\nu_p}{8\pi\,(1-2\,\nu_p)}\,\alpha_b\ f\,(c,\ z,\ r,\ \nu_p) \quad (2.22)$$

5.4. The homogeneous poro-elastic model (Geertsma, 1966, 1973)

We shall see that the displacement expression in a poro-elastic medium only differs from the expression (2.20) for an elastic medium by a coefficient depending on the characteristics of the poro-elastic medium.

Hypotheses : the subsoil is made to approximate a homogeneous, isotropic, semi-infinite poro-elastic medium.

5.4.1. Displacement expression

The vertical component of the displacement (using the strain nucleus concept) for a unit volume and for a unit pressure variation in the nucleus, is (Geertsma, 1966) :

$$\overset{*}{\xi}_z = -\frac{1+\nu_p}{12\pi\,(1-\nu_p)}\,\alpha_b\ f\,(c,\ r,\ z,\ \nu_p), \quad (2.23)$$

in which f is defined by the expression (2.18) to (2.20). If we compare (2.22) with (2.23), we deduce the relation between the elastic and poro-elastic models :

$$\overset{*}{\xi}_z\ (\text{poro-elastic}) = \frac{2}{3}\,\frac{1-2\,\nu_p}{1-\nu_p}\,\overset{*}{\xi}_z\ (\text{elastic}) \quad (2.24)$$

5.4.2. Subsidence of disc-shaped reservoirs

It is a generalization of the theory written in the § 5.4.1.

The reservoir is in the form of a circular cylindrical volume (radius R) of small thickness b, at the depth c, in the horizontal plane, i.e. parallel to the free surface of the halfspace (see fig. 2.3.).

Application of equation (2.17) to a disc-shaped reservoir leads to a displacement field induced by a row of tension nuclei distributed around the circumference of the circle of radius * $(0 \le \rho^* \le R)$ situated at the plane z=c (fig 2.4.) :

$$\bar{\xi} = b \ \Delta p \int_0^R \int_0^{2\pi} \bar{\xi}^* \ (r, z, \rho^*, \varphi) \rho^* \ d\rho^* \ d\varphi \ ; \qquad (2.25)$$

$\bar{\xi}^*$ is the displacement per unit volume and pressure change and Δp is the fluid pressure variation described by the poro-elasticity equations (2.15). The integration over the angle φ (Nowacki, 1962) leads to the vertical component ξ_z (Geertsma, 1973), in terms of Hankel integrals (Eason et al., 1955).

The integrals are all of the type

$$I(a,b,d) = \int_0^\infty e^{-q\bar{\alpha}} \bar{\alpha}^d J_a(\bar{\alpha}R) J_b(\bar{\alpha}r) \, d\bar{\alpha}, \qquad (2.26)$$

$$(r > 0, \ R > 0)$$

in which a, b and d represent numerical values 0 and 1 and J_a, J_b are Bessel's functions of the first kind of the orders a, b.

For brevity's sake, the following shorthand

$$I_1 = I(1,1,0) \quad I_2 = I(1,1,1) \quad I_3 = I(1,0,0) \quad I_4 = I(1,0,1) \qquad (2.27)$$

The value of q is indicated by means of the notation $I_n^{(q)}$. With this notation, the vertical component of the displacement ξ_z can be written as

$$\xi_z = \frac{c_m R}{2} b \ \Delta p \left[- \epsilon \ I_3^{-\epsilon(z-c)} - (3 - 4\nu_p) \ I_3^{(z+c)} - 2z \ I_4^{(z+c)} \right], \qquad (2.28)$$

in which c_m is the uniaxial compaction coefficient defined from the generalized law of the effective stress (2.6)

$$c_m = \frac{(1-\beta^*)\ (1-2\ \nu_p)}{2\ \mu\ (1-\nu_p)} \qquad (2.29)$$

$$\beta^* = \frac{\alpha_g}{\alpha_b} = \alpha_g\ K_b \qquad (2.30)$$

$$\epsilon = -\ 1 \text{ for } z > c$$

$$\epsilon = +\ 1 \text{ for } z < c$$

The subsidence being the vertical displacement at $z = o$, obtained from equation (2.28) is :

$$\xi_z\ (r,o) = -\ 2\ c_m\ \ b\ \Delta\ p\ \ I_3^{(c)}\ \ (1\ -\ \nu_p) \qquad (2.31)$$

The surface subsidence above the centre of the disc-shaped depleted reservoir amounts to :

$$\xi_z\ (o,o) = -\ 2c_m\ b\ \Delta\ p\ \ (1-\nu_p) \left[1 - \frac{c/R}{[1 + (c/R)^2]^{½}} \right] (2.32)$$

5.4.3. Reservoir compaction

The reservoir compaction is found by considering the displacements ξ_z at $c \pm\ b/2$. Because b is usually < <c , a good approximation is that those two vertical components are

$$\xi_z\ (r,\ c\ \ \pm \frac{b}{2}) \sim \frac{c_m R}{2}\ \ b\ \ \Delta p\ \left[\pm\ I_3^{(b/2)} - (3-4\ \nu_p)\ I_3^{(2c)} - 2c\ I_4^{(2c)} \right] \qquad \begin{matrix}(2.33)\\(2.34)\end{matrix}$$

The reservoir compaction is the difference between these two values of ξ_z and obviously amounts to

$$t_R\ (r) \sim c_m\ R\ b\ \Delta p\ I_3^{(\frac{b}{2})} \qquad (2.35)$$

5.5. Terzaghi's expressions

The compaction (or the expansions) of the confined aquifer layer can be also estimated by applying the Terzaghi's expressions (2.8) for a normal uniform load distributed over a circular area or (2.14) for an infinite extent load.

6. Consolidation of the aquitards

6.1. One-dimensional consolidation equation

For the aquitards, the gradual compression as a consequence of the gradual transfer of imposed stress from pore water to mineral skeleton is called consolidation. We use the concept of consolidation developed by Terzaghi (1925), generally considered to be the beginning of soil mechanics and also by the more familiar hydrologic terminology according to Domenico & Mifflin (1965).

The one-dimensional consolidation equation is

$$\frac{\partial p_e}{\partial t} = \frac{k'_D}{\rho g(\alpha' + \emptyset'_o \beta)} \frac{\partial^2 p_e}{\partial z^2}, \qquad (2.36)$$

in which p_e is the pore-water pressure in excess of hydrostatic, k'_D, α', $\emptyset'_o$, β are the vertical permeability, the vertical compressibility, the volume porosity of the clay layer.
In a compressible confining layer (Domenico & Mifflin, 1965), the volume of water obtained from expansion of water is negligible compared with that obtained through a change in porosity. The descriptive differential equation (2.36) is then expressed:

$$\frac{\partial p_e}{\partial t} = \frac{k'_D}{\rho g\, \alpha'} \frac{\partial^2 p_e}{\partial z^2}, \qquad (2.37)$$

These equation is a "diffusion equation" : the dimension of the diffusion coefficient $k'_D/\rho g\alpha'$ is L^2T^{-1}. The application of the Terzaghi's (2.5) allows to demonstrate that the vertical flow in a semipervious element, assuming Darcy's law to be valid is verifying (Harr, 1966) :

$$\frac{\partial p_e}{\partial t} = \frac{1 + e}{a_v\, \rho\, g} \frac{\partial}{\partial z}\left(k'_D \frac{\partial p_e}{\partial z}\right), \qquad (2.38)$$

in which the coefficient of compressibility is defined as

$$a_v = - \frac{\partial e}{\partial z} \tag{2.39}$$

As consolidation proceeds, the parameters k'_D, e and a_v all are changing with time and may also vary with z; thus in general, (2.38) is written as

$$\frac{\partial Pe}{\partial t} = c_c\ (z,t)\ \frac{\partial^2 Pe}{\partial z^2} \tag{2.40}$$

If it is supposed that k'_D, e and a_v are constants, then

$$c_c = \frac{k'_D\ (1 + e)}{a_v\ \rho\ g}\ ; \tag{2.41}$$

c_c is called the coefficient of consolidation.

The equation (2.40) with c_c as a constant is Terzaghi's fundamental form of the governing differential equation of the consolidation process.
The dimension of c_c is also L^2T^{-1}, dimension of any diffusion coefficient.

By comparing (2.37) with (2.40), we deduce

$$c_c = \frac{k'_D}{\rho\ g\ \alpha'} \tag{2.42}$$

By analogy with the specific storage S_s defined for a confined aquifer, the specific storage S'_s for a confining layer is defined as (Domenico & Mifflin, 1965) : "the volume of water that a unit volume of confining layer releases from storage, owing to its compression when the average excess pressure with the unit volume undergoes a unit decline"; it is expressed as :

$$S'_s = \rho\ g\alpha' \tag{2.43}$$

The specific storage of confining layer is similar to the specific storage of an adjacent aquifer, differing only in that compressibility of water is neglected in the aquitard. S'_s is then also of L^{-1} dimension. If E'_c is the bulk modulus of compression, i.e.

$$\alpha' = \frac{1}{E'_c} \tag{2.44}$$

from (2.44) and (2.43), it can be deduced

$$S'_s = \frac{\rho g}{E'_c} \qquad (2.45)$$

We can also express S'_s, from (2.41), (2.42) and (2.43) as

$$S'_s = \frac{a_v \rho g}{1 + e} \qquad (2.46)$$

and, from (2.42) and (2.43), we write

$$S'_s = \frac{k'_D}{c_c} \qquad (2.47)$$

From (2.37) and (2.43), we deduce that, in a clay layer, the flow is governed by the equation

$$\frac{\partial p_e}{\partial t} = \frac{k'_D}{S'_s} \frac{\partial^2 p_e}{\partial z^2} \qquad (2.48)$$

By comparing (2.48) written for an aquitard with (2.15) written for an adjacent aquifer, we remark that the ratio k_D/S_s influences the response of a groundwater system to a pumping stress, in the same manner as the ratio k'_D/S'_s influences the response of excess pore water in a confining layer. For a confining layer, the time required for development of "cone of depression" due to vertical movement of water out of the layer, is more appropriately thought of as time required to achieve full consolidation.

6.2. Time rate of consolidation

The equation (2.40) is a diffusion equation : it can be solved by analogy with the heat flow theory. With (2.47) and (2.45), (2.40) is written as :

$$\frac{\partial p_e}{\partial t} = \frac{E'_c k'_D}{\rho g} \frac{\partial^2 p_e}{\partial z^2} \qquad (2.49)$$

This equation describes the shape of a family of curves (isochrones) showing the proportion of effective and neutral stresses in a confining bed from time $t = o$, when p_e begins declining, to time $t = \infty$, when steady - flow conditions are re-established. This parabolic equation is solved (Melchior, 1986) if one initial condition and one boundary condition are known. To

solve (2.49), Taylor (1948) assigned the boundary and initial values to the internal pressure within a consolidating mass and the external pressure within a consolidating mass and the external pressure at its upper and lower boundary (see Domenico & Mifflin, 1965).
The actual time for a given isochrone to be reached is a constant multiple of some dimensionless time factor F_t, with

$$F_t = \frac{k'_D \, E'_c \, t}{b^2_L \, \rho \, g}, \tag{2.50}$$

where b_L is the distance to a drainage face (fig. 2.5a, b, c)

For an interbedded clay stratum where drainage is possible from both an upper and lower surface, b_L equals $b'/2$ and :

$$F_t = \frac{4 \, c_c \, t}{b'^2} \tag{2.51}$$

(2.50) is also written, from (2.45) and (2.47)

$$F_t = \frac{c_c \, t}{b^2_L} \tag{2.52}$$

In single drainage, i.e, drainage from an upper or lower surface only, b_L is taken as the thickness of the compressible stratum and

$$F_t = \frac{c_c \, t}{b'^2} \tag{2.53}$$

The expression (2.51) and (2.53) are often attributed to Terzaghi & Peck (1948).

A rigorous mathematical solution (Harr, 1966) allows to calculate the "degree of consolidation", often determined by applying the method of finite difference and also using the table of Leonards (1962) that gives the percent consolidation of a clay layer that has occurred at the corresponding time factor. A mathematical study of the consolidation of a clay layer has been developed by Biot (1941) from the poro-elasticity theory.

6.3. Settlement of an interbedded clay layer induced by fluid pressure decline in adjacent aquifers.

The responses of a sandwiched clay layer to adjacent aquifer changes in pressure head can be calculated using the "effective-pressure area" according Domenico & Mifflin (1965) (fig 2.5a, b, c).
The final settlement at equilibrium for changes in aquifer pressures Δh_1 and Δh_2 , above and below the confining layer can be then estimated by

$$\xi'_z = S' \frac{\Delta h_1 + \Delta h_2}{2} \tag{2.54}$$

or

$$\xi'_z = S'_s \frac{\Delta h_1 + \Delta h_2}{2} b' \tag{2.55}$$

and also by the Terzaghi's expression (2.14).

For the clay strata at ROB, we use both Domenico & Mifflin's expressions and Terzaghi's expression that both lead to the same settlements values.

7. The combined problem

To develop a practical mathematical treatment of the subsidence problem, in a multiple aquifer-aquitard system, it is convenient to think of the subsidence process as resulting from two independent phenomena :

- the hydraulic response of the aquifer system to pumpage, i.e. the temporal and spatial head distributions in the aquifers (the groundwater problem).

- the compression of the aquifers and the aquitards due to changing head distributions in the aquifers (the consolidation problem).

Those two phenomena are "coupled". The pressure head distributions obtained from the groundwater problem are used as boundary conditions for the consolidation problem.

If h_i (i = 1,2) are the hydraulic heads in the adjacent aquifers, the flow in the aquifers is governed by the equations (Bredehoeft & Pinder, 1970) :

$$\frac{\partial h_i}{\partial t} + Q_i\ (x,y,t) = \frac{1}{S_i} \left[\frac{\partial}{\partial x} (T_{ix} \frac{\partial h_i}{\partial x}) + \frac{\partial}{\partial y} (T_{iy} \frac{\partial h_i}{\partial y}) \right] \tag{2.56}$$

in which S_i are the storage coefficients, $T_{ix,y}$, the main components of the transmissivity tensors in the directions x and y. The equations (2.56) are then coupled by the leakage terms Q_i ($[Q_i] = LT^{-1}$), that are, provided aquitard storage is neglected (Molz & Hornberger, 1974) :

$$Q_2\ (x,y,t) = \frac{-k'_D\ (h_2 - h_1)}{b'} = - Q_1\ (x,y,t) \tag{2.57}$$

The consolidation problem is described by (2.40).
However, it appears that in most situations involving small (less than 5%) strains and one-dimensional, vertical consolidation, the coupling effects can be ignored (Gambolati, 1973).
The formulation (2.63) and (2.64) can be extended to any number of aquifer-aquitard combinations.
Corapcioglu & Brutsaert (1977) propose a viscoelastic aquifer model to analyze and predict the subsidence; we cannot apply their theory at the ROB missing of the "viscoelastic system parameters".

8. Land displacement and effect on g induced by the three water-level variations at the ROB

To estimate the land surface displacement, we calculate the compaction and the expansion of each layer. We consider the effect of the effective stress variation transmitted to the underlayers.

We apply the theory developed by Gambolati (1973) about the deviations from the Theis'solution *; we conclude that the horizontal displacement may be neglected and that the Theis' solution is valid. Indeed, the consideration of the horizontal strain components results in a modification of the classical diffusion equation to which a further integro-differential term is added. This new equation is solved in a pumped artesian aquifer enclosed in a half space by an iterative finite element technique. The Gambolati's approach has shown that the drawdown deviation from the Theis' solution depends on the values of a parameter W , defined as the ratio between the average depth and the thickness of the aquifer. Especially if $W \geq 2$, the importance of the three-dimensional effect becomes negligible ; the Theis' solution is then valid. For the intermediate and the deepest aquifers at ROB:

* Theis' solution $\equiv \frac{\partial h}{\partial t} = \frac{T}{S} \nabla^2 h$, with $T = k_D\ b$, transmissivity and S, storage coefficient

- in the tuf, we find $W \approx 9.36$ and
- in the bedrock, $W \approx 4.88$

Thus, we admit that Theis' solution may be applied.

We study the *total effect of the three water-levels variations*: we choose the time intervals I_1 (from 85/01/01 to 85/06/30) and I_2 (from 86/06/01 to 86/10/31) during which the largest values of the water table variations were registered, i.e. a 0.07 m rise and a 0.10 m decline; during I_1, the heads in the tuf and in the bedrock respectively increased of 0.45 m and 0.86 m; during I_2, the pressure heads in the tuf and in the bedrock respectively declined of 0.23 m and of 0.35 m (DH, 1988).

In the data sets just now available (from 87/02/25 to 88/12/02, we choose the time intervals I_3 (from 87/09/29 to 88/04/25) and I_4 (from 88/04/25 to 88/11/04) during which the water table shows 0.16 m and 0.18 m rises; in the intermediate and deep aquifer the heads variations don't exceed 0.31 m. We also consider the interval I_5 from 88/11/04 to the end of the available data (DH, 1990b).

On account of the combined problem we have to study and on account of various kinds of water-levels variations that are registered, we classify the water-level variations according to their type (at short or long term) and according to the variations belong to the water table or to the intermediate or deep aquifers.

We also calculate the largest effect during one year : i.e. 0.07m rise in the water-table, 1.40 m increase in the tuf and 0.95m in the bedrock (see DH, 1988).

The settlements or expansions of the clay strata are calculated at the equilibrium; the effect of pumping is the effect induced by the pressure head decline before the recovery phase.

The short term variations corresponding to pressure heads losses during pumpings are registered with amplitudes of 0.01 m to 0.07 m in the intermediate well and of 0.01 m to 0.11 m in the deep well.

To apply all the theories we explained in this chapter, we have to know both the values of the effective stress and the values of elasticity parameters of the ROB layers.

We drawn up the effective stress diagram as a function of the depth, depending on the thickness and the unit weight of each layer (<u>see fig. 2.6</u>).

The Poisson's coefficient ν_p is determined by the Vesic's relation (1972)

$$\frac{\nu_p}{1-\nu_p} = 1 - \sin 1.2\,\hat{\emptyset} \qquad (2.58)$$

$\hat{\emptyset}$ is the internal friction angle.

The volume porosity is calculated from the void ratio by

$$e = \frac{\emptyset_o}{1 - \emptyset_o} \tag{2.59}$$

and

$$\frac{1 - \gamma_n/\gamma_k}{\gamma_n/\gamma_w - 1} = e \frac{\gamma_w}{\gamma_k} \tag{2.60}$$

γ_w, γ_k and γ_n are respectively the unit weights of the water ($\gamma_w = \rho_w g$) , of the material without void and of the layer n.

As we do not know neither the numerical values of the compaction constant C* or expansion constant A* or Young's modulus E_{young}, nor the specific storage S_s, and as the applied loads are weak (it must be noticed that the water table only shows variations of 7 to 18 cm), we have developed a method leading to the estimation of those parameters. A technical method of civil engineering is concerned. We comment some important points.

We first consider similar strata to those at the ROB. The Geotechnical Institute allowed us to use the data of the Brussels underground. An order of magnitude of the parameters values should be found; such a study has been made for each layer except for the bedrock. Let us summary some results.

. For the Brussels sand, for the sample "E/37, 6649/78/527, Annexes 1/1 à 14" (Geotechnical Institute), the constant C* equals 38.
We obtain from (2.14), a settlement induced by a 0.07 m water-level decline, i.e. by a ~ 687 Pa effective stress variation, that is $|\ z_j|$ = 0.35 mm; this compaction is too large compared e.g. with the settlement measured for the drawdown at Focant (0.1 mm induced by a 1 m drawdown) or to others settlements (De Beer et al., 1968), although the strata at the ROB are more compressible than the shales at Focant.
The compression test for the sample F1/49 , similar to the Ypresian clay, 4572/83/24, Annexes 1/1 to 1/3, A/1 to A/63 (Geotechnical Institute), results in C* = 20 and A* = 104; the value of C* leads to a compaction of 0.91 mm, also too large for a weak load.
The reports of the loading test at the laboratory allow to determine the consolidation coefficient c_c. We use the characteristics of the plot of compression dial reading versus the time for the F1/49 clay sample 83/13158 (in the Flanders clay) to apply the two classical procedures, i.e. the Casagrande method and the $\sqrt{t}$ Method. From the two curves (fig. 2.7 and 2.8) we draw for this sample, we obtain c_c = 8.6 10^{-7} m^2 s^{-1} and c_c = 6.7

10^{-7} m^2 s^{-1}. With the mean value 7.65 10^{-7} m^2 s^{-1}, from the Leonards' table and from (2.53), we obtain, a consolidation time equals 7.9 year, too long as a response of a clay stratum to a weak load.

The elasticity parameters values depend on the values of the applied loads. The applied loads at laboratory are larger than the observed loads corresponding to the water-levels variations (0.07 m of water equals a 687 Pa, but 10 to 60 MPa are applied in the test). Nevertheless a sample (20 mm height, 63 mm diameter) does not always show the properties of all the bed stratum : it is also well known that a sample loses its rheological memory ... Thus, the parameter values deduced from experimental test or from references values tables may not be used in our problem. We try another method : we fit the Hardin & Drhevich's expression (Holeyman, 1984) to the case of weak loads. This very long process (DH, 1988) to deduce the shear modulus μ also leads to too large consolidation time (c_c = 2.05 10^{-5} m^2 s^{-1} and t = 107 day).
This discussion leads us to adopt the Wallays' expression (Wallays, 1980)

$$(C^* - 25)\ \Delta\sigma_z = 45\ 000, \qquad (2.61)$$

with $\Delta\sigma_z$ in kPa, that, for weak loads, fixes the lowest value of C^* at the 1000 value ($C^* \geq 1000$ if $\Delta\sigma_z \leq 45.32$ kPa). We apply (2.61) to each bed except for the bedrock.
For the 0.07 m water table decline, we find a 0.00001343 m settlement. For the two confining beds at Brussels, that value 1000 leads to consolidation times and layers settlements that seems to be realistic i.e.

- For the Ypresian clay, t = 8.75108 10^6 F_t sec ; 95 % of the settlement are reached with F_t = 1.129 (from Leonard's table) then t ~ 11 day and 5 % are reached after t ~ 25 min.
- For the clay of Waterschei, b = 10.292 10^3 F_t sec ; 95 % of the settlement are reached when t ~ 3.23 hour and 5 % after t ~ 17.5 sec.

We are able to justify the choice of the expression (2.61); we shall see (chapter 5) that the value 1000 will be confirmed by the observed tides analyses and by the response of the water level to the atmospheric pressure variations.

Because the applied loads are weak, we admit that the compaction constant C^* equals the expansion constant A^*.

For the considered time intervals I_1 to I_5, and taking into account the compactions and expansions of each layer due to the *three water-levels variations*, the land surface displacements are given in table 2.1. The decomposition of the problem can be found in DH, 1988 and 1990b. The land surface displacements are very small but we have shown that they are largely varying when we calculate them taking into account the whole aquifer system or the water table only with effective stress variation transfer to the deep layers or neglecting that transfer (DH, 1990b).

Let us remember that the effect on g is obtained by using the mean vertical gravity gradient (2.1).

Except for the water table, we admit that the beds are of infinite extent; the water table is considered to be a circular aquifer with 1 km radius R; but applying the expression (2.8) with the influence factor, we find an effect of - 4.1 nanogal that equals the effect calculated if we consider the water table to be of infinite extent.

We used the Terzaghi's expression (2.14) and the Domenico & Mifflin's expression (2.54) to estimate the settlement (or the expansion) of the aquitards : the effects obtained by applying those theories are equal.

The effects of the pressure heads variations in the tuf and bedrock aquifers calculated according to the Geertsma's theory using the strain nucleus concept (§ 5.4.2) or by applying the Terzaghi's theory (§ 5.5) are also equal.

During the I_1 interval, all the compactions and expansions of each layer due to the three water-levels variations result in an expansion of 0.22 mm i.e. an effect on g of - 69.6 nanogal; during the I_2 interval, the effect equals + 50.7 nanogal (cf. table 2.1).

CHAPTER 3. ATTRACTION VARIATIONS INDUCED BY THE WATER-LEVELS VARIATIONS

1. Introduction

After having studied the land surface displacement effect, we are going to estimate the effect on gravity of the attraction variations induced by the variable water masses.

The fundamental principle of the gravitational attraction is that of the Bouguer's formula (§ 2) : we extend it to establish the expressions which allow to calculate the gravitational effect of the various kinds of layers : we consider an unconfined aquifer (§ 3), a confined aquifer (§ 6), a layer that is neither aquifer nor aquiclude (§ 4), an aquitard layer (§ 5) and the rigid bedrock (§ 7).

We firstly present the hypotheses we put to develop our study.

2. Bouguer's formula and hypotheses

2.1. Attraction of a thin circular slab

The attraction A of a thin circular slab (fig.3.1.) with radius R, with thickness ϵ_c and volumic mass ρ , on an unit mass, located at the distance c along the symmetry axis, is easily calculated by the Bouguer's formula (Melchior, 1971):

$$A = 2\pi\ G\ \rho\ \epsilon_c\ i_R \tag{3.1}$$

if we define the "influence factor i_R" as :

$$i_R = 1 - \frac{c}{\sqrt{R^2 + c^2}} \tag{3.2}$$

The influence factor is as a function of the radius R and of the distance c (called depth if the unit mass is located at the land surface).

A is maximum when i_R = 1 which corresponds to an infinite radius:

$$A = 2\pi\ G \rho\ \epsilon_c \tag{3.3}$$

To study the attraction effect induced by water-levels variations, we extent the expressions (3.1) to (3.3) and we put a set of hypotheses.

2.2. Hypotheses

2.2.1. Axial symmetry

The geometrical configuration at the ROB is such that we may consider an axial symmetry and apply the simplified expression (3.1) : it is then to be integrated over the whole thickness of the layer. A calculus we performed allows to show that a more rigorous solution such as that of a finite cylinder (proposed by Ducarme, 1974) is not necessary : indeed, if a 10 m thickness layer is subdivided into 10 cm thickness sub-layers, the variation of the influence factors from one sub-layer to another one is only of 10^{-9}.

2.2.2. Land surface displacement

We don't follow the hypothesis usually put by most of the authors studying the effect of the water-levels variations on the gravimeters registrations : they assume that no significant change in the station elevation has occurred (e.g. Lambert & Beaumont, 1977). We think that the attraction effect depends on the compressions and expansions of the various beds and on the total land surface displacement. We use the compressions and expansions values we calculated according to the theory we developed in the chapter 2.

2.2.3. Nature of the strata

We write attraction formulas for each kind of beds; indeed the boundary conditions for a confined flow differ from the unconfined flow boundary conditions; water table variations correspond to changes in the various hydrostatic "regimes" (occurences of phases) in the upper zone and lead consequently to attraction changes; in a confined aquifer, the water compressibility is to be taken into account while in an aquitard the water compressibility may be neglected.

2.2.4. Regimes in the upper unconfined aquifer

To estimate the gravitational effect induced by a small variation of the water table (e.g. 0.07 m water-level variation), we have to consider the three kinds of regimes defined according to the theory of the capillary pressure in porous media.

In a porous medium the theory of capillary pressure is the hydrostatics of two immiscible fluids or phases that can exist simultaneously.

Experimental investigations have shown (Versluys 1917, 1931) that there are three general types of occurence of one of the two phases, or regimes of saturation with that phase (Scheidegger, 1963).

- Saturation regime : the porous medium is completely saturated with one phase.

- Pendular regime: the porous medium has the lowest possible saturation with one phase. This phase occurs in the form of pendular bodies that do not touch each other so that there is no possibility of flow of that phase.

- Funicular regime : an intermediate saturation with both phases is exhibited by the porous medium. If the pendular bodies of the pendular regime expand through addition of the corresponding fluid, they eventually become so large that they touch each other and merge. The result is a continuous network of both phases across the porous medium. It is thus possible that simultaneous flow of both phases occurs along what must be very tortuous funicular paths.

In an unconfined aquifer, the zone above the water table is also divided into three zones corresponding to the three regimes, called "capillary zones" (De Beer, 1956, Grondmechanica, deel I). The saturated zone is the continuous capillary water zone or capillary fringe. Although some authors call the thickness of the capillary fringe and of the funicular zone, the capillary height, without noticing it (Zjoukovsky, 1920, Polubarinova-Kochina, 1962), we keep the individuality of the three zones :

- the <u>saturation zone</u>, rising up to the height h_c capillary fringe thickness.

- the part extending above that fringe is the zone in which the regime is <u>funicular</u>, with a thickness h_f and in which saturation pressure diminishes down to a minimum value in the <u>pendular</u> part with height h_p.

At the ROB, a small increase h_{WT} of the water table doesn't mean the change of the dry regime into a saturated regime as we could think it a priori : in fact, it is the replacing of a funicular zone part by a saturated regime and the replacing of a pendular zone part by a funicular regime (cf. <u>fig 3.2</u>).

The theories about water attraction usually don't take account of those three zones; e.g. according to Goodkind (1986) "an infinite slab of water in material of 10 % porosity produces an attraction of 4.2 μGal per meter of thickness": this assertion means that the gravitational effect is induced by a quite saturated soil slab taking the place of a quite dry soil slab. We think that those approximations are not available if the water-level variations are small variations (e.g. 0.07 m) such as in the upper well at the ROB.

It must be noticed that the regimes changes produced by water-level increase or decrease are not reversible phenomena (De Beer, 1954, 1956). Nevertheless, we consider the approximation of a linear reversible distribution of the soil moisture content as a function of the water height above the phreatic level : on account of the small effect calculated a posteriori on g, we think it is not necessary to consider a more complicated distribution.

2.2.5. Schematic configuration

We define the various notations and we deduce some expressions that will be introduced in our further theoretical developments. The geometrical schematic configuration of the set of strata can be seen on the figure 3.3 that also shows the initial state i (before change of the aquifer water-level) and the final state F (after change of the aquifer water-level).

$(b_j)_i$: thickness of the j^{th} layer at the initial state

$(b_j)_F$: thickness of the j^{th} layer at the final state

$|\xi_{zj}|$: expansion along z of the j^{th} layer

χ_j : unit expansion of the j^{th} layer

$$\chi_j = \frac{\xi_{zj}}{(b_j)_i} \qquad (3.4)$$

$$(b_j)_F = (b_j)_i + |\xi_{zj}|$$

$$= (b_j)_i + \chi_j\,(b_j)_i$$

$$(b_j)_F = (b_j)_i\,(1 + \chi_j) \qquad (3.5)$$

$(z_s)_{i,F}$: vertical coordinate of the land surface from the bed-rock, at the initial and final state.

n : number of layers

$(z_n)_{i,F}$: vertical coordinate of the top of the last layer (phreatic aquifer)

h_c : capillary water height, of saturation zone

h_f : funicular zone height

h_p : pendular zone height

$$(z_s)_i = (z_n)_i + (h_c)_i + (h_f)_i + (h_p)_i \qquad (3.6)$$
$$(z_s)_F = (z_n)_F + (h_c)_F + (h_f)_F + (h_p)_F$$

$$(z_n)_i = \sum_{j=1}^{n} (b_j)_i \qquad (3.7)$$

$$(z_n)_F = \sum_{j=1}^{n} (b_j)_i \ (1 + X_j) + \Delta h_{WT} \qquad (3.8)$$

$$(h_p)_F = (h_p)_i - \Delta h_{WT} \qquad (3.9)$$

$$(h_c)_F = (h_c)_i \qquad (3.10)$$

$$(h_f)_F = (h_f)_i \qquad (3.11)$$

The total expansion of the land surface $|\xi_z|$ is defined as

$$|\xi_z| = (z_s)_F - (z_s)_i \qquad (3.12)$$

By (3.4), (3.6) to (3.11), (3.12) finally becomes :

$$|\xi_z| = \sum_{j=1}^{n} |\xi_{zj}|, \qquad (3.13)$$

that is the sum of the expansion of all the strata.

2.2.6. Volumic mass

We establish the expressions of a stratum volumic mass also called density [ML^{-3}] at the initial state (ρ_i) and at the final state (ρ_F)

The unit weight γ [$ML^{-2}\ T^{-2}$] is defined as $\gamma = \rho g$. We use the notations:

γ_k = unit weight of material without voids
γ_w = unit weight of water

At the initial state (before expansion), the weight of a layer with section Ω, height b is

$$P = \Omega\ b\ [(1-\emptyset_o)\ \gamma_k + \emptyset_o\ \gamma_w] \qquad (3.14)$$

At the final state, after a soil expansion X, the water quantity in an unit section column has varied of :

$$b(1 + X) - (1 - \emptyset_o)\ b = b\ (\emptyset_o + X) \tag{3.15}$$

The final weight is then, by (3.14) and (3.15)

$$P + dP = \Omega b\ [1 - \emptyset_o)\ \gamma_k + (\emptyset_o + X)\ \gamma_w] \tag{3.16}$$

Since

$$\rho_i = (1 - \emptyset_o)\ \frac{\gamma_k}{g} + \emptyset_o\ \frac{\gamma_w}{g}\ , \tag{3.17}$$

we deduce from (3.14) and (3.16)

$$\rho_F = \frac{(1 - \emptyset_o)\ \dfrac{\gamma_k}{g} + \dfrac{\gamma_w}{g}\ (\emptyset_o + X)}{1 + X} \tag{3.18}$$

3. Unconfined aquifer contribution to attraction

We study the effect on g of an unconfined aquifer with infinite extent and also with a radius of 1 km to 3 km, like at ROB.

Since we keep the individuality of the three zones h_c, h_f, h_p, above the water table, we have to estimate the funicular and pendular zones contributions (§ 3.1) because the water contents in those zones can be modified. Moreover, in the saturated part with thickness b_n, although no density variation occurs, the soil expansion and the total displacement of all the layers induce an attraction variation : this contribution is studied in the § 3.2. We deduce the complete contribution of an unconfined aquifer in the § 3.3., i.e. *the contribution of the funicular, pendular and saturated zones.*

3.1. Contribution of the funicular and pendular layer

3.1.1. Layer of finite extent

For a linear distribution, the unit weight variation as a function of the height, with $\Delta h_{WT} < h_c$, is represented on the fig 3.4. We divide the funicular zone into m substrata with thickness $b_l = h_f/m \approx \Delta h_{WT}$ (fig 3.5).

z_l is the ordinate of the upper boundary of a substratum l.
b_l is the thickness of a substratum l.
γ_l is the unit weight of a substratum l.

At the initial state, the depth of a substratum is $(z_s)_i - (z_l - b_l/2)$, which means the depth at half-stratum. The final state is characterized by the replacing of the substratum l by the under-substratum l-1, with unit weight $\gamma_{l-1} > \gamma_l$.

With our notations, $(A_{f+p,l})_i$ is the attraction of the substratum l in the funicular and pendular zone at the initial state and $(A_{f+p,l})_F$ is the attraction of the substratum l at the final state. The contribution of the substratum l to the attraction is then

$$\Delta A_{f+p,l} = (A_{f+p,l})_F - (A_{f+p,l})_i \tag{3.19}$$

$$\Delta A_{f+p,l} = \frac{2\pi G}{g} \Delta h_{WT} \, (\gamma_{l-1} - \gamma_l) \, \{i_R^l\} \tag{3.20}$$

with $\{i_R^l\}$, the influence factor that is

$$\{i_R^l\} = \left\{ 1 - \frac{(z_s)_i - (z_l - \frac{b_l}{2})}{\sqrt{R^2 + [(z_s)_i - (z_l - \frac{b_l}{2})]^2}} \right\} \tag{3.21}$$

The complete contribution of the funicular and pendular zones is:

$$\Delta A_{f+p} = \frac{2\pi G}{g} \Delta h_{WT} \sum_{l=1}^{n} (\gamma_{l-1} - \gamma_l) \, \{i_R^l\} \tag{3.22}$$

3.1.2. Layer of infinite extent

If the aquifer is of infinite extent, we obtain :

$$\Delta A_{f+p} = \frac{2\pi G}{g} \Delta h_{WT} \sum_{l=1}^{m} (\gamma_{l-1} - \gamma_l) \qquad (3.23)$$

We draw the diagrams 3.4 and 3.5 with the values of all the parameters for the borehole at the ROB. We have first to evaluate the porosity {by using (2.59) and (2.60)}. We then determine the unit weight $_n$ in the capillary fringe h_c, we estimate the unit weight γ_p in the pendular zone h_p by taking into account the water content distribution suggested by De Beer (1949) and we deduce the unit weight γ_f in the funicular zone h_f. We obtain

$$\emptyset_o = 0.3939, \ \gamma_n = 19.613 \text{ kN m}^{-3}, \ \gamma_p = 16.534 \text{ kN m}^{-3}$$

The diagrams are drawn in the figure 3.6.

- If the aquifer is of infinite extent, applying (3.23), we obtain :

  . during the interval I_1, for a 0.07 m water table rise

$$\Delta A_{f+p} = + 921.446 \text{ nanogal} \qquad (3.24)$$

  . during the interval I_2, for a 0.10 m decline,

$$\Delta A_{f+p} = - 1316.351 \text{ nanogal}$$

- If the radius of the aquifer is R = 1 km, the attraction is obtained by calculating the expressions (3.20) and (3.21) for each substratum l (l = 1,12). The values of the influence factors $\{i_R^l\}$ and of the attractions $\Delta A_{f+p,l}$ are given in the table 3.1

The attraction variation effect is :

$$\begin{aligned} &. \text{ during } I_1 : \Delta A_{f+p} = 890.563 \text{ nanogal} \qquad (3.25)\\ &. \text{ during } I_2 : \Delta A_{f+p} = -1272.233 \text{ nanogal} \end{aligned}$$

We also calculate the contribution of an aquifer with radius R = 2 km, 3 km and 4 km (DH, 88). The contributions of all the strata are identical to the tenth of nanogal (cf table 3.2) : with respect to the actual precision of the gravimeter registrations, we can conclude that the differentiation of each of the substrata by the taking into account of their depth may be neglected.

3.2. Contribution of the saturated part of the unconfined aquifer

3.2.1. Approximation

We first suppose that Bouguer's formula (3.1) written for a thin stratum is valid for a finite thickness layer; we also suppose that the stratum j mass is concentrated at the half-stratum.

At the initial state, the attraction of the stratum j is :

$$(A_j)_i = 2\pi\, G\, \rho_i\, (b_j)_i\, \{i_R^j\}_i \qquad (3.26)$$

with ρ_i defined by (3.17) and $\{i_R^j\}$, influence factor of the stratum j defined as :

$$\{i_R^j\}_i = \left\{ 1 - \frac{(z_s)_i - (z_j - \frac{b_j}{2})}{\sqrt{R^2 + [(z_s)_i - (z_j - \frac{b_j}{2})]^2}} \right\} \qquad (3.27)$$

At the final state, ρ_F is defined by (3.18). Taking into account the displacements of all the strata, we obtain the expressions of the attraction of the stratum j, at the final state :

$$(A_j)_F = 2\pi\, G\, \left[(1 - \emptyset_o)\, \frac{\gamma_k}{g} + (\emptyset_o + \chi_j)\, \frac{\gamma_w}{g}\right] (b_j)_i\, \{i_R^j\}_F \qquad (3.28)$$

with $\{i_R^j\}_F$, defined as

$$\{i_R^j\}_F = \left\{1 - \frac{\sum_{j=1}^{n} b_j \chi_j + (z_s)_i - (z_j)_i + \frac{(b_j)_i}{2}(1 - \chi_j)}{\sqrt{R^2 + \left[\sum_{j=1}^{n} b_j \chi_j + (z_s)_i - (z_j)_i + \frac{(b_j)_i}{2}(1 - \chi_j)\right]^2}}\right\}$$

(3.29)

The contribution of the stratum j is then

$$\Delta A_j = (A_j)_F - (A_j)_i \tag{3.30}$$

with $(A_j)_F$ defined by (3.28) and (3.29) and $(A_j)_i$ defined by (3.26) and (3.27).

The saturated part of the unconfined aquifer at the ROB, if the water table rises of 0.07 m , has a contribution

$$\Delta A_6 = 0.532 \text{ nanogal} \tag{3.31}$$

3.2.2. Numerical integration

We calculate the contribution of the stratum by dividing it into m substrata l (l = 1, m) (cf fig 3.7) and by adding the contribution of each substratum.

The attraction of the substratum l belonging to the stratum j, at the initial state is :

$$(A_{j,\ l})_i = 2\pi\ G\ \rho_i\ \frac{(b_j)_i}{m}\ \{i_R^l\}_i \tag{3.32}$$

with

$$\{i_R^l\}_i = \{1 - \frac{(z_s)_i - \left[(z_j)_i - \dfrac{(m - 1 + \frac{1}{2})(b_j)_i}{m}\right]}{\sqrt{R^2 + \{(z_s)_i - \left[(z_j)_i - \dfrac{(m - 1 + \frac{1}{2})(b_j)_i}{m}\right]\}^2}}\}$$

(3.33)

and ρ_i defined by (3.17)

At the final state, taking into account the distances variations and the expansions, we obtain

$$(A_{j,\ l})_F = 2\pi\ G \left[(1 - \emptyset_o)\ \frac{\gamma_k}{g} + (\emptyset_o + X_j)\frac{\gamma_w}{g}\right] \frac{(b_j)_i}{m}\ \{i_R^l\}_F$$

(3.34)

with $\{i_R^l\}_F$ =

$$\{1 - \frac{\sum_{j=1}^{n} (b_j)_i\ X_j + (z_s)_i - (z_j)_i + \frac{(b_j)_i}{m}\ [m - 1 + ½\ (1 - X_j)]}{\sqrt{R^2 + \{\sum_{j=1}^{m}\ (b_j)_i\ X_j + (z_s)_i\ - (z_j)_i + \frac{(b_j)_i}{m}\ [m - 1 + ½\ (1 - X_j)]\}^2}}\}$$

(3.35)

The contribution of the substratum l (substratum of the stratum j) is obtained by

$$\Delta A_{j,l} = (A_{j,l})_F - (A_{j,l})_i \tag{3.36}$$

from (3.32), (3.33), (3.34) and (3.35)
The total attraction of the stratum j is

$$\Delta A_j = \sum_{l=1}^{m} \Delta A_{j,l} \tag{3.37}$$

We subdivide the saturated part of the unconfined aquifer with thickness ≈ 12.80 m in m substrata, with m varying from 2 to 100 and we calculate ΔA_j. With R = 1000 m, with m = 13, i.e. the thickness of each substratum equals 1 meter, the influence factors $\{i_R^l\}_i$ and $\{i_R^l\}_F$ only differ at 10^{-8}. We find for j = 6 and l = 12

$$\Delta A_{6,12} = 0.037600 \text{ nanogal.} \tag{3.38}$$

On the other hand, if we neglect the depth variation of the substratum l induced by the expansion, i.e. if we put

$$\{i_R^l\}_i = \{i_R^l\}_F, \tag{3.39}$$

we find a contribution

$$\Delta A_{6,12} = 0.041787 \text{ nanogal} \tag{3.40}$$

i.e. a difference of 10%; for the ROB unconfined aquifer, we conclude that we may neglect the depth variation of each substratum since that effect of variation is only of 4 10^{-3} nanogal, which has no significance.

Thus, the contribution of the substrata 1 can be calculated by applying (3.37), (3.32) and (3.34) but by considering the substrata depths to be constants, i.e. applying (3.39). The formulas are then :

$$A_{j,1} = 2\pi \; G \; (\chi_j \; \frac{\gamma_w}{g}) \; \frac{(b_j)_i}{m} \; \{i'_R\} \tag{3.41}$$

with

$$\{i'_R\} = \{1 - \frac{(z_s)_i - \left[(z_j)_i - \dfrac{(m - 1 + \frac{1}{2})(b_j)_i}{m}\right]}{\sqrt{R^2 + \{(z_s)_i - \left[(z_j)_i - \dfrac{(m - 1 + \frac{1}{2})(b_j)_i}{m}\right]\}^2}}\} \tag{3.42}$$

The total contribution ΔA_6 of the saturated part obtained by adding the partial contributions of the substrata is

$$\Delta A_6 = 0.540 \text{ nanogal} \tag{3.43}$$

It must be noticed that this result only differs of 8 10^{-3} nanogal from the contribution obtained by (3.31) without numerical integration.

For the borehole at ROB, we can conclude that the expression (3.1) established by Bouguer for a thin layer can be applied to a finite thickness layer. The expressions (3.41) and (3.42) we propose are the generalization of Bouguer's formula in which we take into account the land surface displacement and the expansions or compressions of the layers.

3.2.3. Unconfined aquifer of infinite extent

If R ⟶ ∞, the influence factors (3.27) and (3.29) approach 1 and the contribution becomes

$$\Delta A_j = 2\pi \; G \; \chi_j \; \frac{\gamma_w}{g} \; (b_j)_i \tag{3.44}$$

expression also obtained by adding the substrata 1 contributions calculated with (3.32) and (3.34). We obtain at the ROB

$$\Delta A_6 = 0.563 \text{ nanogal}, \tag{3.45}$$

i.e. $2\ 10^{-2}$ nanogal more than the contribution obtained by (3.43) with $R = 1000$ m. The difference between the contribution calculated for the saturated part considered to be infinite and the contribution calculated if $R = 1000$ m is not significant : at ROB, the approximation of an infinite extent of the saturated part of the upper aquifer is then sufficient.

3.3. Complete contribution of the unconfined aquifer

The complete contribution of the unconfined aquifer is obtained by adding the contribution of the funicular and pendular zone A_{f+p} and the contribution of the saturated part A_6. It is given in the table 3.2.

At the ROB, the attraction contribution of the unconfined aquifer, if the radius equals 1 km, during the I_1 time interval equals 891.103 nanogal and - 1273.004 nanogal during the I_2 time interval. We must notice that the contribution calculated according to our method is 20 % smaller than the effect usually estimated by other authors applying the classical Bouguer's expression (3.1) without taking into account the three zones. We can remark that the saturated part only has a very weak contribution, as we are going to see it for the other underlayers.

4. Contribution of the saturated (neither aquifer nor aquitard)

The water table variations induce expansions or compressions of each underlayer by transfer of the effective stress variation. At the ROB, we obtain, during I_1, a contribution of the Forest sand bed by applying (3.44)

$$\Delta A_5 = 0.628 \text{ nanogal} \tag{3.46}$$

5. Contribution of a confining aquitard layer

We can apply the expressions of the § 2 to estimate the attraction effect of an aquitard that responds to :

- the water table variations,
- the pressure heads variations in the adjacent aquifers that are the boundary conditions. The various contributions are given in the table 3.3 obtained by (3.44).
  At long term, the various contributions only reach an amplitude of the nanogal.

6. Contribution of a confined aquifer layer

6.1. Finite extent aquifer

The process to establish the various formulas is identical to that developed in the § 3.2 but an additional contribution appears due to the water compressibility (that compressibility β is taken into account in the storage coefficient and the specific storage defined for a confined aquifer).

For a stratum j, divided into m substrata 1, we write the expressions of :

- the attraction of the substratum 1, at the initial state

$$(A_{j,1})_i = 2\pi G \frac{(b_j)_i}{m} \rho_i \{i_R^1\}_i \tag{3.47}$$

with $\{i_R^1\}_i$ defined by (3.32) and ρ_i defined by (3.17)

- the attraction of the substratum 1, at the final state

$$(A_{j,1})_F = 2\pi G \frac{(b_j)_i}{m} \{(1 - \emptyset_o) \frac{\gamma_k}{g} + (\emptyset_o + X_j) \frac{\gamma_w}{g} + \Delta\rho_w (1 + X_j)\} \{i_R^1\}_F \tag{3.48a}$$

with $\{i_R^1\}_F$ defined by (3.35) and $\Delta\rho_w = \rho^2_w \beta g \Delta h$. (3.48b)

The contribution of the substratum 1 is then

$$\Delta A_{j,1} = (A_{j,1})_F - (A_{j,1})_i \tag{3.49}$$

The complete contribution of the confined layer j is obtained by

$$\Delta A_j = \sum_{1=1}^{m} \Delta A_{j,1} \tag{3.50}$$

6.2. Infinite extent aquifer

The contribution to the attraction of the aquifer layer is obtained from (3.50), in which $R \rightarrow \infty$:

$$\Delta A_j = 2\pi \; G \; (b_j)_i \; [\, \chi_j \frac{\gamma_w}{g} + \Delta \rho_w \; (1 + \chi_j)] \qquad (3.51)$$

At the ROB, we calculate the attraction contributions for $j = 3$ and $j = 1$, for the tuf and for the bedrock aquifers (see table 3.3). The numerical results show that the effect of the water compressibility in the intermediate aquifer ($j = 3$) represents 57 % of the expansion effect. In the bedrock aquifer, the water compressibility is six times larger than those induced by the expansion of the bed. That water compressibility effect can not be neglected. But the total effect is nevertheless very weak (nanogal or tenth of nanogal).
The maximum amplitude pumping (- 0.07 m) in the tuf aquifer induces an effect

$$\Delta A_3 = - 0.396 \text{ nanogal},$$

and in the bedrock aquifer, the largest pumping only induces

$$\Delta A_1 = - 0.658 \text{ nanogal}$$

7. Contribution of the rigid part of the bedrock

At the ROB, the rigid bedrock part can be considered to be of infinite extent and thus it doesn't contribute to the attraction effect. However, if a bedrock is of finite dimension, it will contribute to the attraction on account of its depth variations resulting from the expansions and compressions of the overlying beds. In order to verify the amplitude of that gravitational effect, we deduce expressions allowing to calculate that effect and we perform some numerical estimations.

The depth variation c_s (at half-stratum) of a substratum s with radius R, thickness b_s (with $\Sigma \, b_s = b_j$ and $j = o$ which corresponds to the bedrock part that insn't aquifer) (cf. fig. 3.8) induces an attraction contribution given by :

$$\Delta A_j = 2\pi \; G \; \rho_j \; b_s \; [\{i_R^s\}_F - \{i_R^s\}_i] \qquad (3.52)$$

with

$$\{i_R^s\}_i = \{ 1 - \frac{c_s}{\sqrt{R^2 + c_s{}^2}} \} \qquad (3.53)$$

and

$$\{i_R^s\}_F = \{ 1 - \frac{c_s + |\xi_z|}{\sqrt{R^2 + (c_s + |\xi_z|)^2}} \} \qquad (3.54)$$

From our numerical estimations (DH, 88), we conclude that the contributions are weak. For instance, down to 500 m depth and with R = 10 km, the effect equals 10^{-2} to 10^{-1} nanogal. We must however notice that the bedrock contribution is opposed to the contribution of the other layers.

8. Total attraction variation effects.

The attraction variations effects for the time intervals I_i ($i = 1,5$) are given in the table 4.1 and 4.2 (next chapter). We calculate them by considering :

- (1) the set of the three aquifers and the responses of all the underlayers to water table and pressure heads variations (i.e. in the whole aquifer system).
- (2) the water table variations only and the transfer of the effective stress variations due to those variations to each underlayer.
- (3) the water table variations only.

The results deduced according to (1), (2) and (3) are similar. Except for the contribution of the water table variations which is the main perturbing effect, the contribution of the other underlayers are indeed very small.

9. Conclusion

We proposed a method to estimate the attraction variation effect induced by water-levels variations of various kinds of aquifers (unconfined and confined ones) taking into account all the underlayers, the displacement of the land surface, the expansions and compressions of each layer and the various regimes in the aquifers. Our formulas are refinements with respect to the other authors who only calculate the attraction effect of any infinite saturated layer. We think those refinements are needed on account of the precision of the gravimeter registrations.

CHAPTER 4. THE TOTAL EFFECT ON GRAVITY OF THE WATER-LEVELS VARIATIONS

The "hydrogeological perturbing effects" (land surface displacement and attraction variations effects) during the time intervals I_i (i = 1,5) are given in the tables 4.1 and 4.2, obtained taking into account all the layers of the aquifer system (1), the water table variations including their transfer to the underlayers (2) and the water table variations only (3).

The largest pressure heads declines during pumping in the intermediate well (-0.07 m) and in the deep well (-0.11 m) induce 4.602 nanogal and 1.184 nanogal respectively.

By using the tidal water-level responses models we show that the tidal oscillations induce less than 0.3 nanogal (DH, 1988).

The water-levels variations in the intermediate and deep aquifers (at long term, at short term and tidal ones) are only inducing negligible perturbing effects on the superconducting gravimeter registrations but the effect of the water table drift is at the limit of the actual precision of the superconducting gravimeter registrations.

CHAPTER 5. EARTH TIDES IN THE WELLS

1. Introduction

We study the barometric responses and the tidal responses of the water-levels. We use those responses to estimate the in situ parameters of the layers.

2. Barometric responses at short term

The figure 5.1 displays the response of the three wells to a sudden atmospheric pressure decrease with a 4.7 mbar amplitude, recorded during a thunderstorm (July, the 11th 1984). We observed :

- a 48 mm increase of the water table,
- a 9 mm pressure head increase in the intermediate well and
- a 19 mm pressure head increase in the deepest well.

Moreover, we notice that, at the ROB, the water table is instantaneously and faithfully reflecting the atmospheric pressure variations. This response differs from the water table barometric fluctuations described by Weeks (1979). In Brussels, the unconfined aquifer is a barometer : it can be seen on the figure 5.2.

On the other hand, the water-levels in the two confined aquifers are responding with atmospheric signal disturbances and with lags of about 1.5 h and 0.6 h, respectively in the tuf and in the bedrock.

. Water table response

We write the barometric water table response db_{wt} as (see figures 5.3a and 5.3b).

$$db_{wt} = - \frac{b_{wt}}{\emptyset_o} \epsilon_{pa} , \qquad (5.1)$$

in which b_{wt} is the unconfined aquifer thickness, $\emptyset_o$ the volume porosity and ϵ_{pa} the cubic dilatation of the aquifer induced by the d_{pa} atmospheric pressure variation.
(5.1) shows that the water table variation is larger with a thicker aquifer and a smaller porosity.
Since the atmospheric loading is vertical, we can write

$$|\epsilon_{pa}| = \frac{|\xi_z|}{b_{wt}} , \qquad (5.2)$$

with $|\xi_z|$, the compaction (or the expansion) of the aquifer. For an uniform circular load, $|\xi_z|$ may be calculated by applying the Egorov's theory (1958); if we introduce the Young modulus E_{young} and the Poisson coefficient ν_p, we obtain:

$$|\xi_z| = \frac{2\ R\ dp_a\ (1-\nu^2{}_p)}{E_{young}} \qquad (5.3)$$

We introduce for E_{young} 574 MPa (5.4), value we deduce from the value 1000 of C* or A* we have retained for weak loadings (cf chapter 2). From Warburton & Goodkind (1978), the waves frequencies in atmospheric pressure cells are depending on the extent of those air masses. Applying their conclusions, we estimate that the atmospheric perturbation radius R is between 10 and 15 km. With d_{pa} = 4.7 mbar, R = 12.5 km, ν_p = 0.27 and $\emptyset_o$ = 0.3939 (DH 88), we calculate the water table increase :

$$|db_{wt}|_{calculated} = 48.2 \text{ mm}, \qquad (5.5)$$

which is corresponding with the observed value of 48 mm.
This result means that the E_{young} value (5.4) is realistic: this confirms the approaches we followed to estimate the layer parameters by using soil mechanics considerations (chapter 2). Thus, the water table response to the atmospheric pressure variations allows to determine the Young modulus (or another elasticity parameter), if the Poisson coefficient ν_p and the porosity $\emptyset_o$ are known.

. Intermediate and deep pressure heads responses
==

We use the observed barometric short term responses of the intermediate and deep water-levels (see figure 5.1) to deduce an approach of a rheological model for each of those two wells (DH 88). We consider the wells as Kelvin bodies (Melchior, 1972); the water-level h(t) in the well responds to the atmospheric pressure variation p_a (t) (with p_a (t) = 0 if t $\leq$ 0 and p_a (t)= p_a if t > 0) according to :

$$h(t) = h_M\ (1-e^{-t/T_r}) \qquad (5.6)$$

with h(t) = 0 if t = 0 , h(t) = h_M if t = ∞. T_r is the retardation time (Melchior, 1972).

The water-levels h(t) verify the following responses (h(t) in mm of water) :

$$h(t) = 9\ (1-e^{-t/1368}), \qquad (5.7)$$

in the tuf well-aquifer system and

$$h(t) = 18.6\ (1 - e^{-t/960}), \qquad (5.8)$$

in the bedrock well-aquifer system.

3. Barometric Efficiency (BE) and Tidal Efficiency (TE)

In hydrogeology, the Barometric Efficiency (BE) is traditionally defined by the following expressions (see figure 5.4):

$$BE = \frac{\rho g \, dH}{dp_a}, \qquad (5.9)$$

where dH is the water-level variation in the well and dp_a is the atmospheric pressure variation (e.g. Walton, 1970) and

$$BE = -\frac{1}{\dfrac{\alpha}{\emptyset_o \beta} + 1} \text{ (Jacob, 1950).} \qquad (5.10)$$

With the two confined aquifers parameters values that we have estimated on the basis of rock and soil mechanics (DH, 88), we calculate the theoretical barometric efficiencies $|BE|_{theor}$ defined by (5.10) and compare them with the observed values $|BE|_{obs}$: the results are given in the table 5.8. The observed values $|BE|_{obs}$ are in agreement with the theoretical values.

Introducing (5.10) into the expression (5.7), we obtain

$$\frac{-1}{BE} = \frac{S_s}{\emptyset_o \beta \rho g}, \qquad (5.11)$$

an expression which allows to express the barometric efficiency as a function of the specific storage S_s and of the porosity $\emptyset_o$. We use (5.11) to estimate the S_s and $\emptyset_o$ values from the barometric response and the well tides.

4. Earth tidal observations in the wells

4.1. Historical note

The first observations of periodic water-levels changes go back to antiquity : Pliny in his "Historia naturalis" and in his letter to Licinius described observed tides in some wells in Spain and in Italy.

Arago (1840) studied tides in the artesian wells. Grablowitz (1880) attributed the fluctuations to the dilatation produced by the tide.

Young (1913), Michelson & Gale (1919), Theis (1938), Robinson (1939), Lambert (1940), Pekeris (1940), ... reported on water-level fluctuations which were of a tidal nature...

Melchior & Gulinck (1956) and Melchior, Sterling & Wery (1964) discussed Earth tides in the wells at Turnhout and Basècles.

As the theoretical tidal dilatation is everywhere the same one, the water-level variation should have to be the same one too. This is in contradiction with the various observed amplitudes : the explanation, given by Bredehoeft (1967), is that the amplitudes depend on the aquifer parameters : it is the beginning of the connection of Earth tides to Hydrogeology. Since 1967, the reports on Earth tides in wells are always more numerous (Sterling & Smets, 1971, Robinson & Bell, 1971,...).

At the ROB continuously since 1984, we have the opportunity to study the tides in two aquifers in the same borehole.

4.2. Tides in the wells at the ROB

Periodic water-levels fluctuations are continuously recorded in the intermediate and the deepest wells. Moreover, the water table doesn't show any tidal oscillations. The figure 5.5 shows water-level registrations in the deep well. In that well, periodic oscillations of about 5 cm amplitude are registered while in the intermediate well, the amplitude of the water-level fluctuations is only of about 1 cm. These oscillations in the intermediate well and in the deep well are represented at the same scale on the figure 5.6.

5. Tidal analyses of the water-levels at the ROB

5.1. Experimental results

The hourly observations data, converted into the standard format (Ducarme, 1975, 1978) used by ICET, are smoothed to eliminate the pumpings . We use the classical Venedikov filters method (Venedikov, 1966 a, b) to separate the diurnal , semi-diurnal and ter-diurnal waves before we determine the amplitude and the phase of the main waves by the least squares method. We remove the barometric effects by using the impulse responses (cf table 1.1, chapter 1).

The tables 5.1a and 5.1b show the results of the tidal analysis performed for the water table, for the intermediate and deep wells, before and after having removed the barometric effect. The amplitudes and the mean square errors are expressed in mm. The results deduced from this complete set of data are similar to those deduced from the analyses previously performed on the three sets of data covering respectively one year, twenty and thirty four months (Delcourt-Honorez, 1986a,b, 1989a). We summarize them :

- The atmospheric pressure corrections drastically reduce the mean square errors of 30 %.

- No tidal oscillation is observed in the water table; in that water-level, S_2 has an atmospheric origin.

- The observed oscillations in the fluid pressure of the two confined aquifers are due to Earth tides phenomena, according to the two criteria proposed by Melchior (1956): the phases are about 180° and the amplitude ratios agree with the theoretical ones.

5.2. Stability of the amplitudes and phases

We test the stability of the results by subdividing the total data set in nine sub-sets, each covering a six months time interval. The tables 5.2 and 5.3 show for the two confined wells the amplitude and phase of the main tidal waves for the analyses performed after having applied the atmospheric pressure correction. The various waves are stable and show only a slight variation in amplitude and phase from a sub-set to another one. The amplitude ratios for the deep aquifer are very stable.

Seasonal variations

The equilibrium tidal theory predicts no seasonal variation of the various waves in the water-levels. Nevertheless, since a 54 months data set is now available, we look for seasonal variation as it is investigated by the meteorologists for the barometric tides.
Let us remember the conventional meteorological seasons (cf DH, 1986c), noted as D, E, J and Y, which are respectively defined as :

D - months : November - December - January - February
E - months : March - April - September - October (centered on the Equinoxes)
J - months : May - June - July - August
Y - a whole year.

To determine the seasonal variations, we subdivide the whole data set into sub-sets covering those conventional seasons. It conducts to average each of the following waves : M_2, N_2, O_1 and the S_2 K_2 and P_1 S_1 K_1 groups. The tables 5.4a and 5.4b show for the two confined wells the amplitude (in mm) and phase of those main tidal waves for the analyses performed before and after having applied the atmospheric pressure correction for the D - J - E seasons. For the yearly series, we only give in the tables 5.5a and 5.5b the results of the analyses performed after the barometric effect correction. The amplitudes ratios are also given in the tables 5.4a, b and 5.5a and b.
We also analyse the same conventional atmospheric pressure data sub-sets and for the same time interval as the registrations of the water-levels (i.e. from 84/06/01 to 88/12/02); indeed some seasonal variations have been detected in Brussels (DH, 1986c). The results are given in the table 5.6 with the classical notation M_2 used in Earth tides analysis instead of the L_2 as noted by the meteorologists.

In the intermediate well, the barometric effect correction is the largest on the M_2, N_2 and O_1 waves during the D - season : that corresponds to the maximum amplitude of the atmospheric pressure variations during that season too. For those waves M_2, N_2 and O_1 we deduce a slight systematic variation in amplitude through the D - J -E seasons (see figure 5.7a) but S_2 K_2 and P_1 S1 K_1 don't vary in the same manner. The M_2 barometric wave shows the same variation in amplitude as the M_2 amplitude in the water-level.
In the water-level, the M_2 phase doesn't vary through the seasons but the phases of N_2, O_1, S_2 K_2 and P_1 S_1 K_1 show some variations (see figure 5.7b).
From the analyses performed on a yearly basis, we can also detect for the various waves small variations and thus in the amplitudes ratios too.

In the deepest well, the amplitude and phases are very stable. As for the intermediate well, we can also notice that the barometric effect correction is the greatest on M_2, N_2 and O_1 during the D - season during which those waves are the most perturbed.
The various waves and the amplitudes ratios are very stable from year to year.

At the ROB, the water-levels registrations are the most perturbed during the D - season i.e. in the winter. The registered noise seasonally varies, with a larger perturbing effect in the intermediate water-level than in the deep one : it is due to the smaller waves amplitudes detected in that intermediate well. According to our results, it is thus more convenient to get large amplitude tides in water-levels to be used for the aquifer parameters estimations. Nevertheless, at the ROB, for the intermediate water-level, we are studying the effect of this slight seasonal variations on the in situ parameters values: preliminary results show that the values lie in the same range of magnitude as that deduced from the whole data set.

5.3. Discussion of the amplitudes

In response to the Earth tides, the water-level variations in an unconfined aquifer is given by (Bredehoeft, 1967) :

$$dH = - \frac{\epsilon_t}{\phi_o} b_{wt} \qquad , \qquad (5.12)$$

in which ϵ_t is the cubic dilatation due to the Earth tide, b_{wt} is the unconfined aquifer thickness, and ϕ_o is the porosity.
To show a tidal response, the aquifer should thus be thick and of low porosity. In Brussels, with ϕ_o = 39 % and b_{wt} = 13.50 m, we calulate the water-level variation by (5.12); we obtain an undetectable variation

$$dH = - 3.43 \ 10^{-4} \ \text{mm}$$

From the results of the analyses in the table (5.1b), we can deduce that the amplitudes of the tidal waves are larger in the deepest well in the aquifer of the bedrock than in the intermediate well in the tuf of Lincent, what we had seen on the raw registrations. This is due to the elastic and hydrogeological properties of the two aquifer layers (the values of the parameters of these layers are summarized in the table 5.7). The porosity ϕ_o of the tuf of Lincent is of 33 % while the porosity of the bedrock is 9 % : these two different values explain the larger amplitude for the tides in the aquifer in the bedrock; indeed, according to e.g. Bredehoeft (1967), Morland et al. (1984), a decrease in the porosity value increases the amplitude. Moreover the bedrock permeability k_D (k_D = 4.44 10^{-5} ms^{-1}) is greater than the tuf permeability (k_D = 2.37 10^{-5} ms^{-1}): this also induces, according to Morland et al. (1984) a larger amplitude in the deep well.
On the other hand, Melchior et al. (1964) have concluded that an increase in the depth increases the amplitude, which is also confirmed with our observations.

To compare the amplitudes values with those in other stations, the M_2 wave amplitude is reduced to the equator (Melchior et al., 1964). For the intermediate well, we obtain 1.86 mm and for the deep well, 13.44 mm.
Compared to other stations (Melchior, 1983), these amplitudes seem to be somewhat low but, as we shall see, they are nevertheless justified by the specific storage S_s values (cf expression ((5.38),§ 7).

5.4. Discussion of the phase lags

A phase lag of about one hour (cf table 5.1b) is observed between the maximum of gravity and the maximum of the water-level in the wells. We study this "inelastic response" (cf § 7).

6. Tidal Efficiency

A Tidal Efficiency TE may be defined by

$$TE = \frac{\dfrac{\alpha}{\emptyset_o \beta}}{\dfrac{\alpha}{\emptyset_o \beta} + 1}, \qquad (5.13)$$

usually characterizing in hydrogeology (e.g. Jacob, 1950, Walton, 1970) the effect of rivers, lakes levels changes on the well but that expression is also valid for the elastic Earth tidal well response.

. The Tidal Efficiency TE and the Barometric Efficiency BE are thus related by the simple relation.

$$|BE| + |TE| = 1 . \qquad (5.14)$$

We calculate, for the two confined wells of the ROB, the theoretical tidal efficiency $|TE|_{theo}$ and also deduce $|TE|_{obs}$ from the observations (cf table 5.8).

The observed values of the Tidal Efficiency are in agreement with but lower than the theoretical values. This means that the waves amplitudes are attenuated.

7. Interpretation of the results of the analyses

7.1. Estimation of the permeability and the specific storage of the complex aquifer system

To explain the water-level responses in the intermediate and deep wells, we make some numerical explorations.

The observed phase lags of one hour (cf table 5.1b) associated with the amplitude attenuation show that an elastic theory doesn't perfectly describe the behaviour of the wells.

The phase lags cannot be ascribed to the "Nivocaps" transducers. The three transducers are indeed similar and in the upper water table well, the registrations don't show any phase lag. Experimental observations in laboratory demonstrate that the nivocap doesn't distort the signal (Van Ruymbeke and Delcourt, 1986).

. We apply the water-levels inelastic response theories to Earth tides usually called the "dynamic problem" in hydrogeology.

In response to a wave with a period $\tau_p = 2\pi/\omega$,the fluid pressure fluctuates according to the equation (cf <u>figure 5.8</u>).

$$p = \rho g\ (H + z) + p_o \sin \omega t \tag{5.15}$$

causing the water-level in the well to oscillate; this oscillation is

$$x_2 = x_o \sin\ (\omega t - \Phi)\ , \tag{5.16}$$

where Φ is the phase lag.

The amplification factor A, according to Cooper et al. (1965), afterwards referred as C 65, is to be: "the ratio of the amplitude of the oscillation of the water-level in the well x_o to the amplitude $h_o = p_o / \rho g$ of the pressure head fluctuation in the aquifer". Accordingly, we have

$$A = \frac{x_o}{h_o} \tag{5.17}$$

To deduce the expression of A, we need the following parameters (C 65):

- $$H_e = H + \frac{3}{8} b \tag{5.18}$$

  (H_e is the effective height of the water column)

- $$\alpha_w = r_w \left[\frac{\omega S}{T} \right]^{1/2} , \tag{5.19}$$

  in which r_w in the well radius, S is the storage coefficient defined by (5.8), **T** is the aquifer transmissibility defined by $T = k_D b$ (5.20)

- $$\omega_w = \left[\frac{g}{H_e} \left(1 - \frac{r_w^2 \omega}{2\ T} \text{kei}\ \alpha_w\right) \right]^{1/2} \tag{5.21}$$

-

$$\beta_w = \frac{r_w^2 \, g}{4\,\omega_w \, T \, H_e} \ker \alpha_w \qquad (5.22)$$

In (5.21) and (5.22) , ker and kei are the Kelvin functions, real and imaginary parts of K_o (α_w $i^{1/2}$) which is the modified Bessel function of the second kind of order zero.

The amplification factor is found to be

$$\frac{\rho\, g x o}{p_o} = A = [(1 - \frac{\pi \, r_w^2}{T \tau_p} \operatorname{kei} \alpha_w - \frac{4\pi^2 H_e}{\tau_p^2 g}) + (\frac{\pi r_w^2}{T \tau_p} \ker \alpha_w)^2]^{-1/2}$$

(5.23)

If the vertical oscillation of the well aquifer system is described by (cf figure 5.8).

$$x_1 = x'_o \sin \omega t, \qquad (5.24)$$

the water-level as recorded by an instrument moving with the land surface is then

$$x = x_2 - x_1, \qquad (5.25)$$

with x_2 and x_1 defined by (5.16) and (5.24).

The amplification factor A':

$$A' = \frac{x_o}{x'_o} \qquad (5.26)$$

is as a function of A, with

$$A' = \frac{4\pi^2 \, H_e}{\tau_p^2 \, g} \, A , \qquad (5.27)$$

We deduce the observed amplification for the water-level measure:

$$A_{observed} = A \, (1 - \frac{4\pi^2 H_e}{\tau_p^2 g}) \qquad (5.28)$$

The phase lag is

$$\Phi = \operatorname{Atan} \frac{2\beta_w \omega_w \omega}{\omega^2 - \omega_w^2} , \qquad (5.29)$$

in which ω_w and β_w are given by (5.21) and (5.22)

The expressions (5.23), (5.28) and (5.29) show that the water-level response in the well to a wave is depending on the wave period and on the well aquifer system parameters : well radius r_w and effective height of the water column H_e , transmissivity T and storage coefficient S of the aquifer.

For tidal waves periods, we deduce from (5.28)

$$A_{observed} = A = \frac{\rho g x_o}{p_o} = \frac{x_o}{h_o} \qquad (5.30)$$

This expression is verified by the numerical values given in the <u>table 5.9</u>. We may consequently calculate A by (5.23) only.
A and Φ are written in the <u>table 5.9</u>.
Thus, the calculated phase lags are not in agreement with the observed phase lags.

. We also apply the Morland and Donaldson's theory (1984); according to their study, we consider the parameter n_p given as

$$n_p = \frac{\bar{k}}{k_i} , \qquad (5.31)$$

in which k_i is the intrinsic permeability ($k_i = \frac{k_D \eta}{\rho g}$, with η , the dynamical viscosity) and with

$$\bar{k} = \frac{\eta \omega r_w^2}{\rho g b} . \qquad (5.32)$$

That parameter n_p is required to lie in an approximated range

$$0.04 \leq n_p \leq 0.2 \qquad (5.33)$$

to obtain a one centimeter amplitude and a greater than eleven degree phase lag.

The validity of the condition (5.33) is governed by a right combination of the aquifer parameters, the waves period and the radius of the well r_w. To verify it for the two wells we should have

- for the system "intermediate well - tuf of Lincent aquifer" :

$$0.27 \text{ m} \leq r_w \leq 0.60 \text{ m}$$

- for the system "deep well - bedrock aquifer" :

$$0.56 \text{ m} \leq r_w \leq 1.25 \text{ m}$$

Those two conditions are not realistic since the well radius value is 0.10 m.

We look for other factors to explain the amplitude attenuation and the phase lag : the inertial effect of the water in the aquifer and in the well and the "bore effective radius".

- The inertial effect of the water in the aquifer may be neglected if the condition (C 65)

$$\frac{r^2_w}{2b\emptyset_o} \ln \frac{r_i}{r_w} << H_e \qquad (5.34)$$

is verified ; r_i is the influence region radius.

- The inertial effect of the water in the well may be neglected if the condition (C 65)

$$x_o < \frac{\pi r^3_w g}{10 \text{ f } T \text{ } H_e} \text{ ker } \alpha_w \qquad (5.35)$$

is verified ; f is the pipe friction.

For the two confined wells of the ROB, the two conditions (5.34) and (5.35) are always verified (DH 88). Thus the inertial effect of the water in the aquifer and in the well are not responsible of the observed phase lags.

- We consider the effective radius effect in the following way : since, according to de Marsily (1981), "the well radius r_w is not well defined, it is admitted that it exists for the borehole a "bore effective radius (r_e)" that is to be taken into account for the water-level interpretations and that is somewhat greater than the true well radius r_w ". We calculate A by (5.23) and Φ by (5.29) for the two wells introducing in those expressions a set of r_e values larger and larger (cf table 5.10).
  To obtain a Φ value in agreement with the observed one, the required r_e values are (cf table 5.10)

- for the intermediate well, $r_e = 0.53$ m
- for the deep well, $r_e \geq 0.60$ m

These values are not realistic since, according to hydrogeological considerations the effective radius is only 0.06 m to 0.10 m greater than the true well radius value (Huisman, 1972). These unrealistic large r_e values are moreover in agreement with the unrealistic large radius values we deduced from the theory of Morland et al. (1984).

. According to a recent investigation performed by Hsieh et al. (1987), to determine the aquifer transmissivity from Earth tides analysis, the expression of the phase lag is:

$$\Phi = A \tan \frac{\dfrac{r^2_w}{2} \ker \alpha_w}{1 - \dfrac{\omega r^2_w}{2T} \operatorname{kei} \alpha_w} \qquad (5.36)$$

It also leads to a too low phase lag value which doesn't correspond to the observations.

All these theories are thus in good agreement with themselves but no theory allows to explain the observed phase lags.

Looking for the permeability k_D and specific storage S_s values that could explain the observed phase lags, we use the expression given by Gieske (1986) for the phase lag

$$\Phi \approx \operatorname{Atan} \frac{r^2_w \, K_o \left(r_w \sqrt{\dfrac{\omega S_s}{k_D}}\right)}{2b \, k_D} \qquad (5.37)$$

It must be noticed that for tidal waves, (5.37) is identical as (5.29) proposed by (C 65) but, we prefer the formulation (5.37) that is more suitable.
From (5.37) for diurnal and semi-diurnal waves, we solve the equations systems with the two k_D and S_s unknowns, for each aquifer.

- For the intermediate aquifer, the phase lags values (for M_2, $\Phi = 22°$ and for O_1, $\Phi = 13°$) lead to $k_D = 7.0 \; 10^{-8}$ ms^{-1} and $S_s = 1.96 \; 10^{-3}$ m^{-1} .

- For the deep well, we obtain with the observed phase lags values (for M_2, $\Phi = 29°$ and for O_1 $\Phi = 20°$), $k_D = 2.5 \; 10^{-8}$ ms^{-1} and $S_s = 3.70 \; 10^{-3}$ m^{-1}.

From these results, we deduce that:

- These high values determined for S_s ($\approx 10^{-3}m^{-1}$) show that a water volume larger than that separately contained in each aquifer can be restored. We think that this water is coming from the sandwiched clay layer between the two aquifers (see <u>figure 5.9</u>, the sandwiched clay layer is the clay of Waterschei).

- These values deduced for the permeability k_D ($\approx 10^{-8}$ ms^{-1}) are 1000 times lower than the values of k_D in the two aquifers (k_D = 2.47 10^{-5} ms^{-1} in the tuf and k_D = 4.44 10^{-5} ms^{-1} in the bedrock). The values of k_D are of the same order of magnitude as the value of k_D of the clay of Waterschei separating the two aquifers. (The deduced value for the deep well, k_D = 2.5 10^{-8} ms^{-1}, is nearly equal to the clay permeability value we used in the consolidation study on the site of the ROB, let be 2 10^{-8} ms^{-1}, DH 88). This physically means that the flux is slow and largely influenced by the clay properties. We so interprete the observed phase lags as reflecting the <u>total response of the whole aquifer system</u> involving the tuf aquifer, the clay of Waterschei and the bedrock aquifer : the two "confined aquifers" are indeed not independant but they are to be considered as "leaky aquifers", in a multiple aquifer-aquitard complex system. The water-levels responses in the two wells are depending on the vertical leakage in the aquitard, as shown by the required parameters values to explain the observed phase lags.

  This is the reason why we consider the permeability and specific storage determined from the equations systems (5.37) as the aquifer system global permeability $(k_D)_{syst}$ and the aquifer system global specific storage $(S_s)_{syst}$. The parameters had not been determined from tidal observations yet.
  The vertical leakages between each aquifer through the adjacent aquitard layer also attenuate the tidal amplitude and decrease the Tidal Efficiency.

7.2. Estimation of the porosity and the specific storage of the two aquifer layers.

To determine the porosity $\emptyset_o$ and the specific storage S_s in each aquifer, we use the water-level amplitude response to Earth tides assuming that it is elastic (this kind of response is called "the static problem" in hydrogeology). This may be justified by one of the conclusions derived by Morland et al. (1984) who showed that the porosity influences the amplitude only and doesn't influence the phase lag.

Various theories describing the elastic response connect the tides in the wells (tidal dilatation ϵ_t, water-level fluctuation dH or fluid pressure variation dp) to the aquifer parameters (specific storage S_s, porosity $\emptyset_o$).

We apply :

- The Brede hoeft's model (1967) in which dH is expressed as :

$$dH = - \frac{1}{S_s} \epsilon_t , \qquad (5.38)$$

in which ϵ_t is the tidal dilatation defined by Melchior (1983).

- the Narasihman and Kanehiro's procedure (1980,1984) that leads to

$$\frac{S_s}{\emptyset_o} = \rho g \beta \quad (1+ \frac{dp}{K_b \epsilon_t - dp}) , \qquad (5.39)$$

in which K_b is the bulk modulus.

For each aquifer, we deduce from the results of the tidal analysis (cf. table 5.1b) and from the water-levels barometric response also [cf (5.11)] , the ratio $S_s/\emptyset_o$ values and, separately, the S_s and $\emptyset_o$ values.

It must be noticed that the estimations of $S_s/\emptyset_o$ performed from the data set covering one year, from the data set covering twenty months, from the complete set of data (34 months) and from the five sub-sets each covering six months, lead to identical values.

The S_s values according to the various approaches are given in the table 5.11.

The values deduced according to Narasihman et al. (1980) differ more from the hydrogeological ones than those obtained by applying Bredehoeft's theory (1967). We see that the obtained value (3a) in the table 5.8 from Earth tidal observations is nearly equal to the value we estimated by the expression (5.7).
The S_s values are also in good agreement with those we had deduced by a personal research relative to weak loadings in soil and rock mechanics (DH 88). Since α , aquifer skeleton vertical compressibility, appears in the S_s expression (5.7) we can conclude that the analysis of the observed tides in wells allows to justify a posteriori the approaches we followed by using soil and rock mechanics considerations to estimate the layers elasticity parameters.

The combined water-level responses to the atmospheric pressure and to Earth tides allow to determine the porosity $\emptyset_o$ [according to (5.11) and (5.38)]. We obtain

- for the tuf, $\emptyset_o$ = 31 %
- for the bedrock, $\emptyset_o$ = 14 %

For the bedrock, the value is rather greater than that obtained by classical rock mechanics expressions (we obtained 9 %) but for the tuf the porosity value estimated in this way is quite realistic (33 % according to soil mechanics).

8. Conclusion

We showed that the study of water-levels barometric and tidal responses in wells leads to reliable estimation of the aquifer parameters and of the aquifer system parameters. The tidal research we developed validates a process to estimate in situ aquifer parameters differing from classical tests usually performed in hydrogeology.

Monitoring network of tidal water-levels registrations can be used to define the hydrogeological conditions at specific site e.g. during and after underground working but also at site for stocking toxic and nuclear waste products. The interpretation of the well-tidal variations in terms of physically significant parameters can be rightly applied to waste stocking areas because in situ hydrological conditions can be deduced by continuous monitoring in several boreholes at any widespread site during a long time.

Acknowledgements

We are greatly indebted to Professor J. Bouckaert, the director of the Belgian Geological Survey, Brussels, who incites and helps us to publish our study. Professor J. Bouckaert also allowed the borehole was drilled under the responsibility of the Belgian Geological Survey.

Thanks are to be addressed to Professor P. Melchior, the director of the Royal Observatory of Belgium, Brussels (where all our computations were performed), to have been the catalyst for calculating perturbing effect of water-levels on the superconducting gravimeter and for using water-levels as strainmeters.

We would like to thank Dr. P. Laga (Belgian Geological Survey) for answering all our questions on Geology and for his constant help he always gives us in Geology.

At the Royal Observatory of Belgium we thank Professor P. Pâquet and Dr. B. Ducarme for their constant support and comments during this research and Dr. M. Van Ruymbeke who devised the nivocap transducer.

We also thank Professor A. Delmer and ir. M. Wallays for the interviews on rock and soil mechanics. Thanks to the many people who provided data information, reviews and other assistance, especially ir. E. Smets (Hydraulic Laboratory) and Professor F. De Meyer (Royal Meteorological Institute).

REFERENCES

BIOT, M.A., 1941 : General theory of three-dimensional consolidation.
J. Appl. Phys., vol. 12, 155-164.

BIOT, M.A., 1955: Theory of elasticity and consolidation for a porous anisotropic solid.
J. Appl. Phys., vol. 26, n° 2, 182-185.

BIOT, M.A., 1956 : General solutions of the equations of elasticity and consolidation for a porous material.
J. Appl. Mechanics, vol. 23, 91-96.

BREDEHOEFT, J.D., 1967 : Response of well-aquifer systems to Earth tides.
Journal of Geophysical Research, vol. 72, 3075-3087.

BREDEHOEFT, J.D., & PINDER, G.F., 1970 : Digital analysis of areal flow in multiaquifer groundwater systems : a quasi three-dimensional model.
Water Resources Research, vol. 6, 883-888.

BULL, W.B. & POLAND, J.F., 1975 : Land subsidence due to groundwater withdrawal in the Los Banos-Kettleman City Area, California. Part 3.
Geological Survey Professional Paper, 437-G.

CASAGRANDE, A. & FADUM, R.E., 1940 : Notes on soil testing for engineering purposes.
Harvard Univ. Soil Mech. Ser. Bull, vol. 268, n° 8.

COOPER, H.H., Jr., BREDEHOEFT, J.D., PAPADOPOULOS, I.S. & BENNET, R.R., 1965 : The response of well-aquifer systems to seismic waves.
Journal of Geophysical Research, vol. 70, n° 16, 3915-3926.

CORAPCIOGLU, M.Y. & BRUTSAERT, W., 1977 : Viscoelastic aquifer model applied to subsidence due to pumping.
Water Resources Research, vol. 13, n° 3, 597-604.

DARCY, H., 1856 : Les fontaines publiques de la ville de Dijon.
V. Dalmont, Paris.

DAVIS, S.N. & De Wiest, R.J.M., 1966 : Hydrogeology.
John Wiley & Sons, Inc., New York-London-Sydney.

DE BEER, E.E., 1949 : Grondmechanica, Deel II.
Funderingen.
Standaard Boekhandel. Antwerpen-Brussel-Gent-Leuven.

DE BEER, E.E., 1954 : Grondmechanica, Deel III.
Het water in de grond.
Standaard Boekhandel. Antwerpen-Brussel-Gent-Leuven.

DE BEER, E.E., 1956 : Grondmechanica, Deel I.
Inleidende begrippen.
Standaard Boekhandel. Antwerpen-Brussel-Gent-Leuven.

DE BEER, E., DELMER, A. & WALLAYS, M., 1968 : Essais de charge en galerie et en surface avec plaques de grandes dimensions.
Symposium International de Mécanique des roches. Madrid, 13-33.

DELCOURT-HONOREZ, M., 1986 (a) : Earth tide response and barometric effect in three well-aquifer systems. The effect on gravity of the three water-level variations.
Proceedings of the 10th Int. Symp. on Earth Tides, Madrid (Ed. R. Vieira), 843-854.

DELCOURT-HONOREZ, M., 1986 (b): Lunar and solar barometric tides in seven stations of the trans world tidal gravity profile.
Bull. Inf. Marées Terr., n° 97, 6614-6627.

DELCOURT-HONOREZ, M., 1986 (c) : Twenty months water-levels registrations in three well-aquifer systems, on the site of the Royal Observatory of Belgium.
Bull. Inf. Marées Terr., n° 97, 6639-6648.

DELCOURT-HONOREZ, M., 1988 : Sur la contribution des variations de la pression atmosphérique et des fluctuations du niveau des nappes aquifères aux variations de la pesanteur.
Dissertation doctorale, Faculté des Sciences, Université Catholique de Louvain.

DELCOURT-HONOREZ, M., 1989 (a) : Determination of the in situ parameters from the observed tidal oscillations in the well-aquifer systems at the Royal Observatory of Belgium.
Bull. Inf. Marées Terr., n° 103, 7228-7255.

DELCOURT-HONOREZ, M., 1989 (b) : Water-levels registrations at the Royal Observatory of Belgium.
Communication personnelle. ORB, Oct. 1989.

DELCOURT-HONOREZ, M., 1990 (a, in press) : Water-levels fluctuations in a borehole at the Royal Observatory of Belgium : effect on local gravity, Earth-tidal and barometric responses.
Proceedings of the XIth Int. Symp. on Earth Tides, Helsinki.

DELCOURT-HONOREZ, M., 1990 (b, in press): Land surface displacement induced by water-level variations.
Proceedings of the International Workshop on GPS for Geodesy and Geodynamics, Walferdange, Luxemburg.

LAGA, P.& DELCOURT-HONOREZ, M., 1990 (in preparation): Water-level variations in the three wells of the borehole at the Royal Observatory of Belgium.
Professional Paper, Service Géologique de Belgique.

DE MEYER, F., 1982 : A Multi input single output model for Earth tide data.
Bull. Inf. Marées Terr., 88, 5628-5674.

DE WIEST, R.J.M., 1966: Geohydrology.
John Wiley & Sons, Inc. New York-London-Sydney.

DOMENICO, P.A. & MIFFLIN, M. D., 1965 : Water from low-permeability sediments and land subsidence.
Water Resources Research, vol. 1, n° 4, 563-576.

DUCARME, B., 1974 : La base gravimétrique du lion de Waterloo.
Ciel et Terre, vol. 90, n° 6, 455-476.

DUCARME, B., 1975 : The computational procedures at the International Centre for Earth Tides (ICET).
Bull. Inf. Marées Terr., 72, 4156-4181.

DUCARME, B., 1978 : Data standardization in tidal research.
Bull. Inf. Marées Terr., 78, 4712-4719.

EASON, G. et al., 1955 : On certain integrals of Lipschitz-Hankel type involving products of Bessel functions.
Phil. Trans. Roy. Soc. London, A 247.

EGOROV, K.E., 1958 : Concerning the question of calculations for base under foundations with footings in the form of rings.
Mekhanika Gruntov, Sb. Tr. n° 34, Gosstroüzdat, Moscow.

GAMBOLATI, G., 1972 : A three-dimensional model to compute land subsidence.
Bulletin of the Int. Ass. of Hydrol. Sci., vol. 17, 219-226.

GAMBOLATI, G. & FREEZE, A.R., 1973: Mathematical simulation of the subsidence of Venice.
Water Resources Research, vol. 9, n° 3, 721-732.

GAMBOLATI, G., 1973 : Deviations from the Theis solution in aquifers undergoing three-dimensional consolidation.
Water Resources Research, vol. 13, n° 1, 62-68.

GARG, S.K. & AMOS NUR, 1973 : Effective stress laws for fluid-saturated porous rock.
Journal of Geophysical Research, vol. 78, n° 26, 5911-5919.

GEERTSMA, J., 1957: The effect of fluid pressure decline on volumetric changes of porous rocks.
Trans. AIME, vol. 210, 331-340.

GEERTSMA, J., 1966 : Problems of rock mechanics in petroleum production engineering.
Proc. Congr. Int. Soc. Rock Mech. 1st, Lisbon, 585-594.

GEERTSMA, J., 1973: A basic theory of subsidence due to reservoir compaction : the homogeneous case.
Verhandelingen Kon. Ned. Geol. Mijnbouwk. Gen., vol. 28, 43-62.

GEERTSMA, J. & VAN OPSTAL, G., 1973 : A numerical technique for predicting subsidence above compacting reservoirs, based on the nucleus of strain concept.
Verhandelingen Kon. Ned. Geol. Mijnbouwk. Gen., vol. 28, 63-78.

GIESKE, A., 1986 : Phase shifts in the response of boreholes to tidal gravity variations.
Proceedings of the 10th Int. Symp. on Earth tides, Madrid (Ed. R. Vieira), 827-834.

GOODKIND, J.M., 1986 : Continuous measurement of nontidal variations in gravity.
Journal of Geophysical Research, vol. 91 n° B9, 9125-9134.

GRABLOVITZ, G., 1880 : Sul fenomeno di marea osservato nelle miniere di Dun in Bohemia.
Bull. Soc. Adriatica Sci. Naturali Trieste, 6, 34.

HARDIN, B.O. & DRNEVICH, V.P., 1972: Shear modulus and damping in soils: design equation and curves.
J. SMFD Proc. ASCE, Vol. 98, N° SM7, 667-692.

HARR, M.E., 1966 : Foundations of theoretical soil mechanics.
International Student Edition, McGraw-Hill Book Company, New-York.

HOLEYMAN, A., 1984 : Contribution à l'étude du comportement dynamique non-linéaire des pieux lors de leur battage.
Dissertation doctorale, Faculté des Sciences Appliquées, Service de Mécanique des Sols, Université Libre de Bruxelles.

HSIEH, P.A., BREDEHOEFT, J.D. & FARR, J.M. 1987 : Determination of Aquifer Transmissivity from Earth Tide Analysis.
Water Resources Research, vol. 23, n° 10, 1824-1832.

HUISMAN, L., 1972 : Groundwater recovery.

JACOB, C.E., 1950 : Flow of ground water.
Engineering Hydraulics (Ed. Hunter Rouse), John Wiley & Sons, New York.

LAMBERT, A. & BEAUMONT, C., 1977 : Nano variations in gravity due to seasonal groundwater movements : Implications for the gravitational detection of tectonic movements.
Journal of Geophysical Research, vol. 82, 297-306.

LEONARDS, G.A., 1962 : Foundation engineering.
McGraw-Hill Book Company. New York.

LOFGREN, B.E., 1975 : Land subsidence due to ground-water withdrawal, Arvin-Maricopa Area, California.
Geological Survey Professional Paper, Washington, 437-D.

de MARSILY, 1981: Hydrogéologie quantitative.
Masson.

MARTIN, P. & LOUIS, C., 1973 : Tassements consécutifs au rabattement de nappe.
Bulletin du B.R.G.M., Section III, n° 1, 3-34.

McCANN, G.D. & WILTS, C.M., 1951 : A mathematical analysis of the subsidence in the long beach-San Pedro area.
Rep. Calif. Inst. Technol., Pasadena, Calif.

MELCHIOR, P.J. & GULINCK,M,1956 : Sur l'effet des marées terrestres dans les variations de niveau observées dans les puits, en particulier au sondage de Turnhout.
Comm. de l'ORB, Série Géoph., n° 37.

MELCHIOR, P.J., 1960 : Die Gezeiten in Unterirdischen Flussigkerten.
Erdoel Kohle, 13, 312-317.

MELCHIOR, P.J., 1964 : Sur les diverses perturbations dans l'enregistrement des marées terrestres.
5e Symposium international sur les Marées Terrestres.
Comm. Obs. Belg. 236, Sér. Géoph. 69, 352-371.

MELCHIOR, P.J., STERLING, A. & WERY, A., 1964 : Effets de dilatations cubiques dues aux marées terrestres observés sous forme de variations de niveau dans un puits à Basècles (Hainaut).
Comm. de l'ORB, Série Géoph., n° 66.

MELCHIOR, P.J., 1971 : Physique et dynamique planétaires
Vol. 2 (cours de gravimétrie) Vander-Leuven-Bruxelles.

MELCHIOR, P.J., 1972 : Physique et dynamique planétaires.
Vol. 3 (cours de géodynamique), Vander-Leuven-Bruxelles.

MELCHIOR, P.J., 1973 : Physique et dynamique planétaires.
Vol. 4 (cours de géodynamique), Vander-Leuven-Bruxelles.

MELCHIOR, P.J., 1978, 1983 : The tides of the planet Earth.
Pergamon Press, Oxford.

MELCHIOR P.J., 1986 : The physics of the Earth's core.
Pergamon Press.

MOLZ, F.J. & HORNBERGER, G.M. 1974 : Digital simulation of regional land subsidence due to aquifer system pumpage.
Advances in Rock Mechanics, vol. II, part B, 1090-1095.

MORLAND, L.W., 1972 : A simple constitutive theory for a fluid-satured porous solid.
Journal of Geophys. Research, vol. 77, 890-900.

MORLAND, L.W. & DONALDSON, E.C., 1984 : Correlation of porosity and permeability of reservoirs with well oscillations induced by Earth tides.
Geophys. J.R. Astr. Soc., n° 79, 705-725.

NARASIMHAN, T.N. & KANEHIRO, B.Y., 1980 : A note on the meaning of storage coefficient.
Water Resources Research, vol. 16, n° 2, 423-429.

NARASIMHAN, T.N., KANEHIRO, B.Y. & WITHERSPOON, P.A., 1984 : Interpretation of Earth tide response of three deep, confined aquifers.
Journal of Geophysical Research, vol. 89, n° B 83, p. 1913-1924.

NOWACKI, W., 1962 : Thermoelasticity.
English Edition, 1962, 66-74.

NUR, A. & BYERLEE, J.D., 1971 : An exact effective stress law for elastic deformation of rock with fluids.
Journal of Geophysical Research, vol. 76, n° 26, 6414-6419.

POLAND, J.F. LOFGREN, B.E., IRELAND, R.L. & PUGH, R.G., 1975 : Land subsidence in the San Joaquin Valley, California.
Geological Survey Professional Paper, 437-H.

POLUBARINOVA-KOCHINA, P. Ya., 1962 : Theory of Ground Water Movement.
613 pp. Princeton University Press, Princeton, N.J.

ROBINSON, E.S. & BELL, Th. R., 1971 : Tides in confined well-aquifer systems.
Journal of Geophysical Research, vol. 76, n° 8, 1857-1869.

SCHEIDEGGER, A.E., 1963 : The physics of flow through porous media.
University of Toronto Press.

SKEMPTON, A.W. 1961 : Effective stress in soils, concrete and rock, in
Conference on pore pressure and suction in Soils, Butterworth, London, 4-16.

STERLING, A., 1964 : Fluctuations de niveau d'eau observées dans les puits.
Comm. de l'O.R.B., n° 236, Série Géoph., n° 69.

STERLING, A. & SMETS, E., 1971 : Study of Earth tides, earthquakes and terrestrial spectroscopy by analysis of the level fluctuations in a borehole at Heibaart - Belgium. Geophys. J.R., Astr. Soc., n° 23, 225-242.

STERLING, A. & SMETS, E., 1971 : Study of Earth tides by analysis of the level fluctuations in a borehole at Heibaart. Hydraulic Laboratory-Borgerhout-Antwerpen-Belgium, 1-19.

TAYLOR, D.W., 1948 : Fundamentals of soil mechanics. John Wiley & Sons, New York.

TERZAGHI, K., 1925 : Erdbaumechanick auf Bodenphysikalischer Grundlage. Franz Deuticke, Vienna.

TERZAGHI, K. & FROHLICH, O.K. 1936 : Theorie der Setzung von Tonschickten. Vienne, F. Deuticke.

TERZAGHI, K. & PECK, R.B. 1948: Soil mechanics in engineering practice. John Wiley & Sons, Inc., New York, 1948.

THEIS, C.V. 1935 : The relation between the lowering of the piezometric surface and the rate and duration of discharge of a well using groundwater storage. EOS Trans. AGU, vol. 16, 519-524.

THEIS, C.V., 1938 : The significance and nature of the cause of depression in ground water bodies. Econ. Geology, vol. 33, 889-902.

VAN DER KAMP, G. & GALE, J.E., 1983 : Theory of Earth tide and barometric effects in porous formations with compressible grains. Water Resources Research, vol. 19, n° 2, 538-544.

VAN RUYMBEKE, M. & DELCOURT, M., 1986 : A capacitive transducer for water-level measurements : "Nivocap". Proceedings of the 10th Int. Symp. on Earth Tides, Madrid (Ed. Vieira), 95-102.

VENEDIKOV, A.P., 1966 (a) : Une méthode pour l'analyse des marées terrestres à partir d'enregistrements de longueur arbitraire. Comm. de l'O.R.B., Série Géophys., n° 71, 437-469.

VENEDIKOV, A.P. 1966 (b) : Sur la constitution de filtres numériques pour le traitement des enregistrements des marées terrestres. Acad. R. Belg., Bull. Cl. 1 Sc. 5, (b), 827-845.

VERSLUYS, J., 1931 : Cité dans Scheidegger, A.E., 1963.

WALLAYS, M.V. 1980 : Design parameters in Geotechnical engineering.
British Geotechnical Society, London, 134-135.

WALTON, W.C., 1970 : Groundwater resource evaluation.
McGraw-Hill Series in Water Resources and Environmental Engineering. McGraw-Hill Book Company, New York.

WARBURTON, R.J. & GOODKIND, J.M. 1978 : Detailed gravity-tide spectrum between one and four cycles per day.
Geophys. J.R. astr. Soc., vol. 52, 117-136.

WEEKS, E.P., 1979 : Barometric fluctuations in wells tapping deep unconfined aquifers.
Water Resources Research, vol. 15, n° 5, 1167-1176.

UKKEL WELL 102W847

ROYAL OBSERVATORY OF BELGIUM (ROB)

Lithostratigraphy

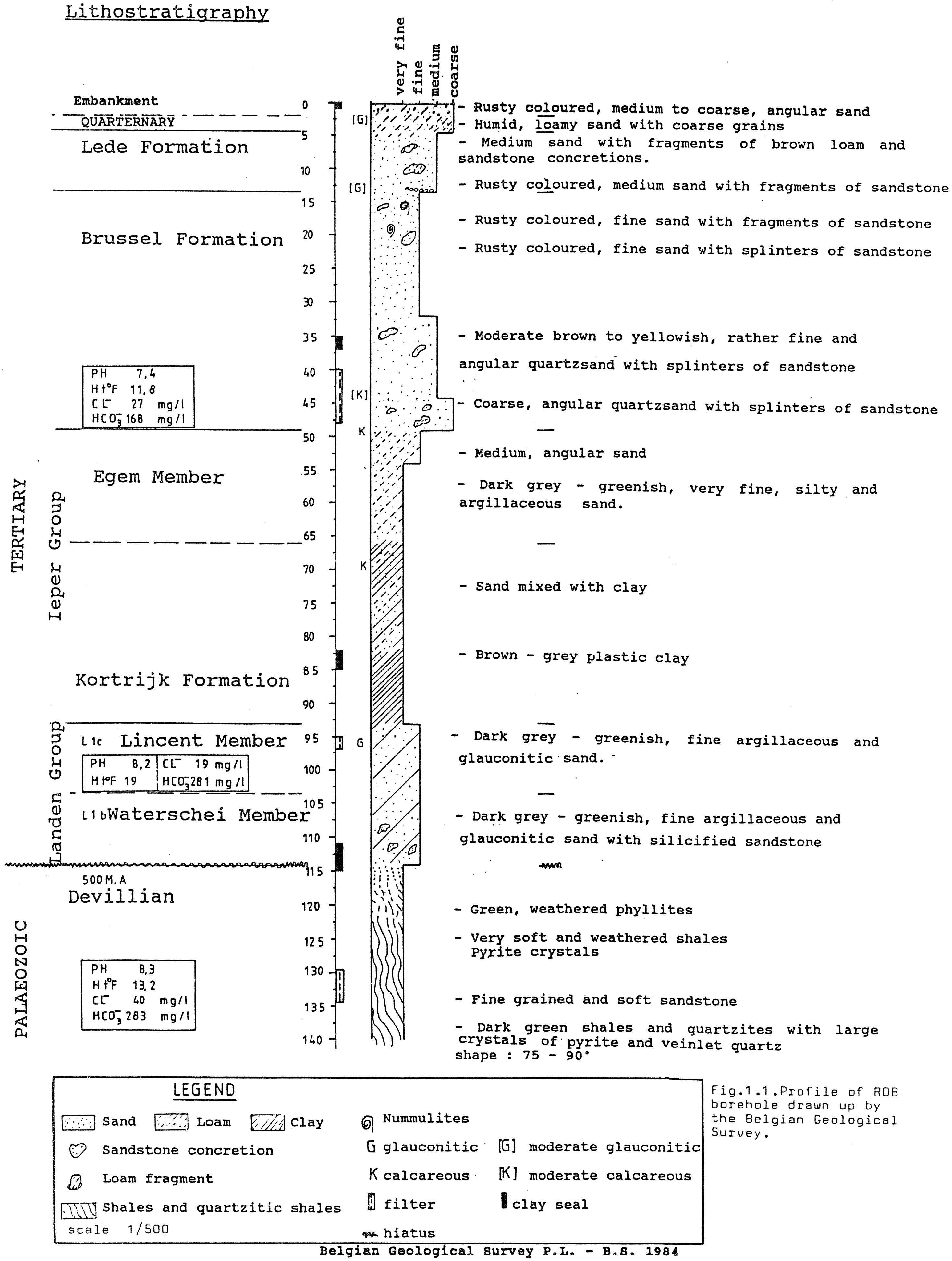

Fig.1.1.Profile of ROB borehole drawn up by the Belgian Geological Survey.

Belgian Geological Survey P.L. - B.S. 1984

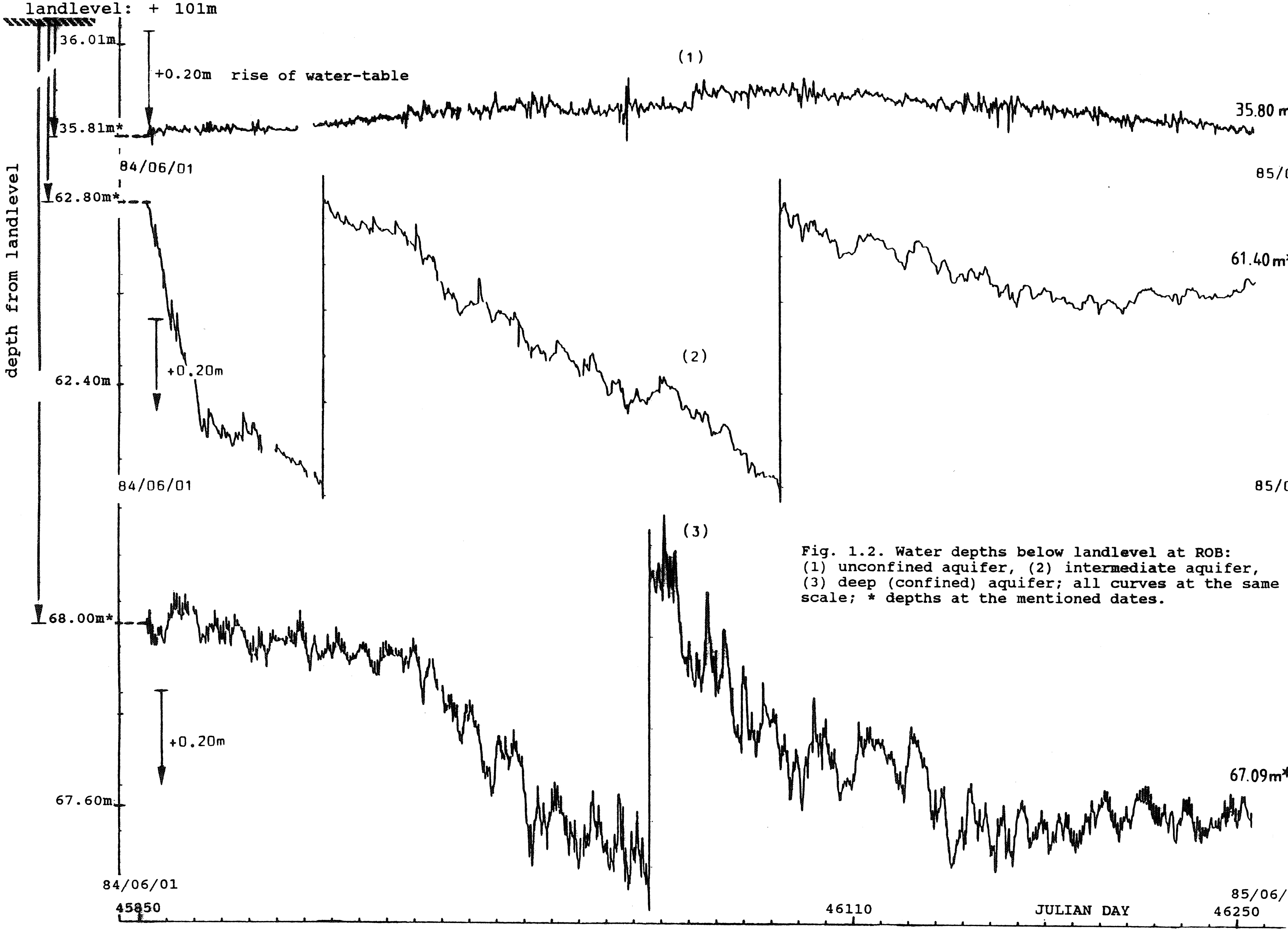

Fig. 1.2. Water depths below landlevel at ROB: (1) unconfined aquifer, (2) intermediate aquifer, (3) deep (confined) aquifer; all curves at the same scale; * depths at the mentioned dates.

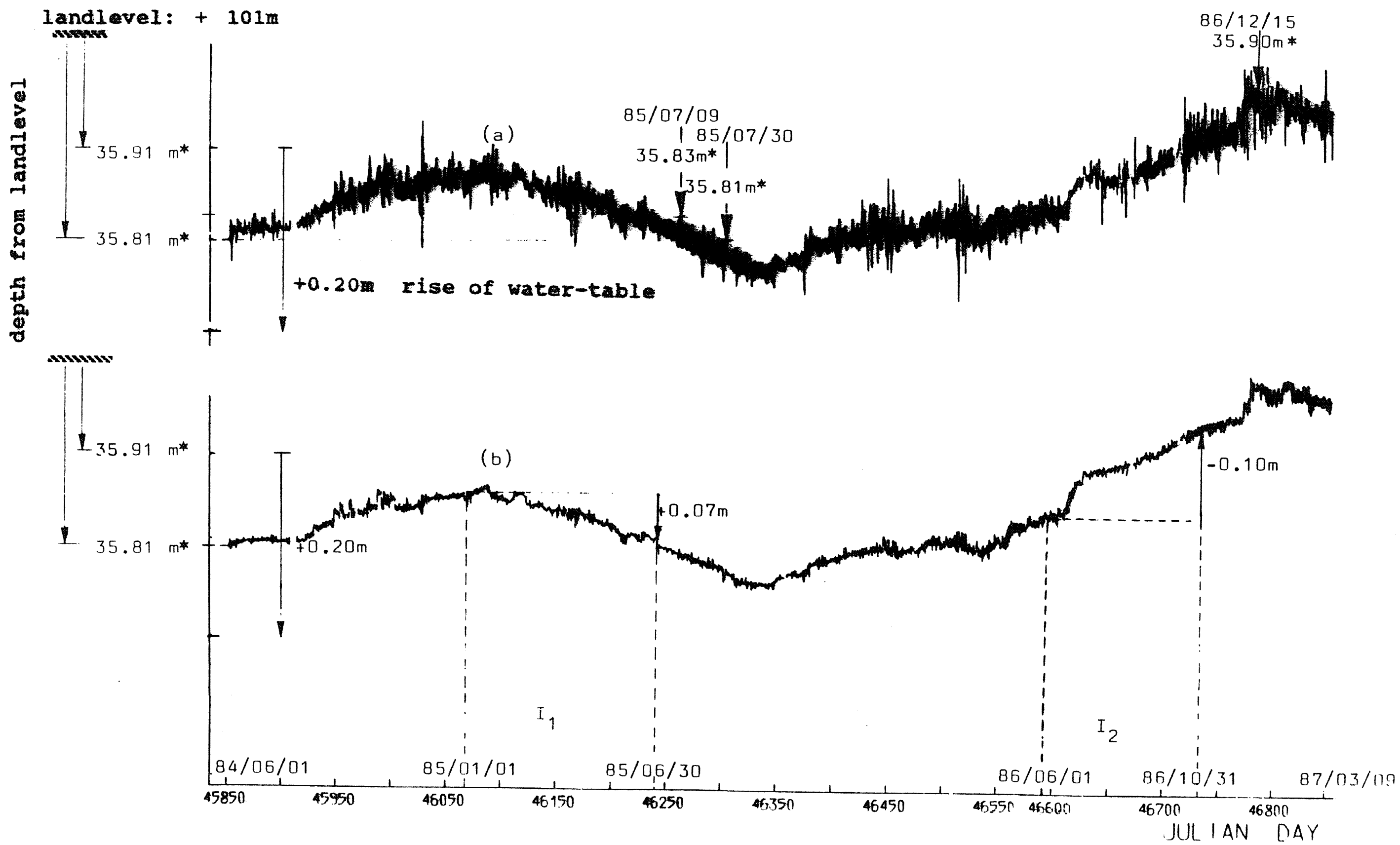

Fig.1.3.34 months(84/06/01 → 87/03/09) registrations in the water table.(a)before barometric effect correction,(b)after barometric effect correction.
*depth from land surface.

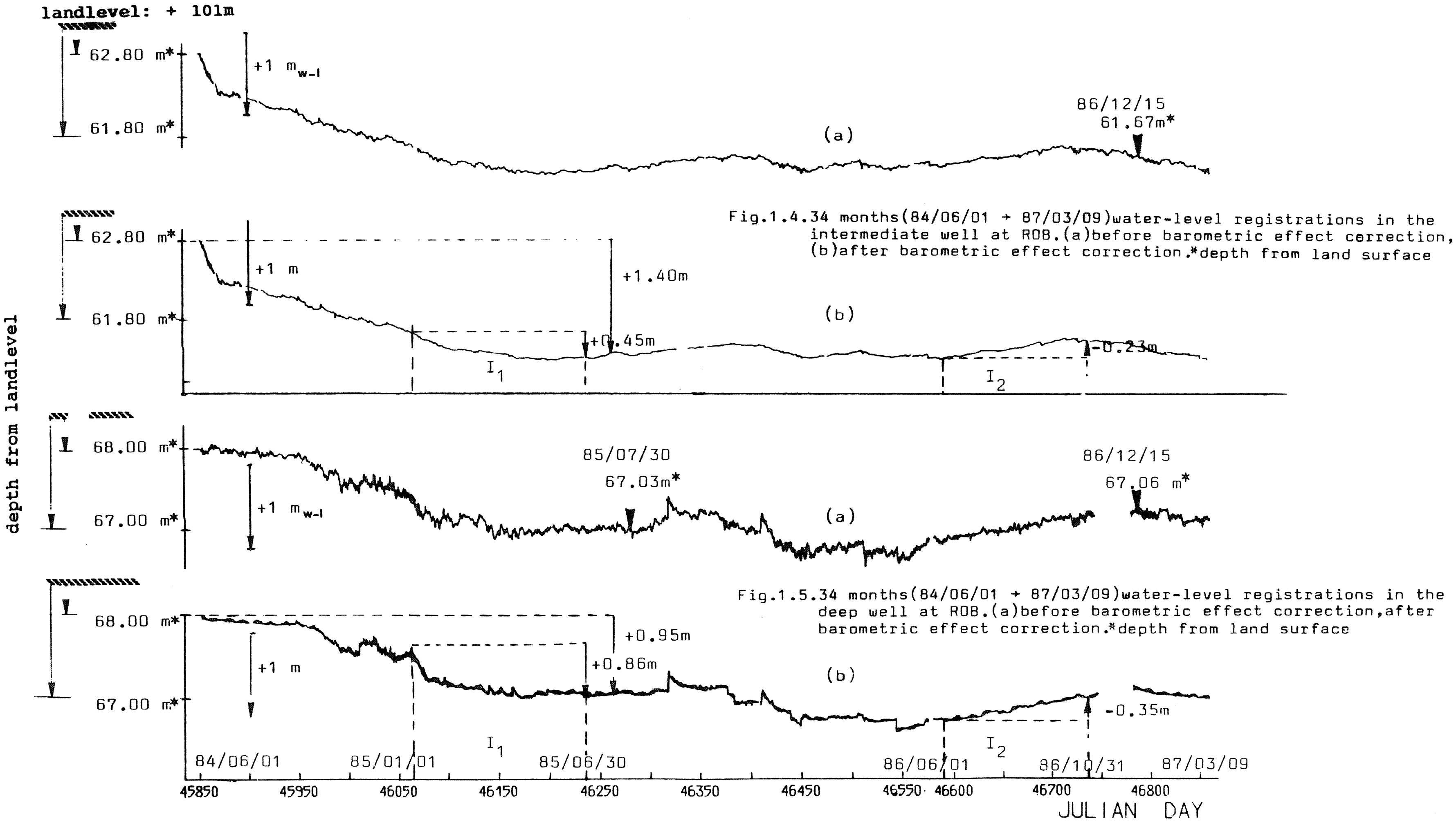

Fig.1.4.34 months(84/06/01 → 87/03/09)water-level registrations in the intermediate well at ROB.(a)before barometric effect correction, (b)after barometric effect correction.*depth from land surface

Fig.1.5.34 months(84/06/01 → 87/03/09)water-level registrations in the deep well at ROB.(a)before barometric effect correction,after barometric effect correction.*depth from land surface

Fig.1.6.Water table variations at ROB.(a)before barometric effect correction.(b)after barometric effect correction(84/06/01→88/12/02)   *depth from land surface

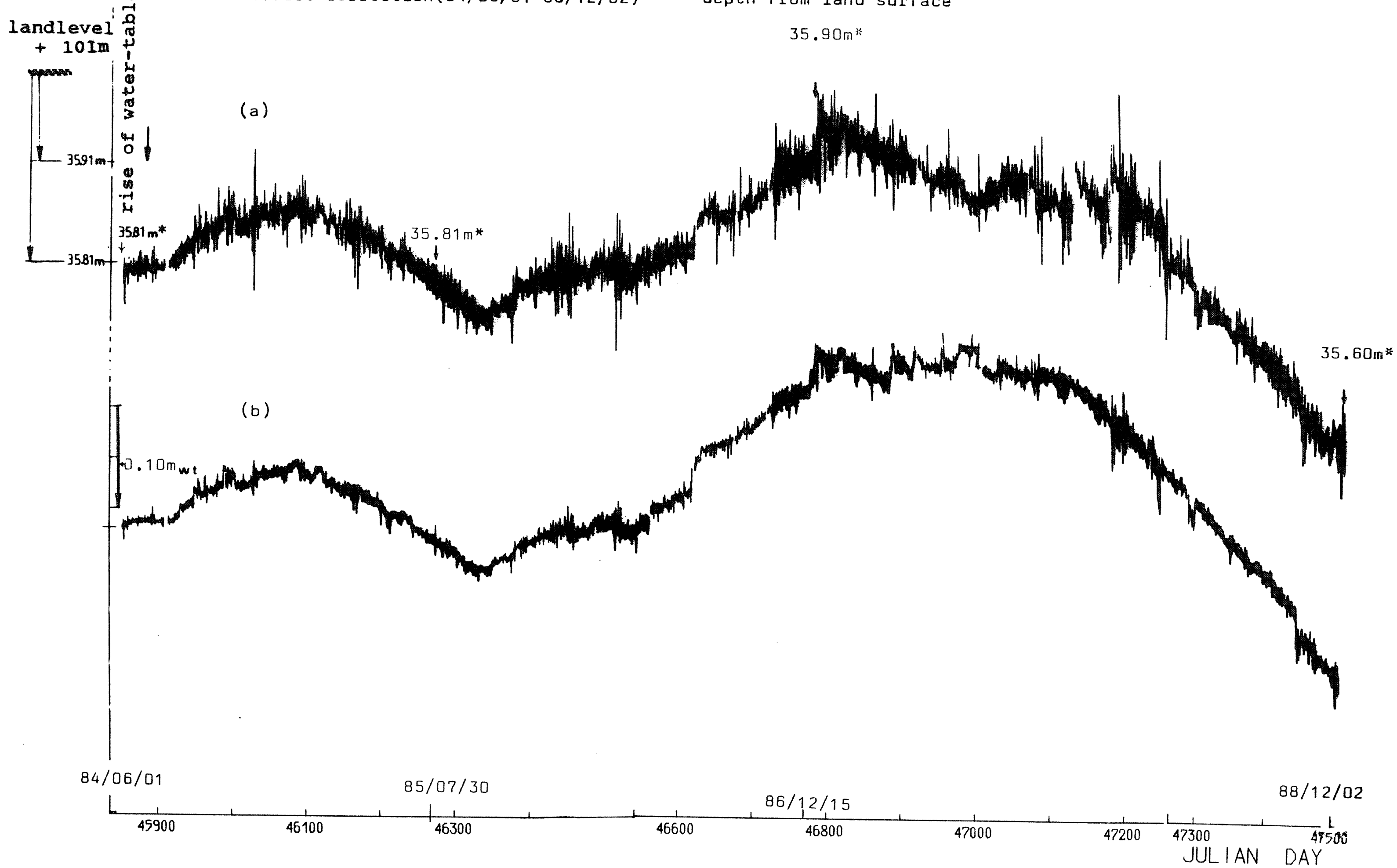

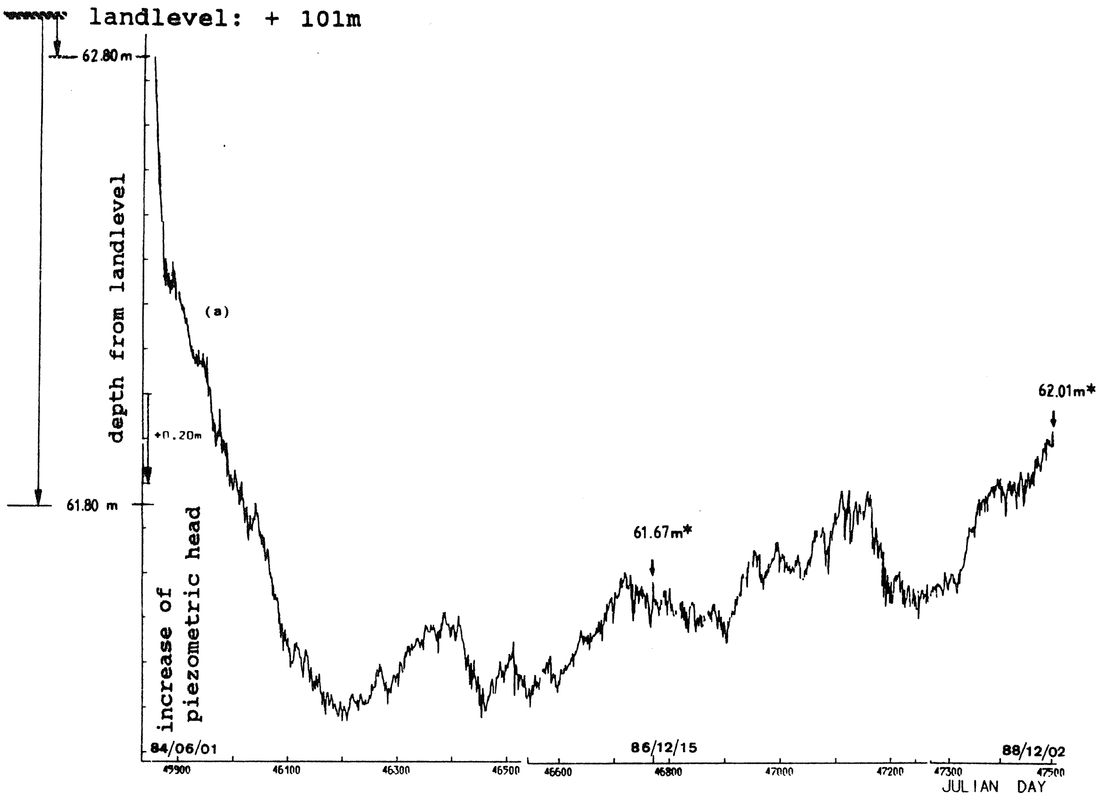

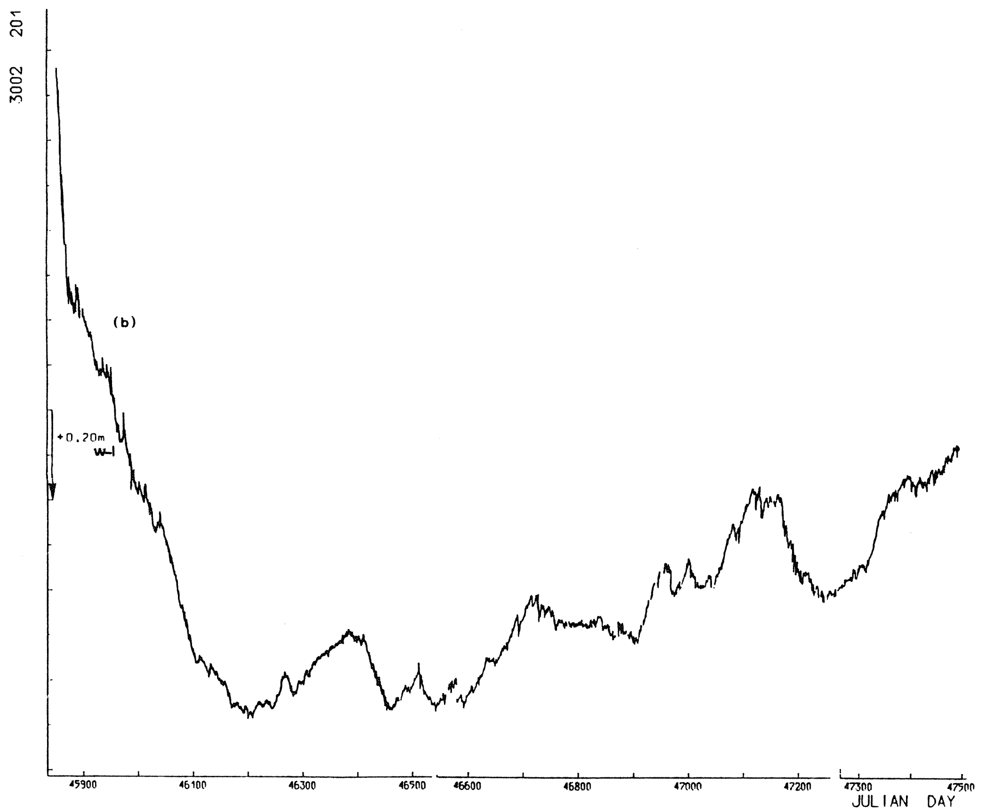

Fig.1.7.Water-level variations in the intermediate well at ROB. (a) before barometric effect correction (b) after barometric effect correction (84/06/01 to 88/12/02) *depth from land surface

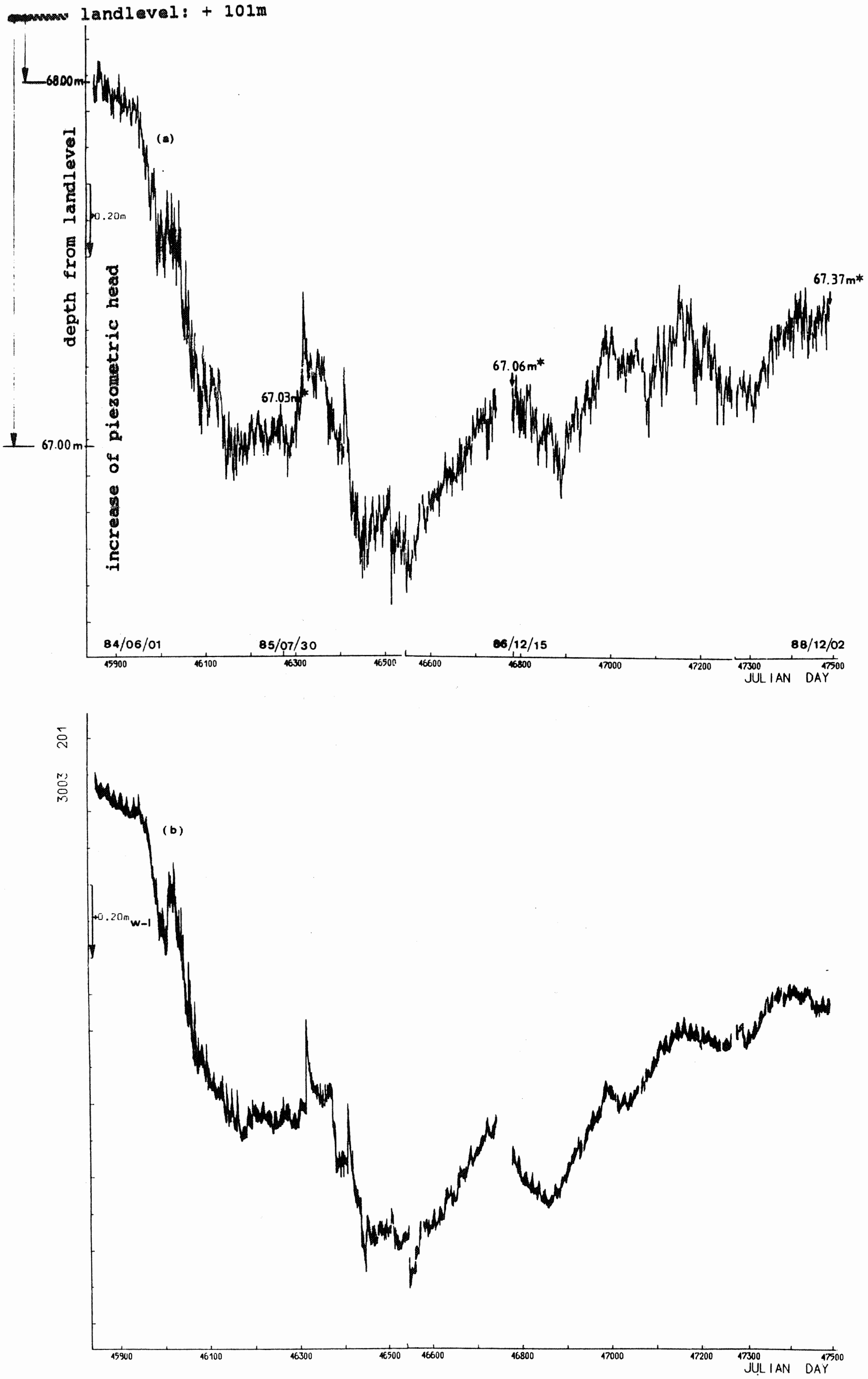

Fig.18.Water-level variations in the deep well at ROB. (a) before barometric effect correction (b) after barometric effect correction (84/06/01 to 88/12/02) * depth from land surface.

Table 1.1

Water-levels impulse responses* to atmospheric pressure variations at ROB calculated by the MISO method.

	*p_t in mbar, numerical coef. in $mm.mbar^{-1}$.	$\lvert BE \rvert_{obs}$ $mm.mbar^{-1}$
Water-table	$6.06766p_t - 0.74237p_{t-1} - 2.15540p_{t-2} - 0.72551p_{t-3} - 1.04399p_{t-4} - 1.39098p_{t-5}$	0.00946
Intermediate well	$0.56367p_t + 0.38000p_{t-1} + 0.31255p_{t-2}$	1.25622
Deep well	$2.04947p_t + 1.59950p_{t-1} - 0.33007p_{t-2} + 1.23010p_{t-3}$	4.54900

Table 1.2.

Long term water-level variations in meter in the three wells of the borehole at the Royal Observatory of Belgium, Brussels.

(* direct measurement; ^ extrapolation of the direct measurement with the "nivocap" transducer)

	watertable H**	interm. well H**	deep well H**
84/06/01	35.81*	62.80*	68.00*
84/06/18	35.82^	62.44^	68.02^
84/06/26	35.82^	62.43^	68.01^
84/07/11	35.82^	62.31^	67.94^
85/01/01	35.87^	61.70^	67.30^
85/01/15	35.78^	61.62^	67.30^
85/06/30	35.81^	61.40*	67.09^
85/07/09	35.83*	61.43^	67.09^
85/07/30	35.81*	61.44^	67.03^
85/09/16	35.77^	61.53^	67.29^
85/12/05	35.78^	61.53^	67.02^
86/03/09	35.83^	61.49^	66.82^
86/06/01	35.83^	61.52^	66.80^
86/10/31	35.90^	61.74^	67.07^
86/12/15	35.90*	61.67*	67.06*
87/02/25	35.93*	61.60*	67.05^
87/03/30	35.93^	61.54^	66.97^
87/04/02	35.90^	61.50^	66.89^
87/04/20	35.90^	61.58^	67.04^
87/05/30	35.93^	61.70^	67.15^
87/07/27	35.93^	61.53^	67.20^
87/09/14	35.93^	61.61^	67.24^
87/09/29	35.91^	61.69^	67.20^
87/12/21	35.88^	61.85^	67.30^
88/04/25	35.76^	61.64^	67.28^
88/11/04	35.57^	61.96^	67.47^
88/12/02	35.60^ 35.60*	62.00^ 62.01*	67.36^ 67.37*

H** : depth from the land surface, in meter
ROB Height = 101 m

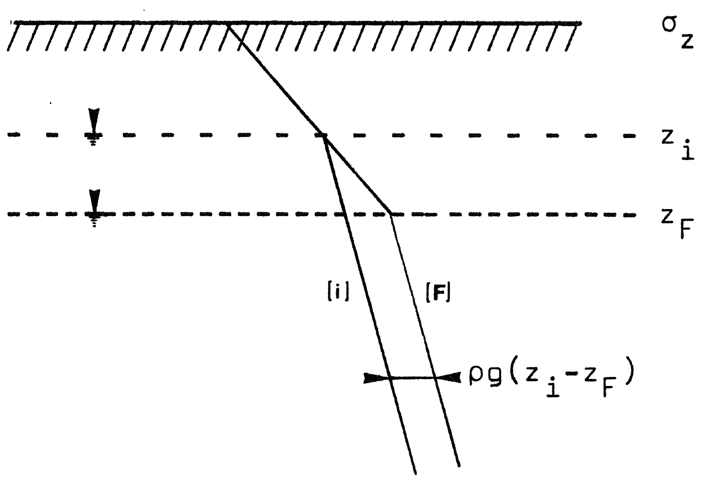

Fig.2.1. σ_z-depth diagram. $\rho g(z_i-z_F)$ effective stress increase due to decline from the initial water table z_i to the final water table z_F.

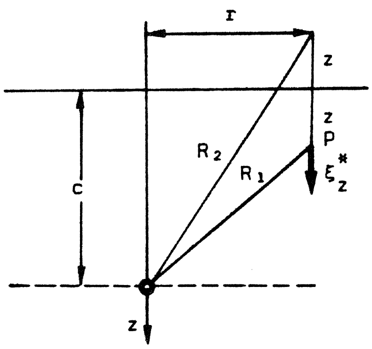

Fig.2.2. Semi-infinite medium with a strain nucleus.

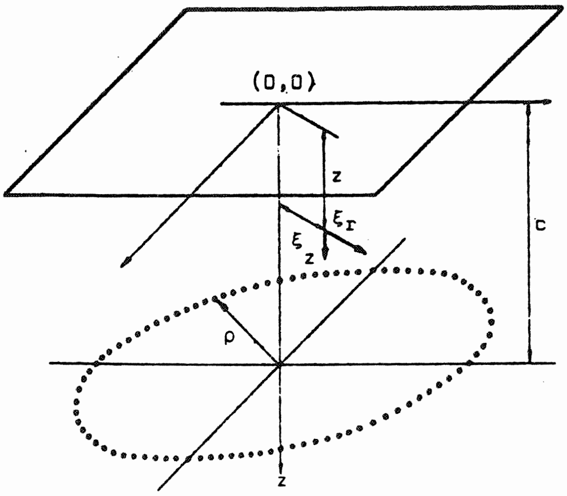

Fig.2.3.Row of nuclei on a circle of radius ρ in the plane z=c below a surface(according to Geertsma,1973).

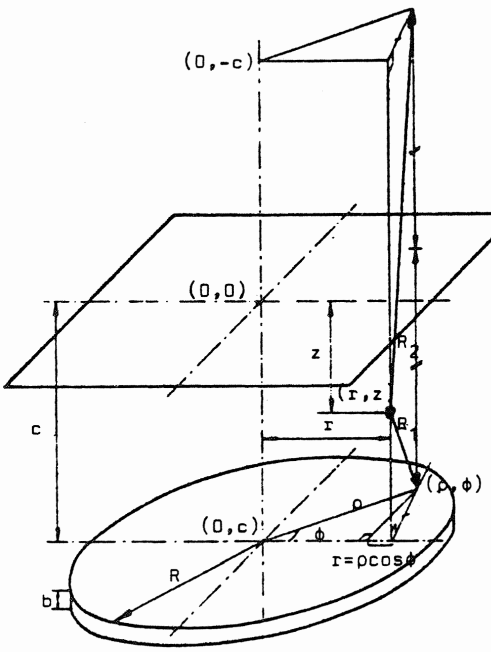

Fig.2.4.Determination of the displacement field around a disc-shaped reservoir in the half space(according to Geertsma,1973).

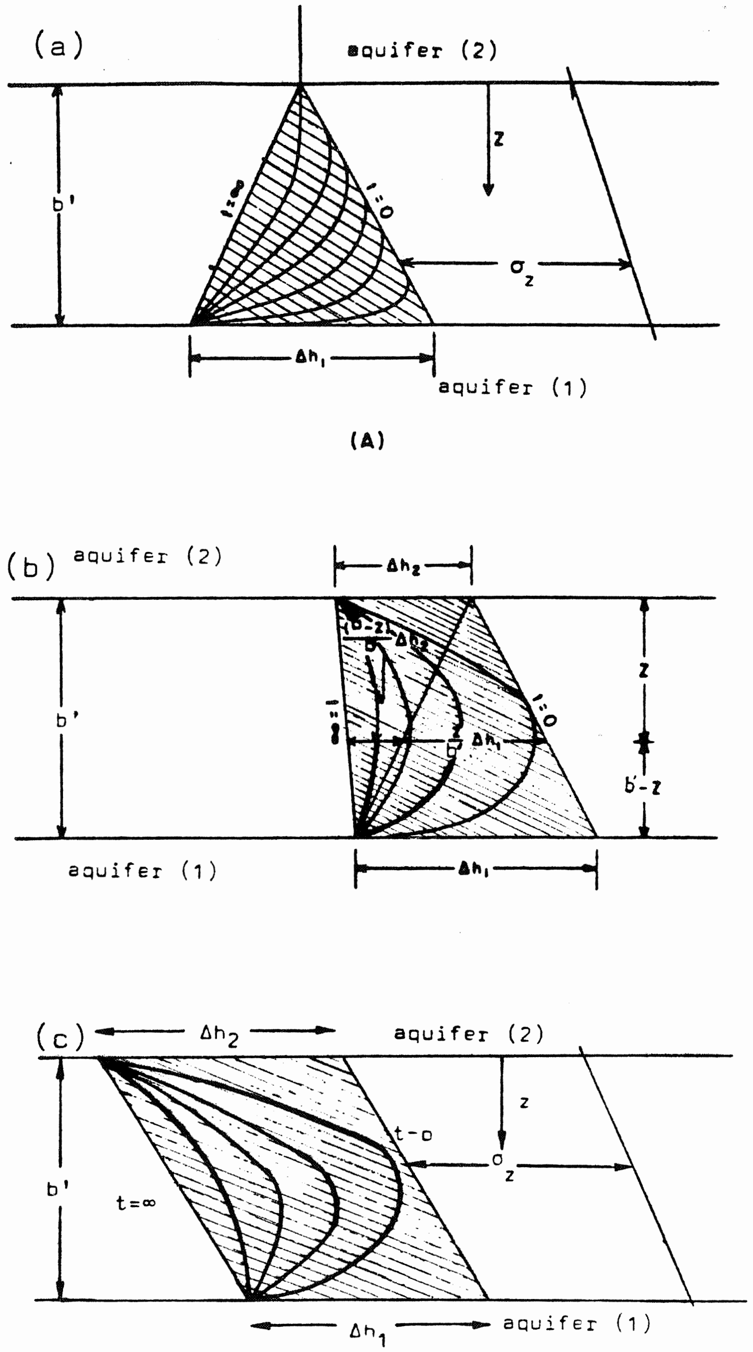

Fig.2.5.Depth-pressure diagrams of a confining layer illustrating effective pressure areas when(a)the head is lowered in one bounding aquifer,and(b)(c)the heads are lowered in both bounding aquifers(according to Domenico&Mifflin,1966).

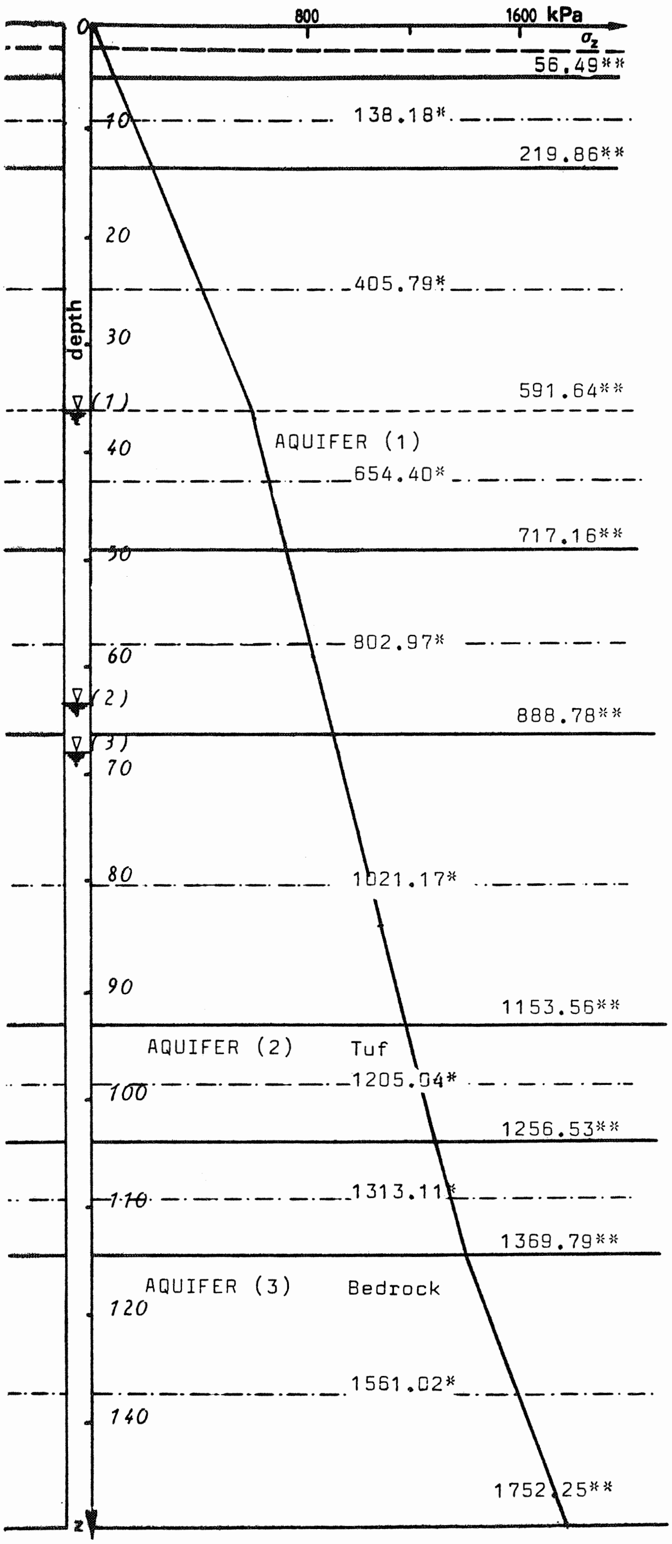

Fig.2.6.Effective stresses diagram at ROB.

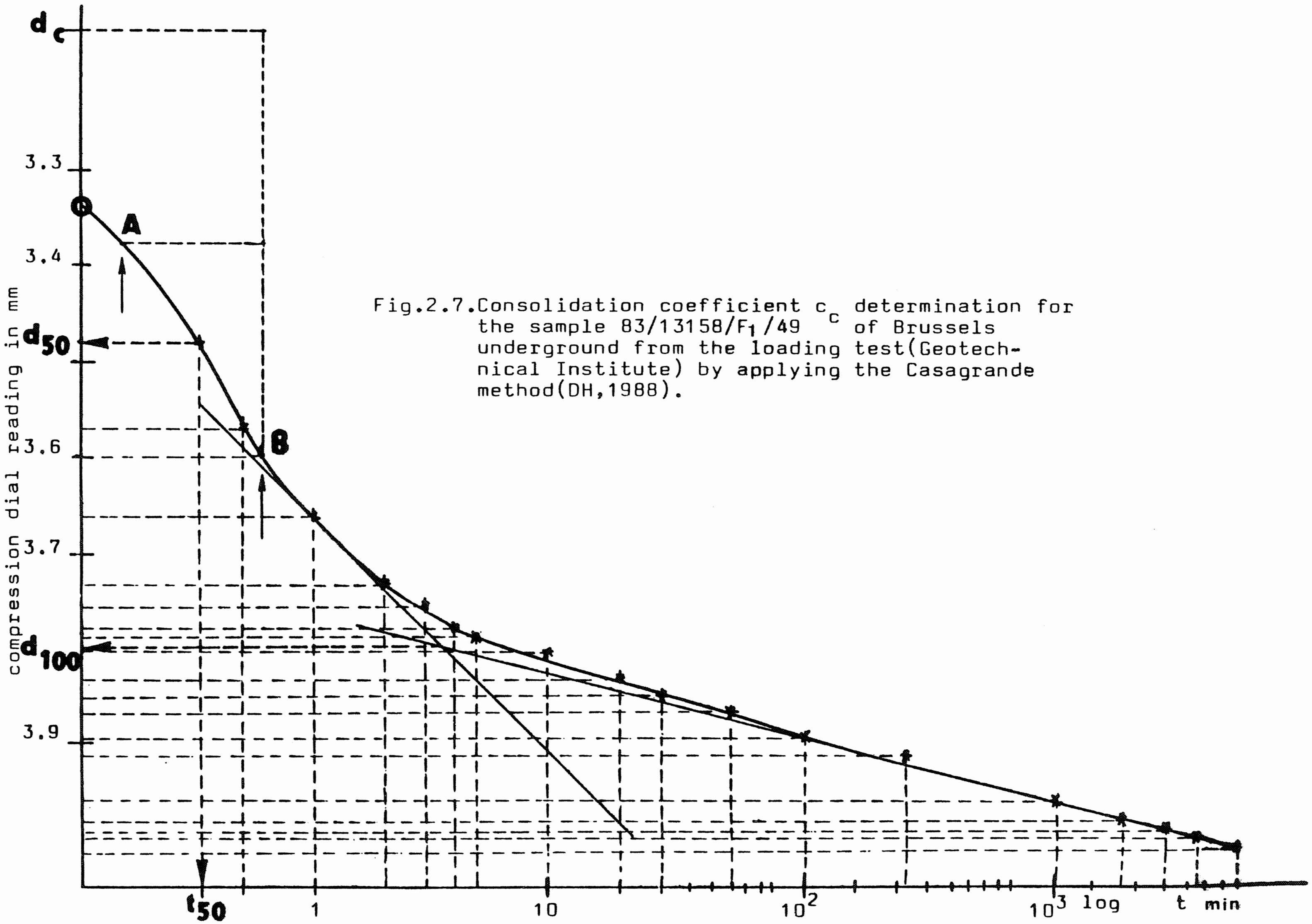

Fig.2.7.Consolidation coefficient c_c determination for the sample 83/13158/F_1/49 of Brussels underground from the loading test(Geotechnical Institute) by applying the Casagrande method(DH,1988).

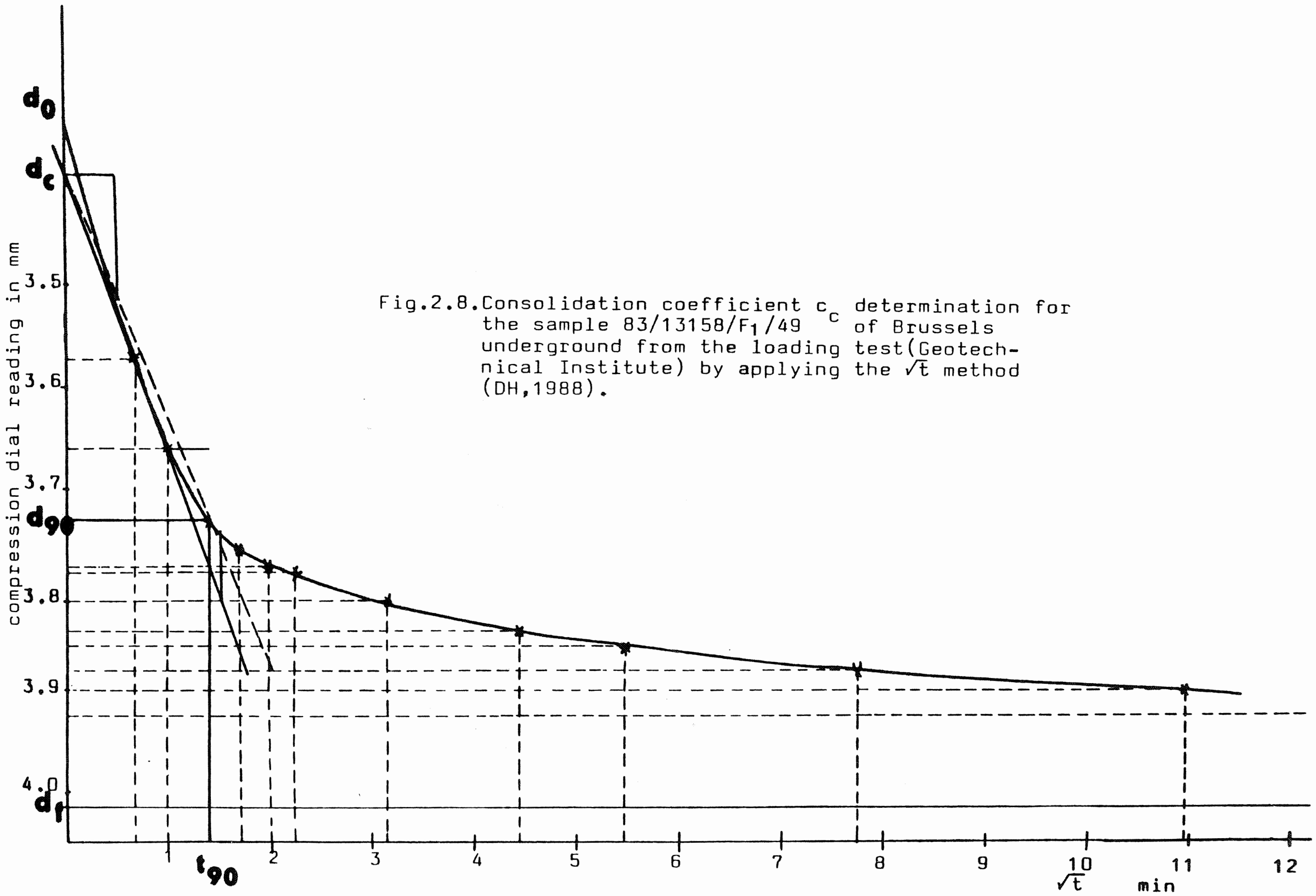

Fig.2.8. Consolidation coefficient c_c determination for the sample 83/13158/F_1/49 of Brussels underground from the loading test (Geotechnical Institute) by applying the $\sqrt{t}$ method (DH,1988).

TABLE 2.1

Effect on g (in nanogal) of land surface displacement induced by the three water-levels variations at ROB, during the time intervals I_i (i = 1,5), from 84/06/01 to 88/12/02.

Time intervals	Expansion in μm	Compaction in μm	Effect on g in nanogal
I_1	220	-	- 69.6
I_2	-	160	50.7
I_3(a)	-	4	1.1
I_3(b)	142	-	- 43.7
I_4	66	-	- 19.9
I_5	30	-	- 9.1

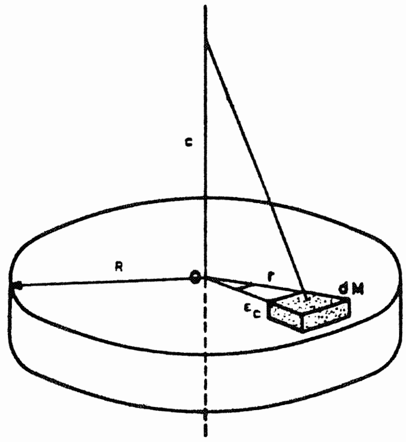

Fig.3.1.Attraction of a circular slab with radius R, with thin thickness ε_c on an unit mass.

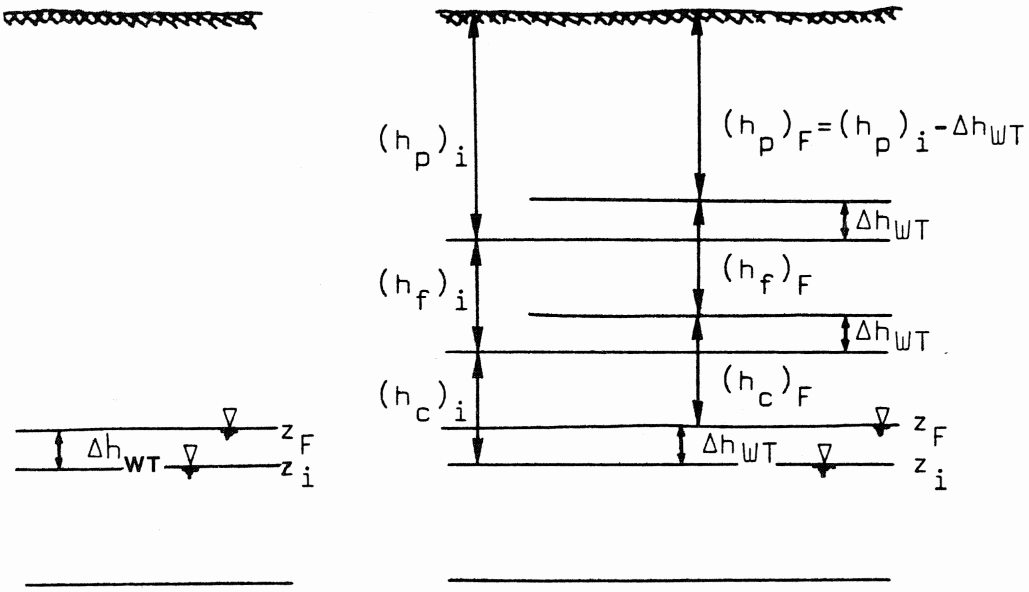

Fig.3.2.Water table variation Δh_{WT};z_i initial state, z_F final state,h_c saturated capillary fringe, h_ℓ funicular zone,h_p pendular zone.

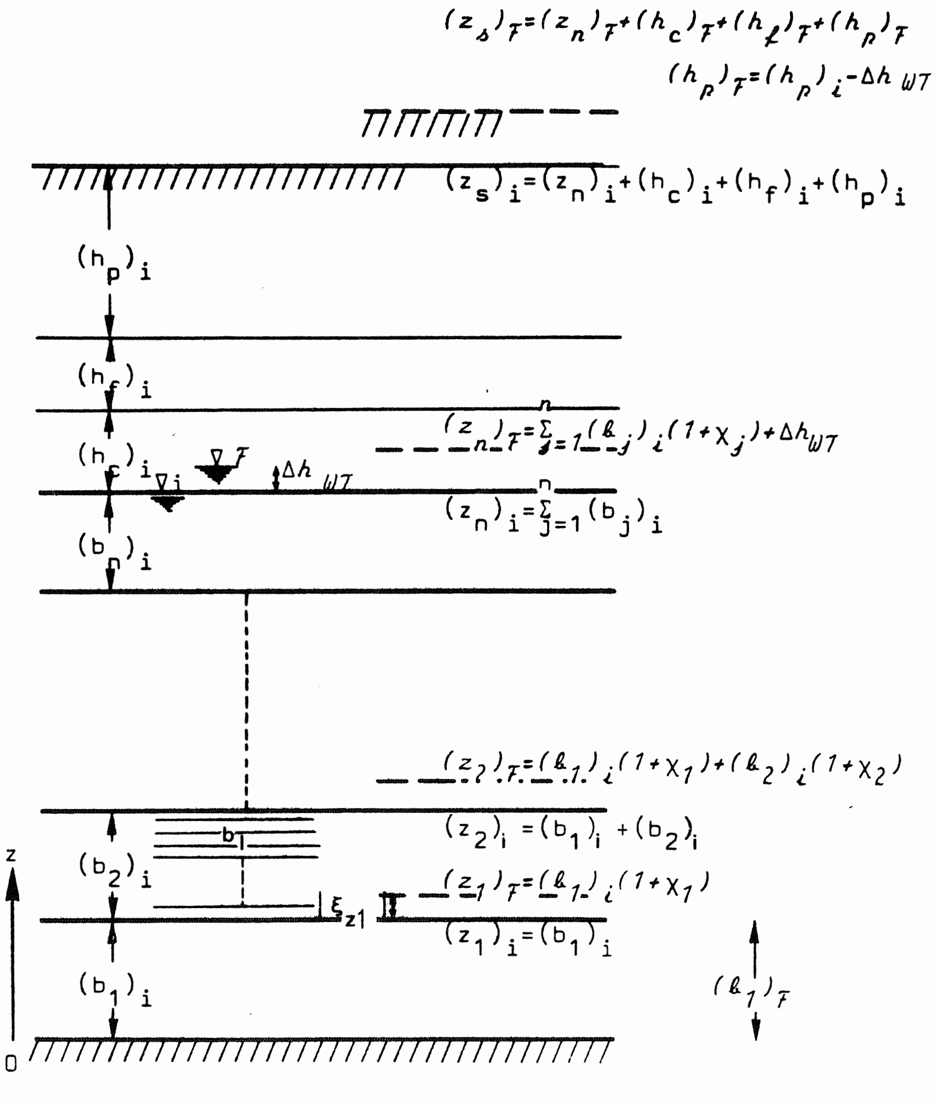

Fig.3.3.Scheme of the geometrical configuration and notations used in attraction calculus of the various strata at ROB.
∇i:initial state
∇F:final state after water table increase Δh_{WT}.

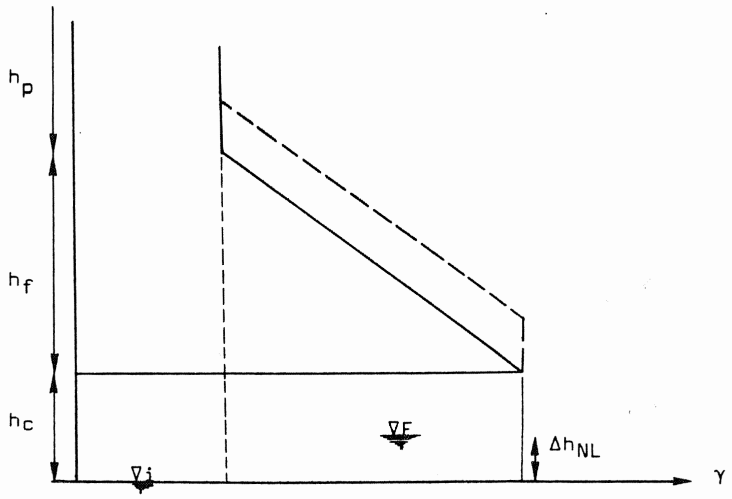

Fig.3.4.Volumic weight distributions in the pendular h_p zone,funicular h_f zone and capillary h_c zone, from the initial state(i) to the final state(F) of the water table.

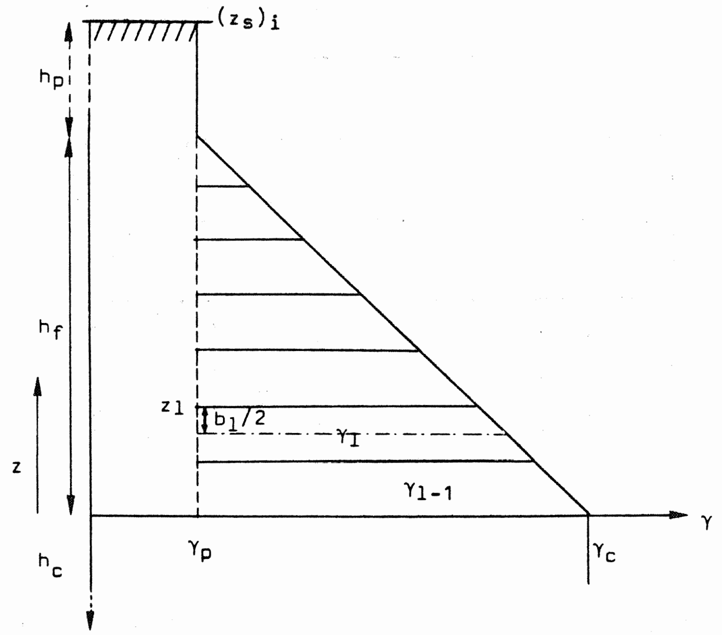

Fig.3.5.Volumic weigth distribution in the funicular zone subdivided into sublayers 1.

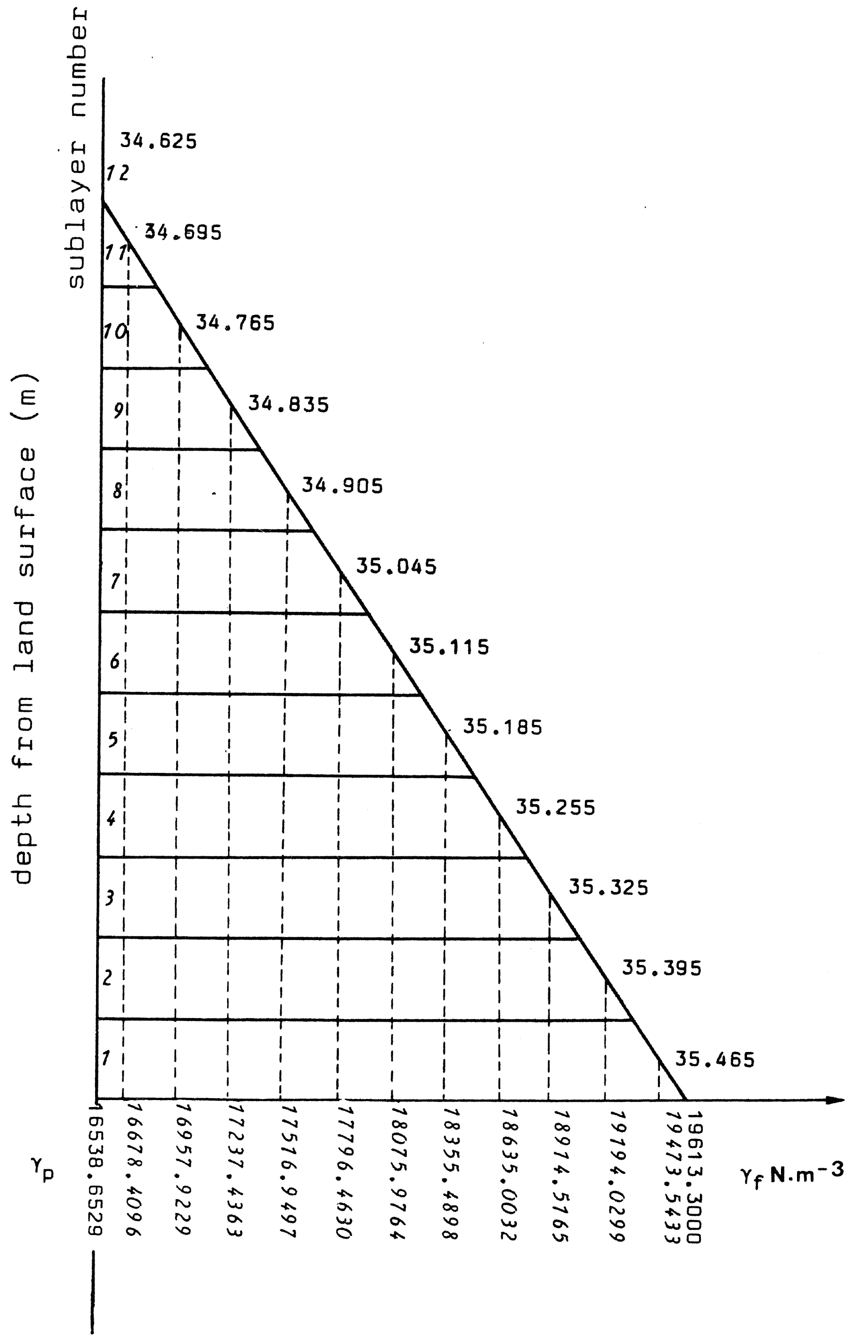

Fig.3.6.Volumic weight distribution in the funicular zone:numerical values at ROB.

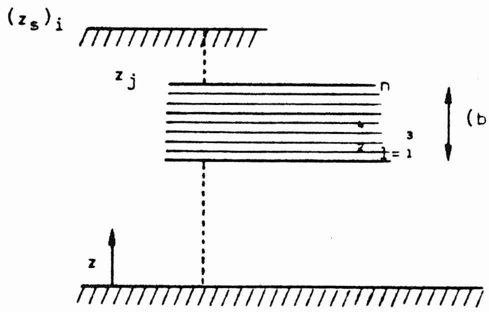

Fig.3.7.Scheme of integration over the layer j thickness.

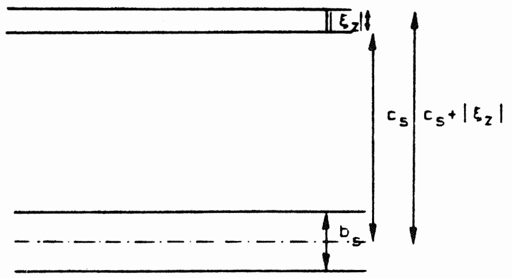

Fig.3.8.Depth variation c_s of a sublayer in the bedrock due to the expansion $|\xi_z|$.

Table 3.1

Calculus of the attraction effect of the funicular and pendular zone of the unconfined aquifer with radius R = 1 km, at the ROB, during the time interval I_1 (85/01/01 to 85/06/30) i.e. for a 0.07 m water table increase.

l	$\{i^l_R\}$	$\Delta A_{p,l}$ (nanogal)
12	0.96532586	41.8838...
l	$\{i^l_R\}$	$\Delta A_{f,l}$
11	0.96525599	80.8573...
10	0.96518612	80.8513...
9	0.96511624	80.8456...
8	0.96504637	80.8397...
7	0.96497650	80.8339...
6	0.96490663	80.8280...
5	0.96483676	80.8222...
4	0.96476689	80.8163...
3	0.96469702	80.8105...
2	0.96462715	80.8046...
1	0.96455728	41.8838...

Table 3.2

Complete contribution of the unconfined aquifer at ROB, induced by an increase of 0.07 m in the water table.

		Attraction (nanogal)			
		R=1km	R=2km	R=3km	R->∞
ΔA_{f+p}	: funicular and pendular zones	890.563	905.463	910.790	921.446
ΔA_6	: saturated part by integration	0.540	0.550	0.553	0.563
	without integration	0.532	0.543	0.547	
$\Delta A_{f+p} + \Delta A_6$		891.103	906.013	911.343	922.009
Bouguer's formula		1116.043*	1136.083*	1142.966*	1156.136
		1107.506"	1131.805"	1140.069"	

* depth c = distance from the land surface to the water table
" depth c = distance from the land surface to the centre of the aquif.

Table 3.3

Contribution of the confined aquifer layers to the attraction calculated by (3.51) (tuf aquifer, j = 3, bedrock aquifer, j = 1)

	j	X_j	$X_j \gamma_w / g$ 10^{-3}kgm^{-3}	$\Delta \rho_w\ (1 + X_j)$ 10^{-3}kgm^{-3}	ΔA_j nanogal
1. 0.07 m water table increase	3	0.00000057	0.57000	0.32896519	+0.396
	1	0.00000055	0.05516	0.32896502	+0.419
2. 1.40 m yearly increase in the tuf aquifer	3	0.00001146	11.45900	6.57937539	+7.942
3. 0.07 m maximum pumping in the tuf aquifer	3	-0.00000057	-0.57000	-0.32896519	-0.396
4. 0.95 m yearly increase in the bedrock aquifer	1	0.00000075	0.75032	4.46452834	+5.685
5. 0.11 m maximum pumping in the bedrock aquifer	1	-0.00000009	-0.08626	-0.51694501	-0.658

Table 4.1

Total "hydrogeological perturbing effect" on g (land surface displacement effect L and attraction variation effect A) at ROB during the time intervals I_i (i = 1,2) taking into account (1) the whole aquifer system, (2) the water table variation including the effective stress variation transfer $\Delta\sigma_z$ and (3) the water table variation only. L and A in nanogal.

Time intervals		I_1 85/01/01 -> 85/06/30	I_2 86/06/01 -> 86/10/30
Water-levels var.		AQ.1 - 0.07 m AQ.2 + 0.45 m AQ.3 + 0.86 m	AQ.1 + 0.10 m AQ.2 - 0.23 m AQ.3 - 0.35 m
(1) the whole aquifer system	L	- 69.543	+ 50.668
	A	+ 905.836	- 1282.004
	L+A	*+ 836.293*	*- 1231.336*
(2) the water table variation	L	- 18.286	+ 26.122
	A	+ 893.537	- 1276.421
$+\Delta\sigma_z$	L+A	+ 875.251	- 1250.299
(3) the water table variation	L	- 4.087	+ 5.838
	A	+ 891.103	- 1273.004
	L+A	+ 887.016	- 1267.166

Table 4.2

Total "hydrogeological perturbing effect" on g (land surface displacement effect L and attraction variation effect A) at ROB during the time intervals I_i (i = 3,5) taking into account (1) the whole aquifer system, (2) the water table variation including the effective stress variation transfer $\Delta\sigma_z$ and (3) the water table variation only. L and A in nanogal.

Time intervals		I_3(a) 87/09/29 -> 87/12/21	I_3(b) 87/12/21 -> 88/04/25	I_4 88/04/25 -> 88/11/04	I_5 88/11/04 -> 88/12/02
Water-levels var.		AQ.1 + 0.05 m AQ.2 - 0.15 m AQ.3 - 0.13 m	AQ.1 + 0.11 m AQ.2 + 0.19 m AQ.3 + 0.00 m	AQ.1 + 0.18 m AQ.2 - 0.31 m AQ.3 - 0.15 m	AQ.1 + 0.03 m AQ.2 + 0.04 m AQ.3 - 0.10 m
(1) the whole aquifer system	L	+ 1.092	- 43.685	- 19.872	- 9.136
	A	+ 635.369	+ 1406.549	+ 2292.606	+ 382.711
	L+A	*+ 636.461*	*+ 1362.864*	*+ 2272.734*	*+ 373.575*
(2) the water table variation	L	- 13.062	- 28.745	- 47.018	- 7.836
	A	+ 638.242	+ 1404.130	+ 2297.665	+ 382.944
$+\Delta\sigma_z$	L+A	+ 625.180	+ 1375.385	+ 2250.647	+ 375.108
(3) the water table variation	L	- 2.919	- 6.422	- 10.508	- 1.751
	A	+ 636.502	+ 1400.304	+ 2291.407	+ 381.901
	L+A	+ 633.583	+ 1393.882	+ 2280.899	+ 380.150

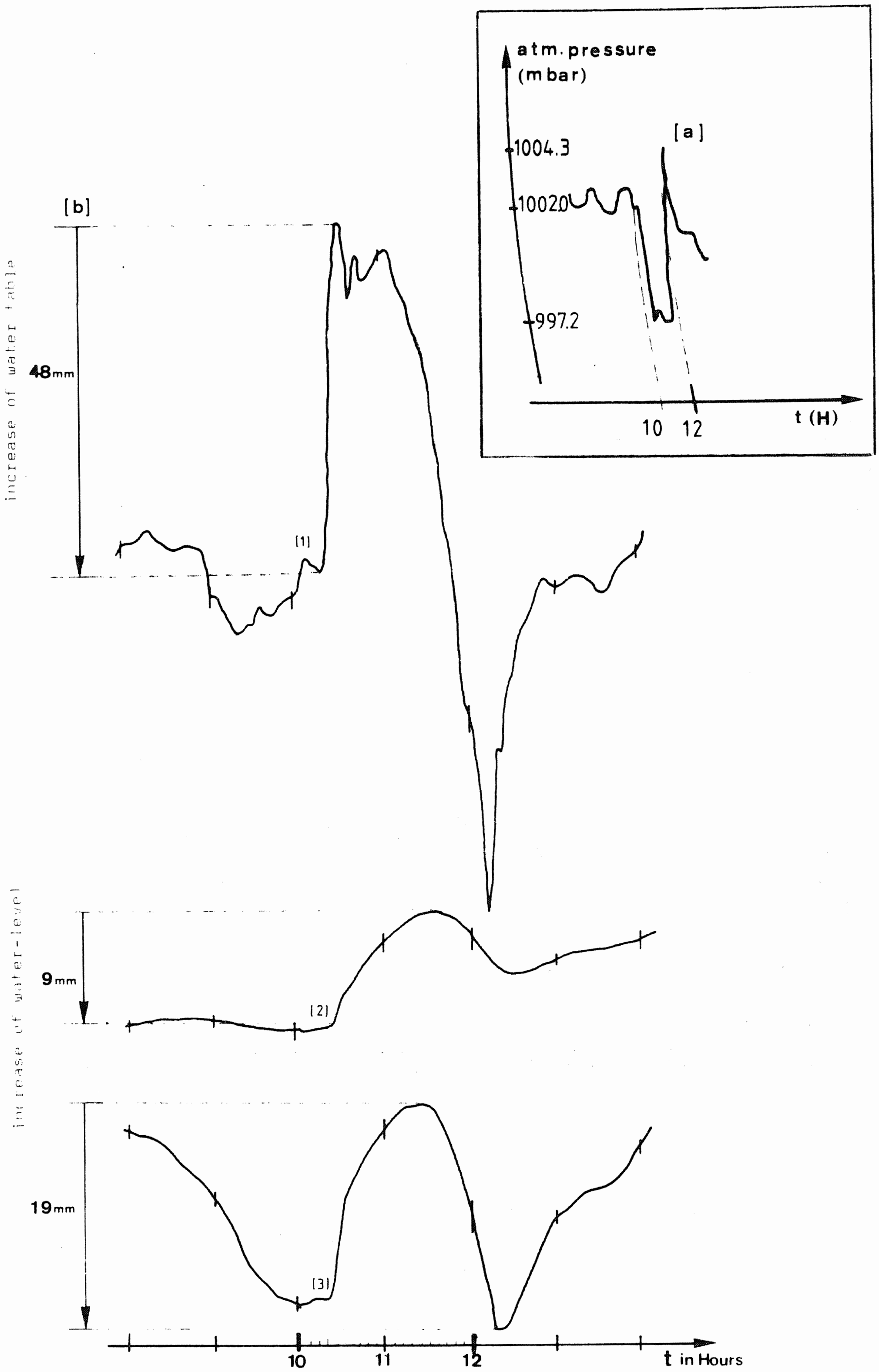

Fig.5.1.Response(b) in the three wells ((1)water table, (2)intermediate well,(3)deep well) to a sudden atmospheric pressure decrease(a) with a 4.7 mbar amplitude,recorded during a thunderstorm(July, the 11th 1984) at ROB.

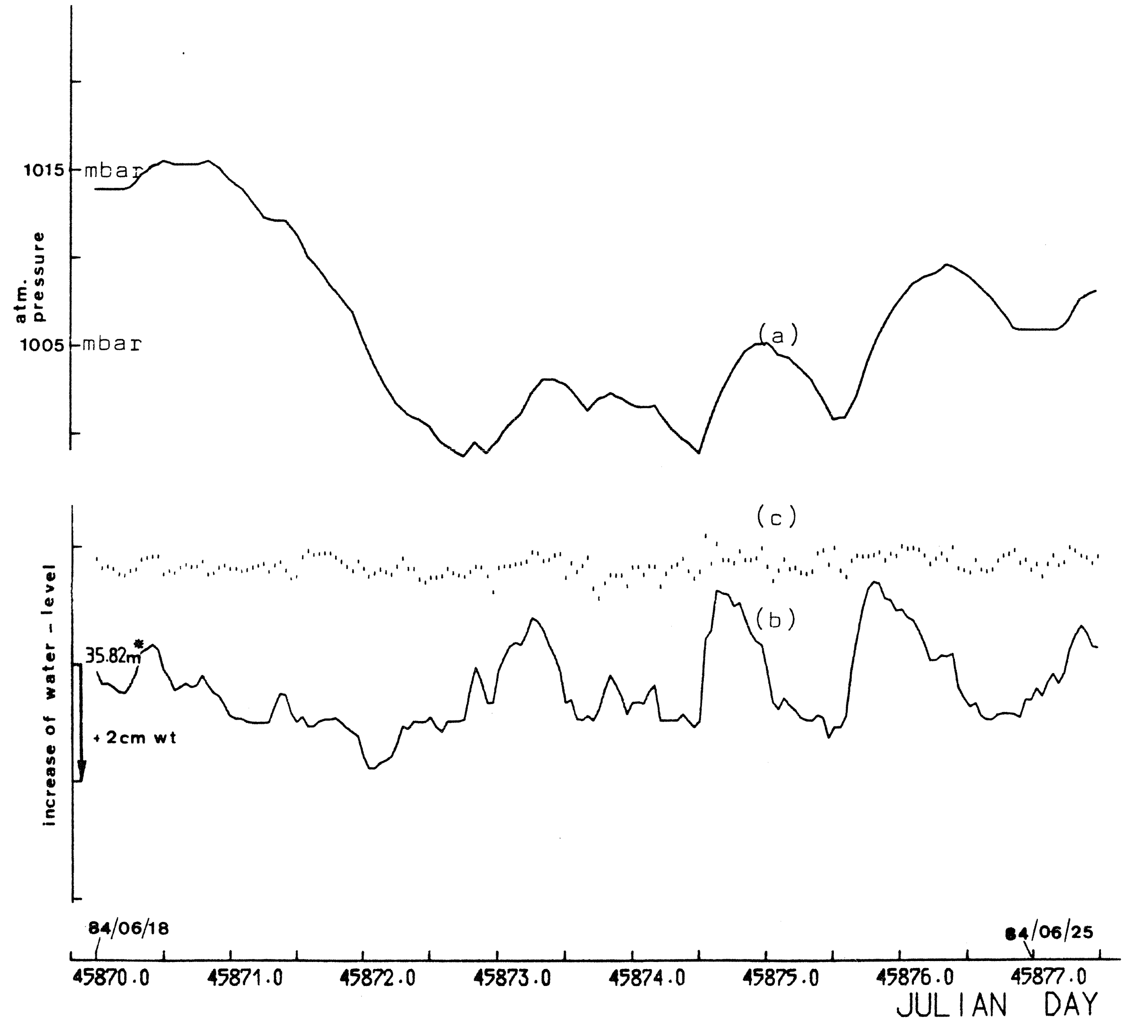

Fig.5.2.Water table response (b) to atmospheric pressure variations (a) registered at ROB.The curve (c) is the water table corrected from barometric effect.

*35.82m=depth from landlevel

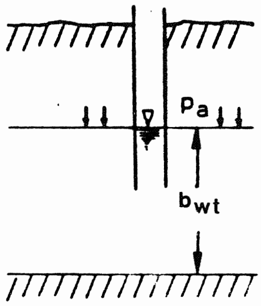

Fig.5.3a.Unconfined aquifer with thickness b_{wt}.

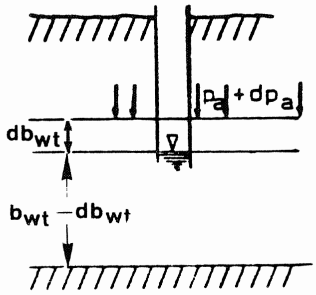

Fig.5.3b.Water table variation db_{wt} induced by atmospheric pressure variation dp_a.

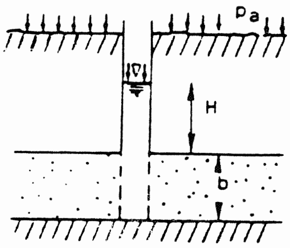

Fig.5.4. **Atmospheric pressure load on a confined aquifer.**

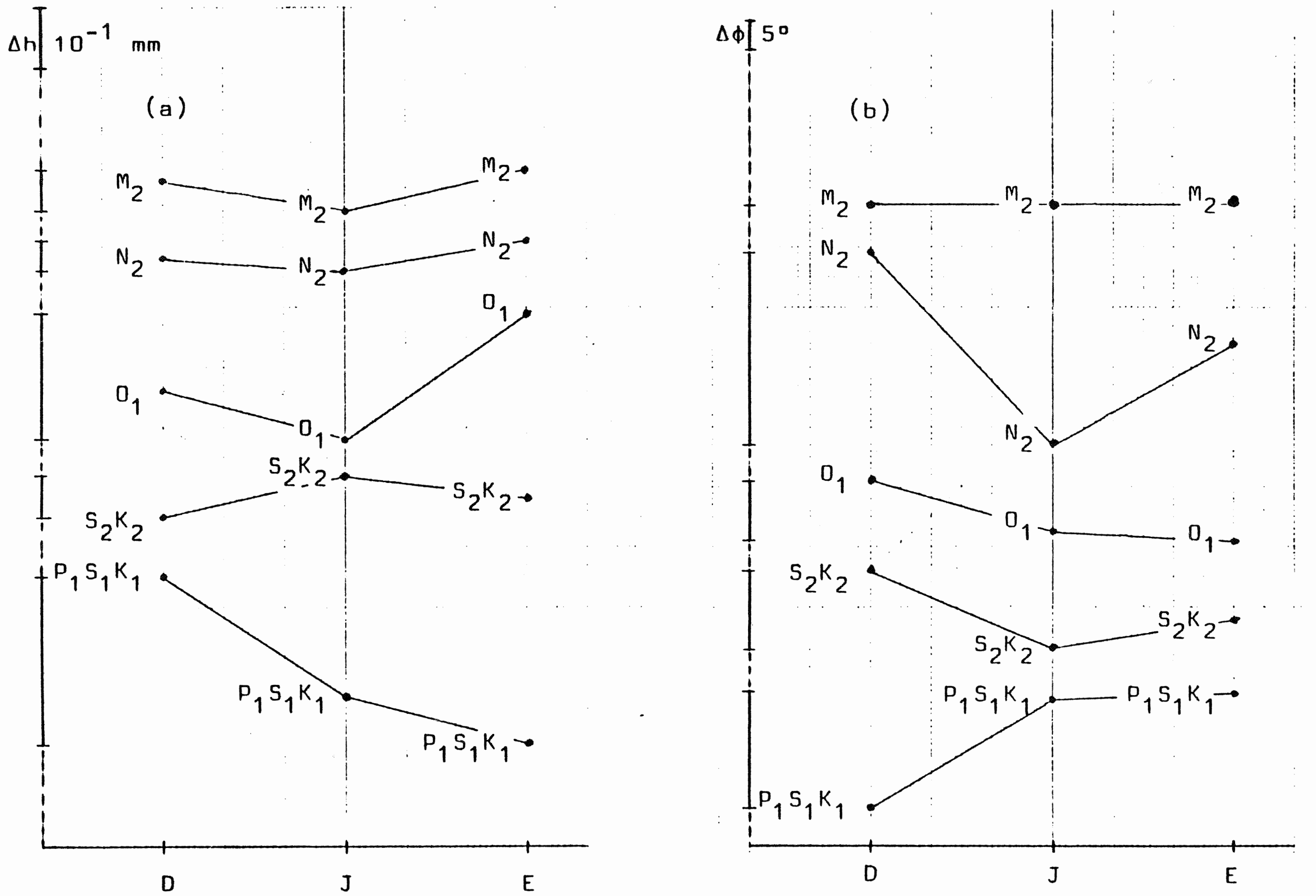

Fig.5.7a&b. Seasonal variations of M_2,N_2,O_1,S_2K_2 and $P_1S_1K_1$ in amplitude(a) and phase(b), in the intermediate water-level at ROB.

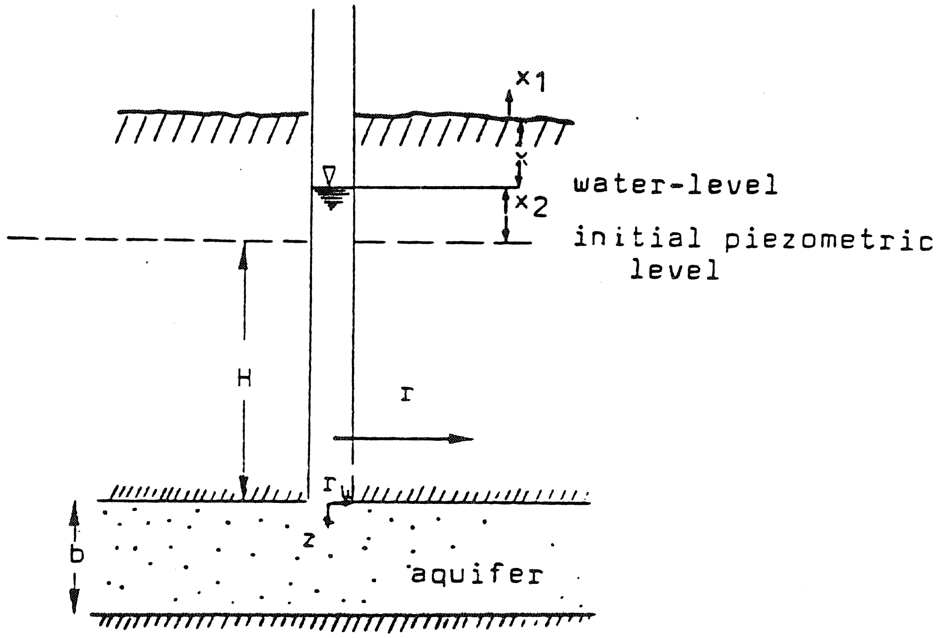

Fig.5.8. **Idealized representation of a well in which water-level fluctuations are caused by oscillation of the fluid pressure in response to a wave. The initial piezometric level is the level before the oscillation (b = aquifer thickness, r,z = cylindrical coordinates, r_w = well radius).**

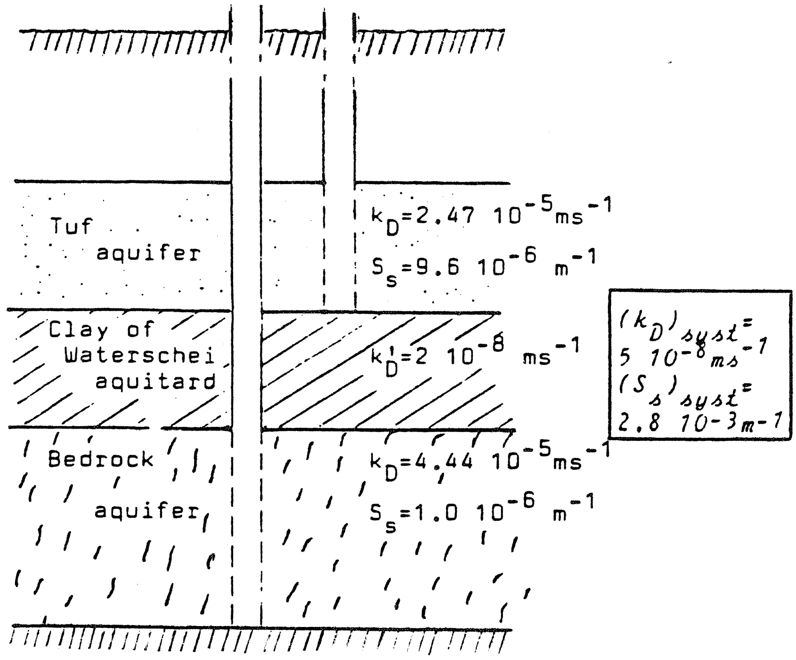

Fig.5.9 **Aquifer system taken into account to study the Earth tidal water-levels response at the ROB. This system involves the tuf aquifer and the bedrock aquifer between which the clay of Waterschei is sandwiched. k_D is the permeability, S_s is the storage coefficient , k'_D is the aquitard permeability.**

TABLE 5.1a.

Water table tidal analyses results before and after having removed the barometric effect.

		UNCONFINED AQUIFER 84/06/01 → 87/02/28 , 1002 d., 23184 h.r.							
		Before atmospheric pressure correction				After atmospheric pressure correction			
	WAVES	A	σ(A)	α	σ(α)	A	σ(A)	α	σ(α)
	M_2	0.18	± 0.06	- 163.6°	±20.0°	0.03	± 0.04	106.2°	±69.1°
	N_2	0.17	± 0.07	-122.7°	±22.7°	0.07	± 0.04	-83.4°	±35.6°
	S_2	2.85	± 0.06	- 81.8°	± 1.2°	0.64	± 0.04	-54.5°	± 3.3°
	K_1	0.40	± 0.15	25.9°	±21.2°	0.11	± 0.05	34.2°	±26.4°
	P_1	0.22	± 0.16	- 87.0°	±41.8°	0.04	± 0.05	68.7°	±72.4°
	O_1	0.11	± 0.14	128.6°	±75.4°	0.10	± 0.05	112.3°	±27.5°
Standard deviation (mm)	D	15.09				5.33			
	SD	5.76				3.56			
	TD	4.10				2.91			

A: Amplitude, in mm σ(A): R.M.S. α: Phase σ(α): R.M.S.

T A B L E 5.1 b.

Water-levels tidal analyses results for the intermediate well (tuf of Lincent confined aquifer) and for the deep well (bedrock confined aquifer) before and after having removed the barometric effect.

		INTERMEDIATE WELL 84/06/01 —> 88/12/05, 1647 d., 35424 h.r.				DEEP WELL 84/06/01 —> 88/12/08, 1652 d., 35376 h.r.			
		Before atmospheric pressure correction		After atmospheric pressure correction		Before atmospheric pressure correction		After atmospheric pressure correction	
	WAVES	A σ(A)	α σ(α)	A σ(A)	α σ(α)	A σ(A)	α σ(α)	A σ(A)	α σ(α)
	M_2	0.81±0.02	156.6°±1.4°	0.80±0.02	156.8°±1.2°	5.40±0.04	148.1°±0.5°	5.31±0.04	148.1°±0.4°
	N_2	0.20±0.02	167.2°±6.2°	0.18±0.02	165.1°±5.7°	1.00±0.05	152.3°±2.6°	0.94±0.04	152.1°±2.3°
	S_2	0.79±0.02	171.0°±1.4°	0.58±0.02	149.3°±1.5°	3.57±0.04	154.9°±0.7°	2.99±0.03	138.8°±0.6°
	K_1	1.08±0.07	162.1°±3.9°	1.07±0.04	161.8°±2.3°	8.18±0.13	157.5°±0.9°	8.30±0.06	158.3°±0.4°
	P_1	0.46±0.08	-179.8°±10.2°	0.46±0.05	170.1°±6.0°	3.32±0.15	162.3°±2.6°	3.36±0.06	157.4°±1.1°
	O_1	0.85±0.07	164.7°±4.8°	0.87±0.05	165.0°±2.7°	7.47±0.13	158.3°±1.0°	7.53±0.06	158.3°±0.4°
Standard deviation	D	9.77		5.64		17.57		7.66	
	SD	2.26		1.85		4.87		4.07	
	TD	0.95		0.84		2.27		2.09	
Amplitudes ratios	(theory)								
S_2/M_2	0.465	0.972		0.721		0.661		0.563	
N_2/M_2	0.194	0.243		0.223		0.186		0.178	
O_1/K_1	0.710	0.787		0.817		0.913		0.907	
M_2/O_1	0.965	0.952		0.915		0.722		0.705	

A : Amplitude, in millimeter   σ(A) : R.M.S.   α : Phase   σ(α) : R.M.S

TABLE 5.2.

Water-levels tidal analyses results of the six months sub-sets of data for the intermediate well after having removed the barometric effect. The amplitudes and their RMS are expressed in mm(*=theoretical amplitudes ratios).

	84/07/01→84/12/31 184 d.,3792 h.r.		85/01/01→85/06/30 181 d.,4128 h.r.		85/07/01→85/12/31 184 d.,4272 h.r.		86/01/01→86/06/30 181 d.,4032 h.r.		86/07/01→86/12/31 185 d.,4224 h.r.	
M_2	0.51 ± 0.05	156.6° ± 4.6°	0.66 ± 0.04	157.7° ± 3.2°	0.76 ± 0.03	159.1° ± 2.3°	0.73 ± 0.04	164.7° ± 3.5°	0.84 ± 0.04	160.9° ± 2.9°
N_2	0.14 ± 0.05	156.6° ± 4.6°	0.13 ± 0.04	168.5° ±16.3°	0.15 ± 0.03	166.3° ±12.8°	0.16 ± 0.05	143.6° ±17.6°	0.20 ± 0.05	165.3° ±13.9°
S_2	0.32 ± 0.05	143.1° ± 8.5°	0.41 ± 0.04	141.7° ± 4.9°	0.50 ± 0.03	151.3° ± 3.4°	0.54 ± 0.04	153.1° ± 4.5°	0.61 ± 0.04	156.5° ± 3.8°
S_1K_1	0.78 ± 0.11	171.8° ± 8.1°	1.00 ± 0.08	162.0° ± 4.7°	0.77 ± 0.08	162.3° ± 6.0°	0.88 ± 0.14	155.8° ± 5.0°	1.08 ± 0.14	179.8° ± 7.4°
P_1	0.46 ± 0.12	-158.0° ±14.8°	0.12 ± 0.09	179.3° ± 43.2°	0.72 ± 0.09	161.0° ± 7.0°	0.57 ± 0.15	-172.4° ±15.3°	0.59 ± 0.16	137.3° ±15.3°
O_1	0.52 ± 0.11	172.0° ±10.2°	0.90 ± 0.08	170.0° ± 5.2°	0.86 ± 0.08	167.6° ± 5.2°	0.73 ± 0.14	158.6° ±10.6°	1.05 ± 0.14	170.3° ± 7.4°
St. Dev. D	4.53		3.56		3.62		6.13		6.35	
SD	1.85		1.43		1.42		1.70		1.69	
TD	0.98		0.74		0.63		0.96		0.83	
S_2/M_2 0.465*	0.528		0.616		0.661		0.737		0.730	
N_2/M_2 0.194*	0.232		0.194		0.194		0.221		0.241	
O_1/K_1 0.710*	0.789		0.894		1.125		0.831		0.968	
M_2/O_1 0.965*	0.989		0.739		0.879		0.995		0.803	

	87/01/01→87/06/28 180 d.,3408 h.r.		87/07/02→87/12/31 185 d.,3840 h.r.		88/01/02→88/06/29 181 d.,3696 h.r.		88/07/02→88/12/05 158 d.,3456 h.r.	
M_2	0.84 ± 0.04	161.7° ± 2.6°	1.01 ± 0.05	158.6° ± 2.7°	0.86 ± 0.06	153.2° ± 3.8°	0.89 ± 0.05	142.6° ± 3.4°
N_2	0.22 ± 0.04	172.4° ± 11.2°	0.22 ± 0.05	176.5° ± 13.9°	0.13 ± 0.06	168.2° ± 26.5°	0.19 ± 0.05	159.1° ± 15.7°
S_2	0.60 ± 0.04	157.7° ± 3.5°	0.74 ± 0.05	156.4° ± 3.5°	0.69 ± 0.05	137.6° ± 4.4°	0.77 ± 0.05	141.5° ± 3.9°
S_1K_1	1.30 ± 0.13	167.3° ± 5.5°	0.87 ± 0.15	161.6° ± 10.0°	1.72 ± 0.18	157.1° ± 6.1°	1.22 ± 0.14	150.3° ± 6.5°
P_1	0.25 ± 0.14	-175.0° ± 33.0°	0.52 ± 0.17	167.3° ± 18.5°	0.42 ± 0.21	-162.7° ± 27.8°	0.85 ± 0.16	147.7° ± 10.7°
O_1	0.76 ± 0.13	166.7° ± 9.3°	0.85 ± 0.14	169.0° ± 10.0°	1.01 ± 0.18	165.5° ± 10.3°	1.16 ± 0.14	155.4° ± 6.8°
St. Dev. D	4.94		6.32		7.72		5.66	
SD	1.32		1.74		2.06		1.89	
TD	0.62		0.90		0.89		0.84	
S_2/M_2 0.465*	0.713		0.726		0.805		0.861	
N_2/M_2 0.194*	0.265		0.219		0.153		0.213	
O_1/K_1 0.710*	0.585		0.970		0.585		0.948	
M_2/O_1 0.965*	1.102		1.196		0.859		0.772	

TABLE 5.3.

Water-levels tidal analyses results of the six months sub-sets of data for the deep well after having removed the barometric affect.
The amplitudes and their RMS are expressed in mm(*=theoretical amplitudes ratios).

	84/07/01→84/12/31 184 d.,4176 h.r.		85/01/01→85/06/30 182 d.,4320 h.r.		85/07/01→ 85/12/31 184 d.,4032 h.r.		86/01/01→86/06/30 180 d.,3504 h.r.		86/07/01→86/12/31 185 d.,3264 h.r.	
M_2	5.83 ± 0.11	158.6° ± 1.1°	5.48 ± 0.07	149.6° ± 0.8°	5.36 ± 0.10	148.8° ± 1.1°	5.21 ± 0.20	147.5° ± 2.1°	5.05 ± 0.08	146.4° ± 0.9°
N_2	1.05 ± 0.11	152.3° ± 5.8°	0.97 ± 0.07	153.5° ± 4.4°	0.98 ± 0.11	166.0° ± 6.4°	0.97 ± 0.22	154.5° +12.9°	0.80 ± 0.09	149.1° ± 6.5°
S_2	3.22 ± 0.11	152.7° ± 1.9°	2.92 ± 0.07	143.5° ± 1.4°	3.01 ± 0.10	140.2° ± 1.9°	3.01 ± 0.19	135.2° + 3.5°	2.94 ± 0.08	132.7° ± 1.5°
S_1K_1	8.66 ± 0.21	164.6° ± 1.4°	8.49 ± 0.16	158.3° ± 1.1°	8.42 ± 0.18	157.0° ± 1.2°	8.30 ± 0.30	159.1° ± 2.1°	7.62 ± 0.13	156.8° ± 1.0°
P_1	3.91 ± 0.22	159.2° ± 3.3°	2.95 ± 0.17	155.4° ± 3.3°	3.78 ± 0.20	155.9° ± 3.0°	2.60 ± 0.33	163.6° ± 7.4°	3.19 ± 0.15	152.0° ± 2.6°
O_1	7.70 ± 0.21	164.5° ± 1.5°	7.54 ± 0.16	159.1° ± 1.2°	7.49 ± 0.17	156.5° ± 1.3°	7.69 ± 0.30	159.4° ± 2.2°	7.03 ± 0.12	159.8 ° ± 1.0°
St. Dev. D	9.06		7.11		7.59		12.21		5.03	
SD	4.35		2.96		3.92		6.95		2.63	
TD	2.55		1.76		1.87		4.00		1.52	
S_2/M_2 0.465*	0.552		0.533		0.561		0.578		0.583	
N_2/M_2 0.194*	0.181		0.176		0.183		0.185		0.158	
O_1/K_1 0.710*	0.889		0.888		0.889		0.926		0.923	
M_2/O_1 0.965*	0.757		0.727		0.716		0.678		0.718	

	87/01/01→87/06/28 180 d.,4032 h.r.		87/07/01→87/12/31 185 d.,3984 h.r.		88/01/02→88/06/27 179 d.,3840 h.r.		88/07/02→88/12/08 161 d.,3552 h.r.	
M_2	5.14 ± 0.06	144.4° ± 0.6°	5.24 ± 0.05	144.4° ± 0.6°	5.16 ± 0.05	145.2° ± 0.5°	5.39 ± 0.08	142.3° ± 0.8°
N_2	0.96 ± 0.07	145.0° ± 4.0°	0.98 ± 0.06	145.1° ± 3.4°	0.78 ± 0.05	142.9° ± 3.5°	0.81 ± 0.08	144.2° ± 5.4°
S_2	2.83 ± 0.06	135.0° ± 1.1°	3.02 ± 0.05	136.2° ± 0.9°	2.92 ± 0.04	133.1° ± 0.08°	3.20 ± 0.07	134.9° ± 1.3°
S_1K_1	7.93 ± 0.11	157.3° ± 0.8°	8.19 ± 0.09	155.5° ± 0.6°	8.53 ± 0.09	155.9° ± 0.6°	8.52 ± 0.12	156.4° ± 0.8°
P_1	3.06 ± 0.12	157.8° ± 2.3°	3.72 ± 0.10	156.6° ± 1.6°	3.28 ± 0.10	159.0° ± 1.7°	3.50 ± 0.13	151.6° ± 2.2°
O_1	7.52 ± 0.11	157.4° ± 0.8°	7.50 ± 0.09	157.2° ± 0.7°	7.67 ± 0.09	156.2° ± 0.6°	7.81 ± 0.12	155.6° ± 0.8°
St. Dev. D	4.91		3.98		3.77		4.82	
SD	2.22		1.99		1.69		2.76	
TD	1.23		1.32		1.39		1.97	
S_2/M_2 0.465*	0.550		0.575		0.566		0.594	
N_2/M_2 0.194*	0.187		0.187		0.152		0.149	
O_1/K_1 0.710*	0.948		0.915		0.898		0.917	
M_2/O_1 0.965*	0.684		0.699		0.673		0.690	

TABLE 5.4 a.

Water-levels tidal analyses results for the intermediate well at ROB, according to the conventional seasons, before and after having removed the barometric effect (84/06/01 to 88/12/09)

	D-season 1497d. 11472h.r.								J-season 1551d. 12432h.r.							
	A	σ(A)	α	σ(α)	A*	σ(A)*	α*	σ(α)*	A	σ(A)	α	σ(α)	A*	σ(A)*	α*	σ(α)*
M_2	0.83	±0.04	156.4°	± 2.7°	0.81	±0.03	157.1°	± 2.1°	0.77	±0.03	157.1°	± 2.2°	0.76	±0.03	156.5°	± 2.0°
N_2	0.19	±0.04	166.2°	±12.7°	0.18	±0.03	178.9°	±10.2°	0.15	±0.03	147.9°	±11.7°	0.15	±0.03	147.0°	±11.3°
S_2K_2	0.75	±0.04	175.2°	± 3.0°	0.55	±0.03	155.8°	± 3.1°	0.83	±0.03	166.2°	± 2.2°	0.62	±0.03	143.4°	± 2.7°
$P_1S_1K_1$	1.30	±0.14	175.0°	± 6.1°	1.25	±0.07	174.6°	± 3.4°	1.01	±0.08	148.6°	± 4.4°	1.04	±0.05	146.4°	± 3.0°
O_1	0.79	±0.15	172.1°	±11.1°	0.86	±0.08	171.1°	± 5.6°	0.76	±0.09	160.9°	± 6.4°	0.78	±0.06	162.7°	± 4.3°
stand. dev. D	12.02				6.53				6.93				4.82			
SD	2.58				1.93				1.97				1.83			
TD	1.11				0.92				0.81				0.77			
N_2/M_2 0.194*	0.233				0.223				0.197				0.191			
M_2/O_1 0.965*	1.049				0.943				1.016				0.974			

	E-season 1523d. 11520h.r.							
	A	σ(A)	α	σ(α)	A*	σ(A)*	α*	σ(α)*
M_2	0.84	±0.04	156.7°	± 2.4°	0.83	±0.03	157.0°	± 1.9°
N_2	0.24	±0.04	174.1°	± 8.6°	0.21	±0.03	164.0°	± 8.0°
S_2K_2	0.74	±0.03	169.3°	± 2.0°	0.54	±0.02	148.0°	± 2.2°
$P_1S_1K_1$	0.99	±0.17	164.7°	± 9.5°	0.97	±0.09	165.8°	± 5.4°
O_1	1.03	±0.13	161.1°	± 7.2°	0.99	±0.07	161.2°	± 4.1°
stand. dev. D	9.93				5.51			
SD	2.30				1.80			
TD	0.90				0.81			
N_2/M_2 0.194*	0.291				0.251			
M_2/O_1 0.965*	0.818				0.834			

A: amplitude, in millimeter σ(A): R.M.S. α: phase σ(α): R.M.S.

A*, α* : amplitude and phase after atmospheric pressure correction

* amplitudes ratios (theory)

TABLE 5.4b.

Water-levels tidal analyses results for the deep well at ROB, according to the conventional seasons, before and after having removed the barometric effect (84/06/01 to 88/12/09)

	D-season 1499d. 10848h.r.								J-season 1552d. 12528h.r.							
	A	σ(A)	α	σ(α)	A*	σ(A)*	α*	σ(α)*	A	σ(A)	α	σ(α)	A*	σ(A)*	α*	σ(α)*
M_2	5.52±	0.09	147.2°±	0.9°	5.39±	0.07	147.5°±	0.8°	5.35±	0.06	149.8°±	0.7°	5.27±	0.05	149.6°±	0.6°
N_2	1.11±	0.10	142.6°±	5.1°	0.98±	0.08	148.4°±	4.6°	0.98±	0.07	153.7°±	3.8°	0.94±	0.06	153.8°±	3.4°
S_2K_2	3.47±	0.09	153.3°±	1.5°	3.02±	0.07	139.6°±	1.4°	3.61±	0.07	154.6°±	1.1°	2.99±	0.06	138.5°±	1.1°
$P_1S_1K_1$	8.65±	0.25	157.8°±	1.7°	8.78±	0.11	158.6°±	0.7°	8.25±	0.16	157.3°±	1.1°	8.30±	0.08	156.6°±	0.5°
O_1	7.05±	0.28	157.3°±	2.3°	7.64±	0.12	157.6°±	0.9°	7.65±	0.17	159.9°±	1.3°	7.45±	0.09	159.7°±	0.7°
stand. dev. D	21.58				9.35				14.06				7.01			
SD	5.75				4.55				4.21				3.61			
TD	2.76				2.39				1.88				1.77			
N_2/M_2 0.194*	0.201				0.181				0.183				0.179			
M_2/O_1 0.965*	0.783				0.706				0.700				0.708			

	E-season 1523d. 12000h.r.							
	A	σ(A)	α	σ(α)	A*	σ(A)*	α*	σ(α)*
M_2	5.33±	0.07	147.1°±	0.8°	5.28±	0.06	147.0°±	0.7°
N_2	0.92±	0.08	158.2°±	4.8°	0.87±	0.06	152.4°±	4.3°
S_2K_2	3.51±	0.05	153.1°±	0.9°	2.93±	0.05	137.7°±	0.9°
$P_1S_1K_1$	7.84±	0.28	159.7°±	2.0°	8.09±	0.12	160.7°±	0.8°
O_1	7.70±	0.22	157.2°±	1.6°	7.53±	0.09	157.5°±	0.7°
stand. dev. D	17.14				7.25			
SD	4.85				4.15			
TD	2.18				2.12			
N_2/M_2 0.194*	0.173				0.165			
M_2/O_1 0.965*	0.692				0.702			

A: amplitude, in millimeter σ(A): R.M.S. α: phase σ(α): R.M.S.

A* , α* : amplitude and phase after atmospheric pressure correction

* amplitudes ratios (theory)

TABLES 5.5 a & b

YEARLY water-levels tidal analyses results for the intermediate well(a) and the deep well(b) at ROB AFTER having removed the barometric effect.

(a)	1985 365d.8400h.r.		1986 365d.8304h.r.		1987 366d.7248h.r.		1988 340d.7152h.r.	
	A σ(A)	α σ(α)	A σ(A)	α σ(α)	A σ(A)	α σ(α)	A σ(A)	α σ(α)
M_2	0.71±0.02	158.4°± 1.9°	0.79±0.03	162.7°± 2.3°	0.94±0.03	160.4°± 2.0°	0.87±0.04	147.2°± 2.6°
N_2	0.13±0.03	168.5°±11.1°	0.19±0.04	155.5°±10.8°	0.24±0.04	177.2°± 8.7°	0.15±0.04	160.7°±16.2°
S_2	0.45±0.02	146.9°± 2.9°	0.58±0.03	154.9°± 2.9°	0.67±0.03	158.4°± 2.6°	0.75±0.04	140.4°± 2.8°
K_2	0.10±0.02	159.4°±10.4°	0.13±0.02	163.2°± 9.7°	0.18±0.02	120.8°± 7.4°	0.11±0.03	149.2°±14.8°
S_1	0.52±0.09	-146.5°± 9.6°	0.44±0.16	149.8°±21.1°	0.36±0.16	-117.0°±24.9°	0.64±0.19	-156.4°±17.0°
K_1	0.88±0.06	162.1°± 3.6°	0.96±0.10	170.0°± 5.8°	1.11±0.10	163.6°± 5.0°	1.46±0.11	156.2°± 4.5°
P_1	0.42±0.06	163.2°± 8.3°	0.54±0.11	163.1°±11.5°	0.37±0.11	177.5°±16.8°	0.60±0.13	171.5°±12.4°
O_1	0.88±0.05	168.2°± 3.5°	0.90±0.09	164.0°± 5.9°	0.81±0.09	168.3°± 6.5°	1.05±0.11	161.6°± 6.0°
stand. dev. D	3.50		6.23		5.72		6.77	
SD	1.34		1.71		1.61		2.00	
TD	0.68		0.89		0.78		0.86	
S_2/M_2 0.465*	0.637		0.733		0.713		0.835	
N_2/M_2 0.194*	0.187		0.289		0.253		0.173	
O_1/K_1 0.710*	0.995		0.939		0.736		0.717	
M_2/O_1 0.965*	0.809		0.875		1.155		0.829	

(b)	1985 365d.8352h.r.		1986 365d.6768h.r.		1987 366d.8064h.r.		1988 343d.7392h.r.	
	A σ(A)	α σ(α)	A σ(A)	α σ(α)	A σ(A)	α σ(α)	A σ(A)	α σ(α)
M_2	5.43±0.06	149.1°± 0.7°	5.10±0.11	146.9°± 1.2°	5.20±0.04	144.4°± 0.4°	5.27±0.05	143.7°± 0.5°
N_2	0.97±0.07	158.5°± 3.9°	0.92±0.12	154.8°± 7.7°	0.97±0.05	144.8°± 2.7°	0.83±0.05	143.4°± 3.5°
S_2	2.96±0.06	141.9°± 1.1°	3.01±0.10	133.7°± 2.0°	2.92±0.04	135.5°± 0.7°	3.07±0.05	134.4°± 0.8°
K_2	0.72±0.05	135.0°± 3.8°	0.75±0.08	147.0°± 6.1°	0.68±0.03	120.4°± 2.4°	0.80±0.03	131.1°± 2.5°
S_1	0.33±0.19	-152.2°±31.9°	0.91±0.30	175.6°±19.3°	0.28±0.12	-138.4°±24.3°	0.43±0.12	173.9°±16.2°
K_1	8.44±0.12	157.8°± 0.8°	7.90±0.18	158.6°± 1.3°	8.09±0.07	156.5°± 0.5°	8.52±0.07	156.4°± 0.5°
P_1	3.33±0.13	155.9°± 2.2°	2.88±0.21	157.0°± 4.1°	3.41±0.08	156.9°± 1.4°	3.38±0.08	156.1°± 1.4°
O_1	7.53±0.11	157.6°± 0.9°	7.33±0.18	158.9°± 1.4°	7.48±0.07	157.1°± 0.5°	7.71±0.07	155.9°± 0.5°
stand. dev. D	7.35		10.55		4.61		4.37	
SD	3.43		5.34		2.14		2.45	
TD	1.81		3.11		1.27		1.69	
S_2/M_2 0.465*	0.546		0.589		0.562		0.582	
N_2/M_2 0.194*	0.179		0.179		0.187		0.158	
O_1/K_1 0.710*	0.892		0.929		0.926		0.904	
M_2/O_1 0.965*	0.721		0.696		0.695		0.683	

A:amplitude, in millimeter σ(A):R.M.S. α:phase σ(α):R.M.S.
*amplitudes ratios(theory)

TABLE 5.6.

BAROMETRIC tidal analyses results in Brussels according to the conventional seasons:D-J-E and Y, during the time interval corresponding to the water-levels registrations(June 84→December 88).

	D-season 1502d.12528h.r.		J-season 1554d.14016h.r.		E-season 1522d.13248h.r.	
	A σ(A)	α σ(α)	A σ(A)	α σ(α)	A σ(A)	α σ(α)
M_2	34±15	-172.7°± 25.0°	14± 9	135.8°± 40.1°	21±11	162.9°± 30.5°
N_2	14±16	57.8°± 67.6°	17±10	-117.2°± 34.0°	21±12	-109.4°± 32.4°
S_2K_2	268±15	-126.2°± 3.2°	279±10	-129.7°± 2.1°	258± 8	-129.8°± 1.8°
$P_1S_1K_1$	77±52	- 93.5°± 38.1°	56±29	- 88.2°± 29.3°	92±64	84.1°± 40.4°
O_1	10±58	- 60.4°±318.2°	42±31	121.5°± 43.3°	64±50	-146.8°± 44.7°

	1985 366d.8784h.r.		1986 364d.8736h.r.		1987 364d.8736h.r.		1988 366d.8784h.r.	
	A σ(A)	α σ(α)	A σ(A)	α σ(α)	A σ(A)	α σ(α)	A σ(A)	α σ(α)
M_2	30±12	-155.6°± 23.3°	9±14	67.7°± 97.4°	22±13	140.1°± 34.7°	24±17	171.0°± 40.8°
N_2	22±13	149.1°± 34.0°	24±17	-124.1°± 40.1°	13±15	-114.4°± 64.6°	27±19	13.8°± 39.3°
S_2	301±12	-130.3°± 2.2°	326±14	-119.5°± 2.4°	278±13	-134.1°± 2.6°	264±16	-123.7°± 3.6°
K_2	47± 9	-125.1°± 11.5°	60±11	-136.8°± 10.1°	36±10	-172.5°± 15.0°	35±13	-173.2°± 20.6°
S_1	119±83	167.9°± 40.6°	220±114	48.7°± 29.1°	58±86	- 52.4°± 86.1°	188±108	-147.8°± 32.7°
K_1	25±53	14.6°±120.6°	168±69	37.7°± 23.6°	139±52	86.2°± 21.7°	104±65	93.1°± 35.9°
P_1	10±58	-118.8°±330.9°	75±77	83.0°± 58.7°	110±59	- 5.5°± 30.6°	86±73	-107.5°± 48.2°
O_1	79±51	-141.8°± 37.3°	197±66	45.3°± 19.3°	21±50	-120.3°±137.1°	144±62	126.7°± 24.7°

A:amplitude,in μbar σ(A):R.M.S. α:phase σ(α):R.M.S.

T A B L E 5.7.

Various parameters values for the well-aquifer systems
("intermediate well - tuf of Lincent aquifer" and "deep well-bedrock aquifer")
at ROB

	Thickness b(m)	Porosity $Ø_o$	Poisson coefficient ν_p	Vertical compressibility α(m^2N^{-1})	Specific storage S_s(m^{-1})	Pemeability K_D(ms^{-1})	Transmissivity T (m^2s^{-1})	Well radius r_w(m)	Effective height H_e (m)
Intermediate well tuf of Lincent aquifer	10.50	33 %	0.27	$8.30\ 10^{-10}$	$9.6\ 10^{-6}$	$2.47\ 10^{-5}$	$25.9\ 10^{-5}$	0.10	5.5625
Deep well bedrock aquifer	26.00	9 %	0.29	$7.78\ 10^{-11}$	$1.0\ 10^{-6}$	$4.44\ 10^{-5}$	$114.4\ 10^{-5}$	0.10	12.4375

TABLE 5.8.

BAROMETRIC EFFICIENCIES |BE| and TIDAL EFFICIENCIES |TE| of the two confined wells at ROB.

	INTERMEDIATE AQUIFER	DEEP AQUIFER
	mean values	mean values
|BE| observed	0.123	0.446
|BE| theoretical by (1)	0.155	0.347
|TE| observed	0.793	0.545
|TE| theoretical by (2)	0.845	0.653
	$\|BE\|_{theor} + \|TE\|_{theor} = 1$	
	$\|BE\|_{obs} + \|TE\|_{obs} = 0.916$	$\|BE\|_{obs} + \|TE\|_{obs} = 0.991$

$$(1)\quad BE = -\frac{1}{\frac{\alpha}{\phi_0 \beta} + 1}$$

$$(2)\quad TE = \frac{\frac{\alpha}{\phi_0 \beta}}{\frac{\alpha}{\phi_0 \beta} + 1}$$

TABLE 5.9.

Amplification factors ($A_{observed}$ and A) and phase lags ϕ values for the M_2 And O_1 waves in the two confined wells at ROB.

		M_2	O_1
Intermediate well	A	0.9977	0.9989
	$A-A_{obs}$	$10^{-8}A$	$10^{-9}A$
	ϕ	1°15	0°59
Deep well	A	0.9995	0.9998
	$A-A_{obs}$	$10^{-7}A$	$10^{-8}A$
	ϕ	0°30	0°15

TABLE 5.10.

Calculated water-levels phase lags ϕ values by (5.37) in the intermediate and in the deep wells, for the M_2 and O_1 waves, as functions of the effective radius r_e ; ker α_w is the real part of K_o ($\alpha_w i^{1/2}$), modified Bessel function of second kind of order zero; $\alpha_w = r_w$ (ω $S/T)^{1/2}$. The α_w and ker α_w numerical values are cut.

		$r_e = r_w = 0.1$ m		$r_e = 0.20$m		$r_e = 0.40$ m		$r_e = 0.50$ m		$r_e = 0.60$ m	
		M_2	O_1	M_2	O_1	M_2	O_1	M_2	O_1	M_2	O_1
INTER-MEDIATE WELL	α_w	0.000739	0.000512	0.001478	0.001025	0.002956	0.002050	0.0003694	0.002563	0.002217	0.003075
	kerα_w	7.326144	7.697047	6.632996	6.998840	5.939850	6.305693	5.716750	6.082552	5.534385	5.900228
	H_e	5.5625	5.5625	4.3437	4.3437	4.0390	4.0390	4.0025	4.0025	3.9826	3.9826
	ϕ	1°14	0°57	4°11	2°09	14°43	7°49	21°16	11°2	28°35	15°47
		M_2	O_1	M_2	O_1	M_2	O_1	M_2	O_1	M_2	O_1
DEEP WELL	α_w	0.000178	0.000123	0.000357	0.000247	0.000714	0.000495	0.000893	0.000619	0.001072	0.000743
	kerα_w	8.745762	9.111562	8.052615	8.418415	7.359468	7.725268	7.136325	7.502125	6.953497	7.319803
	H_e	12.4375	12.4375	10.4218	10.4218	9.9179	9.9179	9.8575	9.8575	9.8246	9.8246
	ϕ	0°31	0°16	1°13	0°57	4°13	2°09	6°25	3°17	8°74	4°45

TABLE 5.11.
In situ parameters S_s , $S_s/\emptyset_0$ values determination for the two confined aquifer layers at ROB from the well tidal observations and from the barometric effect in the wells.

	INTERMEDIATE AQUIFER					DEEP AQUIFER				
waves	K_1	O_1	M_2	N_2	S_2	K_1	O_1	M_2	N_2	S_2
ϵ_T (10^{-8})	1.2	0.86	0.83	0.16	0.38	1.2	0.86	0.83	0.16	0.38
$S_s/\emptyset_0$ ($10^{-6}m^{-1}$) * N.K. (1984)	4.6	4.6	4.6	4.6	4.6	5.2	5.4	5.2	5.1	5.3
S_s ($10^{-6}m^{-1}$) * Bred (1967)	12.8	10.2	11.2	9.4	8.7	1.4	1.2	1.5	1.6	1.1
	Mean values					Mean values				
$S_s/\emptyset_0$ ($10^{-6}m^{-1}$) * N.K. (1984)	4.6 (1a)					5.3 (1b)				
S_s ($10^{-6}m^{-1}$)	1.5 (2a)					0.5 (2b)				
S_s ($10^{-6}m^{-1}$) * Bred (1967)	10.5 (3a)					1.4 (3b)				
S_s ($10^{-6}m^{-1}$) ** Bred (1967)	12.0 (4a)					0.9 (4b)				
S_s ($10^{-6}m^{-1}$) definition ***	9.6 (5a)					1.0 (5b)				

* estimation from tidal response observation
** estimation from barometric response observation
*** Hydrogeological definition

N.K. = Narasimhan & Kanehiro
Bred = Bredehoeft

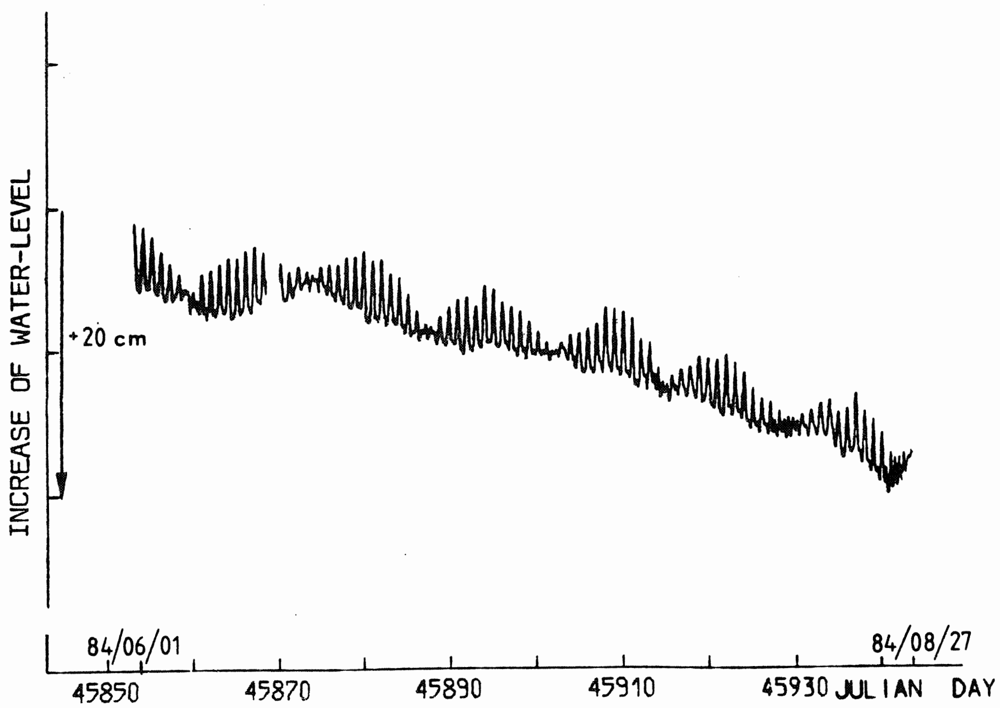

Fig.5.5.Observed tidal oscillations in the deepest well at ROB after having removed the barometric effect.

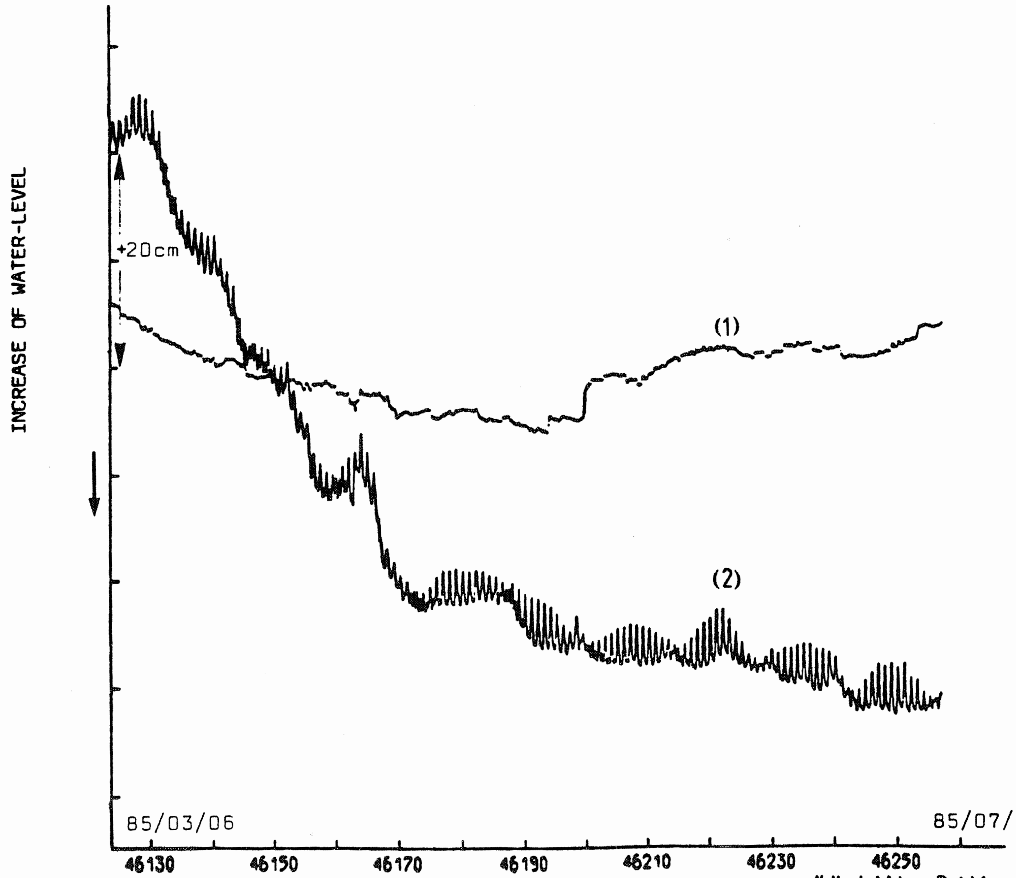

Fig.5.6.Observed tidal phenomena in the intermediate well (curve 1) and in the deep well(curve 2) at the same scale after having removed the barometric effect at ROB.